DISSERTATIONES
MEDICINAE
UNIVERSITATIS
TARTUENSIS
369

VALERIA SIDORENKO

Novel anthracycline-loaded nanoparticles for precision cancer therapy

DISSERTATIONES MEDICINAE UNIVERSITATIS TARTUENSIS
369

DISSERTATIONES MEDICINAE UNIVERSITATIS TARTUENSIS
369

VALERIA SIDORENKO

Novel anthracycline-loaded nanoparticles for precision cancer therapy

UNIVERSITY OF TARTU
Press
1632

Laboratory of Precision and Nanomedicine, Institute of Biomedicine and Translational Medicine, University of Tartu, Estonia

This dissertation is accepted for the commencement of the Doctor of Philosophy in Medicine degree on the 16th of October 2024 by the Council of the Faculty of Medicine, University of Tartu, Estonia.

Supervisors: Ass. Prof. Lorena Simón Gracia, PhD
Laboratory of Precision and Nanomedicine,
Institute of Biomedicine and Translational Medicine,
University of Tartu, Estonia

Prof. Tambet Teesalu, PhD
Laboratory of Precision and Nanomedicine,
Institute of Biomedicine and Translational Medicine,
University of Tartu, Estonia

Reviewers: Piret Arukuusk, PhD
Institute of Technology, University of Tartu, Estonia

Prof. Jyrki Tapio Heinämäki, Dr. Pharm
Institute of Pharmacy, University of Tartu, Estonia

Opponent: Ibane Abasolo Olaortua, PhD
Nanomedicine for Therapeutic Applications (NM4T) CIBER-BBN,
Instituto de Química Avanzanda de Cataluña – CSIC, Barcelona, Spain

Commencement: 13th of December 2024 at 12:00

The University of Tartu grants the publication of this dissertation.

This work was supported by Archimedes Foundation (LMVBS17506 “Innovative anticancer drug candidates based on a novel cytotoxic compound, Utorubicin”), by the European Regional Development Fund Mobilitas Plus postdoctoral fellowship MOBJD11 (to Dr. Simon-Gracia), the European Regional Development Fund (Project No.2014-2020.4.01.15-0012), by EMBO Installation grant #2344 (to Prof. Teesalu), European Research Council grant GLIOGUIDE (780915) from European Regional Development Fund (to Prof. Teesalu), WellcomeTrust International Fellowship WT095077MA (to Prof. Teesalu), and Norwegian-Estonian collaboration grant EMP181 (to Prof. Teesalu). We also acknowledge the support of the Estonian Research Council (grants PRG230, PRG1788, and EAG79 to Prof. Teesalu), EuronanomedIII projects (ECM-CART and iNanoGun to Prof. Teesalu), and TRANSCAN3 (project ReachGLIO to prof. Teesalu) and the Estonian Government through PhD fellowships.

ISSN 1024-395X (print)
ISBN 978-9916-27-744-7 (print)

ISSN 2806-240X (pdf)
ISBN 978-9916-27-745-4 (pdf)

Copyright: Valeria Sidorenko, 2024

University of Tartu Press
www.tyk.ee

TABLE OF CONTENTS

LIST OF ORIGINAL PUBLICATIONS 8

ABBREVIATIONS 9

1. INTRODUCTION 12

2. LITERATURE OVERVIEW 14
   - 2.1. Anthracyclines in cancer treatment 14
     - 2.1.1. Mechanisms of action 14
     - 2.1.2. Anthracycline limitations 15
     - 2.1.3. Novel anthracyclines 16
     - 2.1.4. Utorubicin (UTO) 18
   - 2.2. Improving chemotherapy with nanomedicine 20
     - 2.2.1. Nanocarriers for anthracycline delivery 21
     - 2.2.2. Niosomes (NSVs) 24
     - 2.2.3. Polymersomes (PS) 25
   - 2.3. Passive drug delivery 28
   - 2.4. Enhancing drug delivery to tumors with tumor-homing peptides 28
     - 2.4.1. CendR peptides 30
     - 2.4.2. iRGD peptide 31
     - 2.4.3. LinTT1 peptide 32
   - 2.5. Modulation of tumor microenvironment for enhanced tumor targeting 34
   - 2.6. Targeting tumor blood vessels with vascular disrupting agent CA4P 34
   - 2.7. Summary of the literature 35

3. AIMS OF THE STUDY 37

4. MATERIALS AND METHODS 38
   - 4.1. Peptides (I, II, III) 38
   - 4.2. Polymers and lipids (I, II, III) 38
   - 4.3. Anthracyclines (I, II, III) 39
   - 4.4. Synthesis of NSVs (I) 39
     - 4.4.1. Characterization of NSVs (I) 39
     - 4.4.2. Cell-free binding studies (I) 40
     - 4.4.3. DOX encapsulation efficiency in NSVs and drug release (I) . 40
     - 4.4.4. Stability studies (I) 40
   - 4.5. Synthesis of PS (II, III) 41
     - 4.5.1. Synthesis of FAM-PS (II, III) 41
     - 4.5.2. Synthesis of peptide-targeted PS (TPP-PS) (II) 41
     - 4.5.3. Synthesis of DiR-labeled PS (DiR-PS) for biodistribution studies (II) 41
     - 4.5.4. Anthracycline encapsulation in PS (II, III) 42
     - 4.5.5. Purification (II) 42

4.5.6. Characterization of PS samples (II, III) 42
4.5.7. Efficiency of the peptide conjugation to PS (II) 43
4.5.8. Drug release study from PS (II) 43
4.6. Cell culture (I, II, III) 43
4.6.1. Cellular uptake studies using fluorescence confocal microscopy (I, II) 44
4.6.2. Cellular binding assessment by flow cytometry (I, II) 45
4.6.3. *In vitro* cytotoxicity assay (I, II) 45
4.7. *In vivo* experiments (II, III) 46
4.7.1. Tumor models (II, III) 46
4.7.2. Biodistribution of TPP-DiR-PS (II) 46
4.7.3. Receptor-modulating effects in TNBC breast tumors (III) 47
4.7.4. FAM-PS homing to MKN45P tumors in combination with CA4P and iRGD (III) 47
4.7.5. Tissue immunofluorescence stainings (II, III) 48
4.7.6. Drug combination treatment studies (III) 49
4.7.7. Toxicological studies (III) 50
4.7.8. H&E stainings (III) 50
4.7.9. Statistical analyses (I, II, III) 50

5. RESULTS 51
5.1. Development of TPP-NSVs for effective internalization and DOX delivery to cancer cells 51
5.1.1. Functionalization of NSVs with RPAR and their characterization 51
5.1.2. RPAR-NSVs selectively bind to their target protein NRP-1 .. 53
5.1.3. RPAR-NSVs selectively bind to cultured NRP-1^{+} cells in a receptor-dependent manner 53
5.1.4. Characterization and stability of RPAR-DOX-NSVs 55
5.1.5. Cytotoxicity of RPAR-DOX-NSVs 56
5.2. UTO preclinical development as a nanocarrier payload for effective drug delivery *in vitro* and tumor homing *in vivo* 58
5.2.1. UTO is more potent than DOX in a panel of cultured cancer cells 58
5.2.2. Enhancing PS targeting through peptide density optimization 60
5.2.3. DOX and UTO encapsulation into TPP-PS 62
5.2.4. RPAR-UTO-PS are more toxic in receptor-positive cancer cells 64
5.2.5. TPP-PS home to orthotopic breast tumors *in vivo* 65
5.2.6. LinTT1-UTO-PS specifically deliver drug to breast tumors .. 68
5.3. Evaluation of CA4P-induced molecular changes in TME for iRGD-enhanced secondary UTO-nanotherapy of peritoneal carcinomatosis 70
5.3.1. CA4P treatment enhances iRGD peptide receptor expression in breast and PC tumors 70

5.3.2. CA4P treatment sensitizes IP tumors to iRGD-potentiated nanoparticle delivery 73
5.3.3. iRGD-enhanced secondary nanotherapy reduces peritoneal dissemination and improves the survival of mice with PC 75
5.3.4. Combination therapy of CA4P, iRGD, and UTO-PS does not induce overt toxicities 77

6. DISCUSSION 79
6.1. Significance 79
6.2. Main findings 79
6.2.1. Precision nanoplatform development for anthracycline delivery 80
6.2.2. Anthracyclines' anticancer activity is enhanced via TPP-targeted nanovesicles 80
6.2.3. *In vivo* tumor targeting with TPP-functionalized PS 81
6.2.4. CA4P-induced receptor upregulation enables the enhancement of nanotherapy 82
6.2.5. Safety assessment and clinical potential 83
6.2.6. Future directions 84

7. CONCLUSIONS 86

8. SUMMARY IN ESTONIAN 87

9. REFERENCES 90

ACKNOWLEDGEMENTS 114

PUBLICATIONS 115

CURRICULUM VITAE 161

ELULOOKIRJELDUS 163

LIST OF ORIGINAL PUBLICATIONS

I d'Avanzo, Nicola*; **Sidorenko, Valeria***; Simón-Gracia, Lorena; Rocchi, Antonella; Longo, Francesca; Celia, Christian; Teesalu, Tambet. (2023). C-end rule peptide-guided niosomes for prostate cancer cell targeting *J Drug Deliv Sci Technol*. DOI: 10.1016/j.jddst.2023.105162.

II Simón-Gracia, Lorena*; **Sidorenko, Valeria***; Uustare, Ain; Ogibalov, Ivan; Tasa, Andrus; Tshubrik, Olga; Teesalu, Tambet. (2021). Novel Anthracycline Utorubicin for Cancer Therapy *Angew. Chem. Int. Ed*. DOI: 10.1002/anie.202016421.

III **Sidorenko, Valeria**; Scodeller, Pablo; Uustare, Ain; Ogibalov, Ivan; Tasa, Andrus; Tshubrik, Olga; Salumäe, Liis; Sugahara, Kazuki N.; Simón-Gracia, Lorena; Teesalu, Tambet. (2024). Targeting Vascular Disrupting Agent-Treated Tumor Microenvironment with Tissue-Penetrating Nanotherapy. *Sci Rep.* DOI: 10.1038/s41598-024-64610-7.
* Shared first authorship.

Intellectual property

IV Title of Invention: "Targeted anthracycline delivery system for cancer treatment" By Olga Tšubrik, Andrus Tasa, Ain Uustare, Ivan Ogibalov, Tambet Teesalu, Lorena Simón-Gracia, and **Valeria Sidorenko**
International Publication Number: WO2022023492A1
International PCT No: PCT/EP2021/071321

Contribution to the articles was as follows:

Publication I: I performed experiments and analysis of Figures 3–4 and 6–9, edited the original manuscript draft, and addressed the reviewers' comments with the requested experiments.

Publication II: I conducted the experiments and performed the analysis for Figures 2–6, created Figures 2–6 (including Supplementary Figures S17–S24 and Table 1), contributed to manuscript writing and editing, addressed the reviewers' questions through experimental investigations, and incorporated suggestions from the reviewers into the manuscript.

Publication III: I performed experiments for Figures 2–5 and conducted the analysis presented in Figures 1–5. I also created Figures 1–5 (including Supplementary Figures 1–4 and Table 1), contributed to the experimental design, participated in the manuscript writing and editing process, responded to reviewers' inquiries through written explanations and additional experimental investigations, and incorporated the reviewers' suggestions into the manuscript.

ABBREVIATIONS

22Rv1	a human prostate carcinoma epithelial cell line
A.U.	arbitrary units
AB(s)	antibody(-ies)
ADC	antibody-drug conjugate
Ahx	aminohexaonic acid
ALT	alanine aminotransferase
AML	acute myelogenous leukemia
AMR	amrubicin
AMR-OH	amrubicinol, an active metabolite of amrubicin
ANOVA	analysis of variance
ARRIVE	Animal Research: Reporting of In Vivo Experiments
AUC	area under the curve
BSA	bovine serum albumin
CA4P	combretastatin A4 phosphate, Fosbretabulin
CendR	C-end rule
CPP	critical packing parameter
CREAT	creatinine
CRS	cytoreductive surgery
DAPI	4′6-diamidino-2-phenylindole fluorescent dye
DAU	daunorubicin
DDS	drug delivery systems
DiR	lipophilic, near-infrared fluorescent cyanine dye
DLS	dynamic light scattering
DMEM	Dulbecco's Modified Eagle Medium
DMF	dimethylformamide
DMSO	dimethyl sulfoxide
DNA	deoxyribonucleic acid
DOX	doxorubicin
DOX-NSVs	doxorubicin-loaded niosomes
DOX-PS	doxorubicin-loaded polymersomes
ECM	extracellular matrix
EE (%)	drug encapsulation efficiency (%)
EMA	European Medicines Agency
EPI	epirubicin
EPR	enhanced permeability and retention
Eq(s)	equivalent(s)
FAM	5-carboxyfluorescein
FBS	fetal bovine serum
FC	flow cytometry
FDA	Food and Drug Administration
Fisher's LSD	Fisher least significant difference post hoc test
GI	gastrointestinal

GLUC	glucose
GS	goat serum
H&E	hematoxylin and eosin
HCl	hydrochloride
HIAR	heat-induced antigen retrieval
HIF-1α	hypoxia-inducible factor 1-alpha
HLB	hydrophilic-lipophilic balance
IC50	half-maximal inhibitory concentration
IDA	idarubicin
IFP	interstitial fluid pressure
IP	intraperitoneal
iRGD	internalizing RGD, integrin αvβ3/β5-binding tumor-penetrating peptide, sequence [CRGDKGPDC]
IV	intravenous
IVIS	In Vivo Imaging System
kDa	kilodalton
LinTT1	linear TT1, p32-binding tumor-penetrating peptide, sequence [AKRGARSTA]
Lyp-1	p32-homing tumor homing and penetrating peptide, sequence [CGNKRTRGC]
M21	human melanoma cell line
Mal	maleimide
MCF10CA1a	human triple-negative breast cancer cell line
MDR	multidrug resistance
MeOH	methanol
MKN45P	human high-potential peritoneal dissemination gastric cancer cell line
MRI	magnetic resonance imaging
MTS/PMS	3-(4,5-dimethylthiazol-2-yl)-5-(3-carboxymethoxyphenyl)-2-(4-sulfophenyl)-2H-tetrazolium/phenazine methosulfate assay
MTT	3-(4,5-dimethylthiazol-2-yl)-2,5-diphenyltetrazolium bromide
MWCO	molecular weight cut-off
NIR	near-infrared dye
NP(s)	nanoparticle(s)
NRP-1	neuropilin-1
NSV(s)	niosome(s)
NTA	nanoparticle tracking analysis
OCT	optimal cutting temperature compound
p32	protein 32, also known as gC1q receptor, p33, or hyaluronan binding protein 1 (HABP1)
PBS	phosphate-buffered saline
PBST	PBS with the addition of Tween 20
PC	peritoneal carcinomatosis

PCL	poly(ε-caprolactone) polymer
PDI	polydispersity index
PEG	polyethylene glycol
PEG-PCL	poly(ethylene glycol)-poly(ε-caprolactone) copolymer
PET	positron emission tomography
PFA	paraformaldehyde
PLA	polylactic acid polymer
PLGA	poly(lactic-co-glycolic acid)
PPC-1	human primary prostate cell line
PS	polymersomes
PTX	paclitaxel
RES	reticuloendothelial system
RNS	reactive nitrogen species
ROS	reactive oxygen species
RPAR	prototypic CendR peptide, NRP-1-binding tumor-penetrating peptide, sequence [RPARPAR]
RT	room temperature
SEM	standard error of the mean
TAM(s)	M2 type tumor-associated macrophage(s)
TEM	transmission electron microscopy
TME	tumor microenvironment
TNBC	triple-negative breast cancer (MCF10CA1a cell-derived)
TPP-DOX-NSVs	tumor-penetrating peptide-targeted and doxorubicin-loaded niosomes
TPP-UTO-PS	tumor-penetrating peptide-targeted and utorubicin-loaded polymersomes
TPP(s)	tumor-penetrating peptide(s)
Tw20	Tween 20
uPA	urokinase-type plasminogen activator
UTO	Utorubicin
UTO-PS	Utorubicin-loaded polymersomes
VDA	vascular disrupting agent
VEGF	vascular endothelial growth factor
WHO	World Health Organization

1. INTRODUCTION

Given the diverse nature of cancer types and stages, a multifaceted approach to treatment is essential to treat the disease effectively. Local therapies such as surgery, radiation, and bone marrow transplantation effectively remove localized and accessible tumors; however, the management of distant diseases that have spread throughout the body, as well as unresectable tumors, relies on systemic treatments such as chemotherapy.

Anthracyclines have emerged as promising anticancer drugs with broad-spectrum efficacy against diverse malignancies (Edwardson et al., 2015; Martins-Teixeira & Carvalho, 2020). Renowned members of this drug class, such as doxorubicin (DOX) and daunorubicin (DAU), exhibit potent mechanisms of action by disrupting deoxyribonucleic acid (DNA) replication and inducing apoptosis in rapidly dividing cancer cells. Despite their effectiveness, anthracyclines' clinical utility is restricted by cardiotoxicity, multidrug resistance (MDR), and off-target toxicity (Martins-Teixeira & Carvalho, 2020). Therefore, there is a need for innovative strategies for drug delivery and prodrug design to improve the therapeutic efficacy and safety of anthracyclines. This can be achieved by enhancing their anticancer properties by developing novel anthracyclines with improved properties, such as Utorubicin (UTO).

Introducing drug delivery vehicles is essential for enhancing therapeutic efficacy and reducing the harmful side effects associated with systemic cancer treatments. Traditional systemic drug administration often lacks the precision to selectively target and kill cancer cells, leading to unintended side effects in healthy tissues. Drug delivery vehicles, including lipid and polymeric nanovesicles, provide a strategic solution for controlled and targeted drug transport, resulting in safer options (Wicki et al., 2015). These vehicles not only enhance the pharmacokinetics of therapeutic agents but also facilitate their specific delivery to the tumor site, minimizing off-target effects. Encapsulating drugs within these carriers can shield the therapeutic payload until the intended destination is reached, thereby enhancing the treatment efficacy and reducing systemic toxicity. Furthermore, hydrophobic membranes in nanovesicles enable the encapsulation of drugs in the hydrophilic aqueous core and hydrophobic bilayer, thereby improving the solubility of poorly water-soluble drugs. Consequently, these nanovesicles provide a robust platform suitable for encapsulating and transporting anthracyclines, particularly hydrophobic ones such as UTO.

Targeted drug delivery, particularly using tumor-penetrating peptides (TPPs), can potentially improve the accuracy and effectiveness of cancer treatment (Ruoslahti, 2017). Tumor cells frequently pose challenges to the effective delivery of therapeutic agents, requiring innovative strategies to overcome these obstacles. TPPs, owing to their unique ability to navigate biological barriers within tumor tissues, have emerged as promising tools. These peptides can selectively bind to receptors overexpressed on the surface of tumor-associated endothelial cells and cancer cells, facilitating their internalization and allowing for specific

delivery of drugs or contrast agents to the tumor microenvironment (TME). This targeted approach not only maximizes the concentration of therapeutic agents at the intended site but also minimizes exposure to healthy tissues, thereby mitigating systemic side effects. The versatility of polymersomes (PS) and niosomes (NSVs) as efficient platforms for anthracycline delivery allows for easy functionalization with TPPs, further augmenting their ability to accumulate anthracyclines in tumors. Therefore, integrating TPPs into drug delivery systems (DDS) represents a transformative option for precision medicine, offering promising solutions for developing more effective and tailored cancer therapies.

This thesis focuses on the preclinical development and evaluation of an innovative precision cancer therapeutic, primarily focusing on the novel anthracycline prodrug, UTO, designed to address the limitations associated with traditional anthracyclines. We used 2 types of nanovesicles, namely NSVs and PS, which were optimized and validated in our laboratory (d'Avanzo et al., 2024; Grossen et al., 2017; Lepland et al., 2020; Scodeller et al., 2017; Simón-Gracia et al., 2018). The synthesis of TPP-targeted and anthracycline-loaded nanoparticles (NPs) was first optimized to enhance drug accumulation in cancer cells expressing specific receptors. Our methodology involved comprehensive *in vitro* and *in vivo* binding assays to evaluate the cytotoxicity of DOX- or UTO-loaded TPP-targeted NPs. Furthermore, we investigated the treatment efficacy and synergistic effects of combining the vascular disrupting agent (VDA) combretastatin A4 phosphate (CA4P) and clinical grade TPP iRGD with UTO-loaded PS (UTO-PS) to treat mice bearing peritoneal carcinomatosis, highlighting the potential for significantly improved therapeutic and safety outcomes.

2. LITERATURE OVERVIEW

2.1. Anthracyclines in cancer treatment

Chemotherapy is a critical modality in cancer treatment that utilizes cytotoxic drugs to target and damage cancer cells as well as prevent tumor growth. Several classes of chemotherapeutic agents have been developed for the treatment of cancer. One such class, known as anthracyclines, is considered to be by far the most used and most effective anticancer drugs (Minotti et al., 2004; Weiss, 1992) that most cancer patients receive at some point during their treatment (Mross, 1991). These compounds are derived from *Streptomyces* bacterium, along with most being studied DOX and DAU (Fig. 2). Both anthracyclines have been used in clinical practice for over 30 years for the treatment of various solid and hematological cancers, including lymphomas and breast, leukemia, gastric, uterine, ovarian, bladder, and lung cancers (McGowan et al., 2017; Venkatesh & Kasi, 2023).

2.1.1. Mechanisms of action

Anthracyclines, or anthracycline antibiotics, are chemotherapeutic agents characterized by a tetracyclic ring system (rings A, B, C, and D) with a sugar moiety called daunosamine attached to the aglycone moiety at ring A through a glycosidic linkage (Fig. 1) (Martins-Teixeira & Carvalho, 2020; Minotti et al., 2004). Daunosamine functions as a topoisomerase 2 interacting domain, while the rings B, C, and D form a DNA intercalating domain. These structural features enable anthracyclines to intercalate between DNA base pairs (Gewirtz, 1999), causing DNA deformation (Reinert, 1983) and stabilization of the normally reversible topoisomerase 2-DNA complex (Marinello et al., 2018; Tewey et al., 1984). This, in turn, introduces lethal DNA strand breaks and damages proliferating cancer cells (Capranico et al., 1990; Pommier, 1993; Tewey et al., 1984; Zunino & Capranico, 1990). The resulting DNA-drug interactions disrupt the DNA synthesis, repair, and transcription processes, ultimately inhibiting cell replication and, eventually, leading to cell death (Hortobágyi, 1997; Pommier et al., 2010). Additionally, the quinone moiety can directly damage DNA, proteins, and lipids by forming reactive oxygen species (ROS), causing cytotoxic cellular damage (Gewirtz, 1999; Marinello et al., 2018). Because of their broad anti-tumor activity, anthracyclines have the widest range of clinical use compared to other antitumor drugs used in oncology. For that reason, they are listed by the World Health Organization (WHO) as essential medicines for cancer treatment (World Health Organization, 2023).

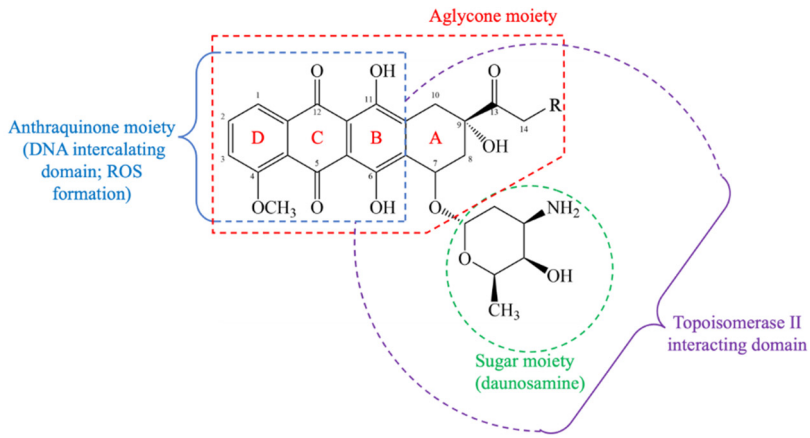

Figure 1. Chemical structure of anthracyclines, highlighting key functional groups. The aglycone moiety is shown as the tetracyclic ring structure (in red), with the anthraquinone moiety (in blue) responsible for DNA intercalation and reactive oxygen species (ROS) generation. The sugar moiety (in green), daunosamine, is shown attached to the aglycone, serving as the topoisomerase II interacting domain. These structural features collectively contribute to the cytotoxic mechanisms of anthracyclines, including DNA deformation, strand break induction, and oxidative damage. Adapted from (Martins-Teixeira & Carvalho, 2020).

2.1.2. Anthracycline limitations

Despite its potent anticancer activity, anthracycline chemotherapy has several limitations (Tacar et al., 2012). Systemically administered drugs do not differentiate between healthy and cancerous cells, causing substantial damage to healthy tissues and contributing to severe side effects. In addition, mechanical and physiological barriers, such as poor and heterogeneous tumor perfusion, dense extracellular matrix (ECM), and high interstitial fluid pressure (IFP), significantly limit the penetration of drugs into solid tumors (Grantab & Tannock, 2012; Jain, 1999; Minchinton & Tannock, 2006). Higher systemic doses of medicines may compensate for poor drug delivery, contributing to the unwanted toxicity and development of multifactorial anthracycline resistance (MDR) in specific cancer cells, which can be both acquired and initial cellular adaptations to the treatment (Chien & Moasser, 2008; Nielsen et al., 1996; Zahreddine & Borden, 2013). The overrepresentation of drug efflux mechanisms, such as MDR transporters, is one of the primary reasons for the reduced intracellular accumulation of anthracyclines (Gottesman, 2002; Nielsen et al., 1996).

In addition, cancer cells have been shown to have increased antioxidant defenses, resulting in resistance to anthracycline-produced ROS in the cell (Chien & Moasser, 2008; Nielsen et al., 1996). Furthermore, modifications in the function of topoisomerase II, such as a decrease in enzyme quantity or alterations in its regular activity due to mutations or other causes, can lead to cellular resistance to

additional doses of anthracyclines (Burgess et al., 2008). Such complex MDR factors contribute significantly to treatment failures in approximately 90 % of patients with metastatic cancer (Solmaz et al., 2015), resulting in tumor relapses (Licht et al., 1991).

Another significant disadvantage associated with non-targeted anthracycline therapies is their dose-dependent toxicity towards cardiomyocytes, resulting in cumulative dose-dependent and irreversible cardiotoxicity (McGowan et al., 2017; Rinehart et al., 1974), accounting for high mortality rates (Minotti et al., 2004; Tacar et al., 2012). However, the mechanisms underlying anthracycline-induced cardiac toxicity are not fully understood. The cardiotoxicity is believed to result from the creation and accumulation of ROS and reactive nitrogen species (RNS) in mitochondria-rich myocardial cells, which can harm DNA and trigger lipid peroxidation in cardiac muscle cells (Farías et al., 2017). In addition, these cells are deficient in primary antioxidant enzymes (such as catalase, superoxide dismutase, and glutathione peroxidase), making them vulnerable to free radical damage (Cappetta et al., 2017).

Despite cardiotoxicity, systemically administered and non-targeted anthracyclines are responsible for liver (Y. Zhang et al., 2020), kidney (Okuda et al., 1986), and gastrointestinal (GI) (Kwon, 2016) toxicities. In addition, they are the cause of side effects such as nausea and vomiting, abdominal pain, hair loss, bone marrow suppression, GI bleeding, and severe seizures (Venkatesh & Kasi, 2023).

Therefore, overcoming challenges such as drug resistance, side effects, and limited drug accumulation in tumors necessitates the development of innovative therapeutic strategies to selectively eliminate cancer cells while sparing healthy ones in cancer treatment.

2.1.3. Novel anthracyclines

The development of novel anthracyclines aims to overcome, or at least limit, the drawbacks associated with conventional formulations of parental drugs (Hulst et al., 2022). For instance, several new anthracyclines have been developed, including epirubicin (EPI) (Plosker & Faulds, 1993), an approximately 30 % less cardiotoxic DOX analog with activity in gastric and breast cancer, and idarubicin (IDA) (Hollingshead & Faulds, 1991), a DAU analog with improved lipophilicity and activity, as induction therapy for acute myelogenous leukemia (AML) (Fig. 2).

This can be achieved by modifying anthracyclines, which considerably influences their antitumor effectiveness and adverse effects. The chemical and genetic production of anthracyclines, including alterations to tetracyclic rings, side chains, and aminosugars, has led to the synthesis of over 2,000 compounds (Minotti et al., 2004). Despite this large number, only a few anthracyclines have been approved for clinical use (Arcamone et al., 1997; Hulst et al., 2022; Mordente et al., 2009; Weiss, 1992). Therefore, there is still a need for novel and more advanced anthracyclines with enhanced antitumor potency and efficacy, which could ultimately lead to the development of improved drug analogs.

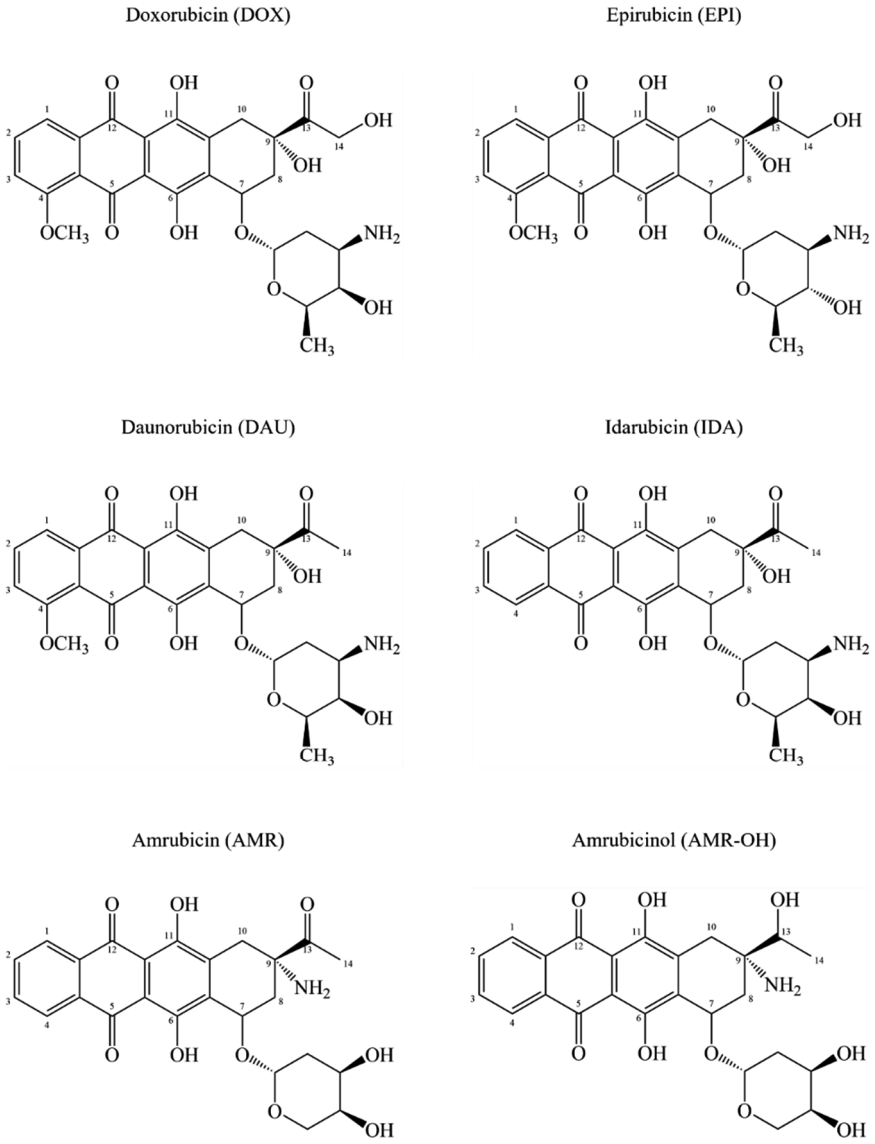

Figure 2. The chemical structures of doxorubicin (DOX), epirubicin (EPI), daunorubicin (DAU), idarubicin (IDA), amrubicin (AMR), and its active metabolite amrubicinol (AMR-OH) are illustrated. In the design and synthesis of UTO (Fig. 3), Amrubicinone (aglycone moiety of AMR) was utilized as the foundational compound. This choice was driven by the favorable attributes of AMR-OH, including lower cardiotoxicity compared to DOX and EPI. Additionally, AMR-OH is exceptionally potent, inhibiting the growth of DOX-resistant cancer cells up to 80 times more effectively than its parent compound, AMR (Yamaoka et al., 1999). Adapted from (Edwardson et al., 2015; Hira et al., 2008).

2.1.4. Utorubicin (UTO)

In this thesis, we developed a novel prodrug called UTO, which was designed to be a more potent and less cardiotoxic anthracycline analog suitable for cancer therapy. UTO, like its precursor amrubicin (AMR), belongs to the category of 9-amino anthracyclines and is known for its reduced cardiotoxicity compared to other anthracyclines, such as DOX and EPI (Morisada et al., 1989; Suzuki et al., 1997). AMR, a synthetic anthracycline approved for treating lung cancer (Kurata et al., 2007), is activated by enzymatic reduction of the carbonyl group into a hydroxyl group (13-OH). In the case of AMR, the resulting metabolite, amrubicinol (AMR-OH), demonstrates potency up to 80 times greater than AMR itself (Yamaoka et al., 1998, 1999). This contrasts with other anthracycline-based anticancer drugs, such as DOX, where metabolites generally have a less potent antitumor effect than the parent compound (Kurata et al., 2007). Despite its anthracycline nature, AMR-OH exhibits limited DNA-binding capability, forming drug-DNA adducts only at the tenth rate of DOX (Hanada et al., 1998).

As UTO shares a quinone moiety structure with anthracyclines (Fig. 1), its reduction to a semiquinone radical generates ROS, impacting cellular processes and inducing cell death (Salvatorelli et al., 2012). The inhibitory effects of AMR and AMR-OH on cell growth appear to be mainly linked to the suppression of topoisomerase II (Hanada et al., 1998).

Further enhancement of cytotoxicity can be achieved by strategically attaching a methylene group to specific sites on the amino and hydroxyl groups, precisely between the respective nitrogen and oxygen atoms of the 1,2-amino alcohol moiety of DAU (Post et al., 2005). This structural modification results in the formation of an oxazolidine cycle, which facilitates the creation of an anthracycline-DNA adduct by binding to the guanine base and intercalating DNA with 4-ring anthraquinone, thus effectively inhibiting cell replication (S. Cutts et al., 2015; S. M. Cutts et al., 2005). As the oxazolidine cycle is unstable in aqueous solutions, a biocleavable protecting group, acetyloxymethyl carbamate, was introduced to protect the reactive oxazolidine cycle (Alexander et al., 1988). This protective measure, also employed in a range of antibiotic, antiviral, and anticancer prodrugs, is cleaved by carboxylesterases in the cytosol upon entry into the cell, a group of enzymes found to be overexpressed in various tumor types (D. Wang et al., 2018; G. Xu et al., 2002). This selective metabolism within tumors minimizes toxicity in healthy tissues, making it a potential advancement in cancer therapy with improved efficacy and reduced side effects (the UTO mechanism of action is depicted in Fig. 3).

Therefore, we aimed to develop a less cardiotoxic 9-aminoanthracycline with enhanced potency and tumor-selective cytotoxic activity.

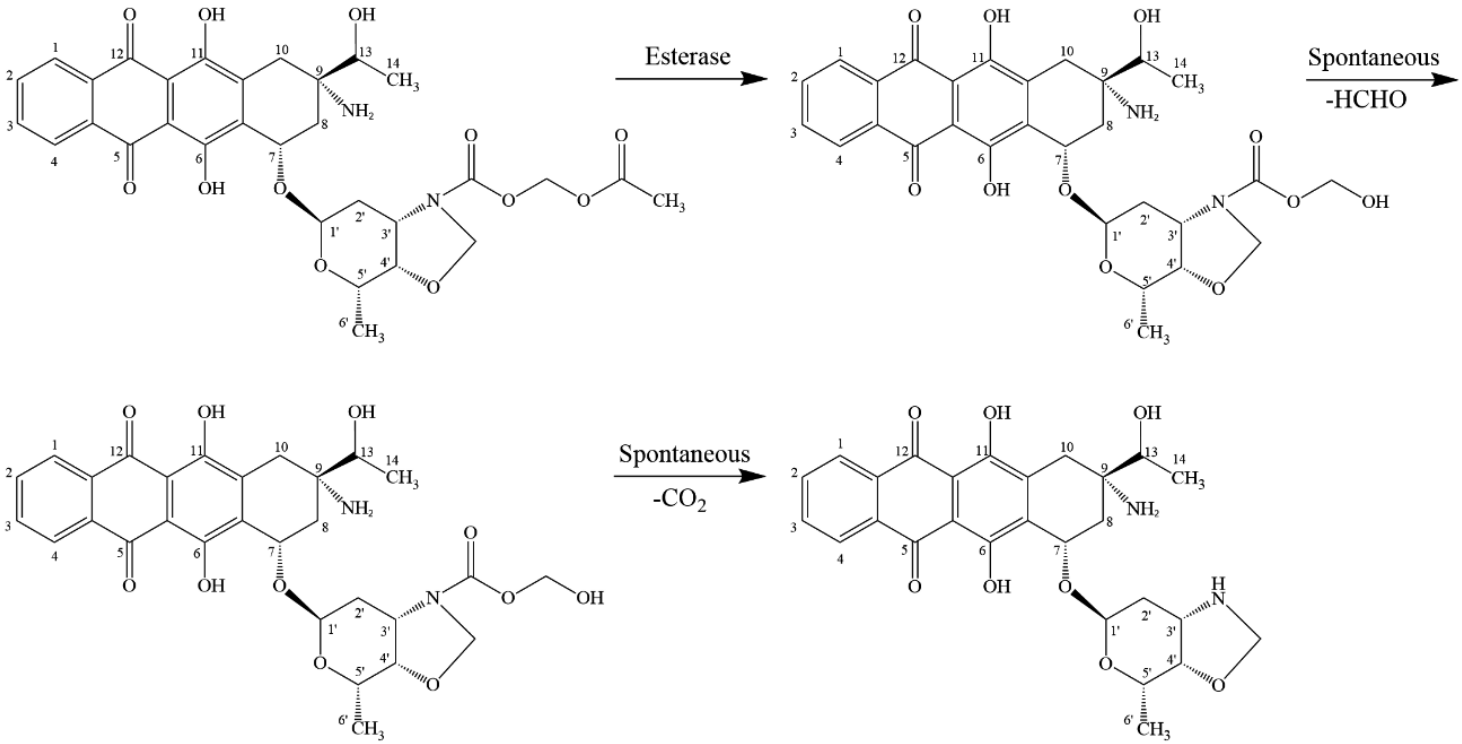

Figure 3. The chemical structure of UTO prodrug and its scheme of cleavage is shown. Esterases hydrolyze the acetyl group from the acetyloxy-methyl carbamate protecting group of UTO, followed by the spontaneous decomposition of the hemiacetal. The oxazolidine cycle then forms an anthracycline–DNA adduct. Adapted from (Simón-Gracia et al., 2021).

2.2. Improving chemotherapy with nanomedicine

Another approach for improving chemotherapeutic safety and potency is their incorporation into nanoparticles (NPs). The use of nanoscale particles ranging in size up to a few hundred nanometers (nm) can enhance the therapeutic effectiveness, bioavailability, biodistribution, and targeting specificity of various anticancer drugs (Duncan & Gaspar, 2011), especially anthracyclines, while minimizing their side effects. Different materials are used in the synthesis of NPs, including polymers (e.g., nanovesicles, micelles, dendrimers), inorganic materials (e.g., metal and silica), lipids (e.g., liposomes and lipid micelles), and biological materials (albumin NPs, viral NPs) (Wicki et al., 2015). Such a wide variety of nanomaterials allows the engineering of NPs with the required characteristics and functionalities to increase their therapeutic index. For example, encapsulation in vesicle- or micelle-like NP can alleviate the problems of solubility and chemical stability of toxic drugs. This is particularly important as poor water solubility limits the bioavailability and development of novel anthracyclines identified during early drug screening (Williams et al., 2013). In patients, hydrophobic drugs such as paclitaxel (PTX) are typically administered with the toxic solvent Cremophor EL, which restricts the amount of taxol that can be administered (Gelderblom et al., 2001; Shimomura et al., 1998; Weiss et al., 1990).

As chemotherapy is most commonly administered intravenously (IV), drug encapsulation in NP can shield it from premature enzymatic degradation in the bloodstream or other biological fluids, often leading to suboptimal drug concentrations. With the drug being protected, its circulation time is prolonged, allowing more time for the drug to reach its site of action before premature degradation. Therefore, lower drug concentrations can be used to achieve the same anticancer effects, thereby reducing the off-target toxicity and potential development of MDR (Hu & Zhang, 2009). Moreover, NPs can be composed of external or internal microenvironment-sensitive materials that allow selective NP degradation in response to internal or external stimuli like pH, temperature, magnetic field, irradiation, or enzymatic activity, allowing controlled drug release specifically at the tumor site (McCoy et al., 2010).

NPs, beyond drug delivery, can be tailored to carry both drugs and imaging agents, either on the surface or encapsulated within the same NP. These customizable NPs, equipped with affinity ligands, enable targeted treatment and real-time monitoring of tumor progression, thus acquiring theranostic properties (Lammers et al., 2011; Zavaleta et al., 2018).

Therefore, NPs act as powerful and versatile tools, offering customization based on the delivered drug and its site of action, thereby enhancing specificity and therapeutic potential.

2.2.1. Nanocarriers for anthracycline delivery

Anthracyclines have been effectively encapsulated in various NPs, including lipidic, polymeric, and inorganic NPs, to enhance their therapeutic index (Ma & Mumper, 2013). 4 of the 15 clinically approved cancer nanomedicines incorporate anthracyclines, as indicated in Table 1 (L. Sun et al., 2023). Notably, all 4 nanoformulations are based on liposomal drug carriers. 2 of these formulations involve liposomal DOX: either polyethylene glycol (PEG)-coated (Doxil®/Caelyx®) (Barenholz, 2012) or non-PEGylated (Myocet®) (Swenson et al., 2001). The other 2 formulations contain DAU alone (DaunoXome®) (Fassas & Anagnostopoulos, 2005) or in combination with other drugs (Vyxeos®) (Krauss et al., 2019). These liposomal anthracyclines have a variety of indications, spanning from the treatment of solid malignancies to various leukemias (L. Sun et al., 2023).

The liposomal nanoplatform has successfully brought anthracyclines to the market by enhancing their blood circulation time, facilitating drug delivery to the tumor site through passive accumulation, and reducing cardiotoxicity (Allen & Martin, 2004; Rodríguez et al., 2022). These liposomes are comprised of double-chain phospholipids and cholesterol, forming a bilayer structure capable of encapsulating hydrophilic drugs in the aqueous lumen and hydrophobic drugs in the hydrophobic bilayer (Barenholz, 2001) (Fig. 4), making them a suitable platform for anthracycline encapsulation and delivery.

Despite their numerous advantages, liposomes face limitations such as biological instability, drug leakage, uncontrolled release, and insufficient drug-loading capacity (Barenholz, 2001). As a result, no marketed liposomal therapy has shown an overall survival benefit compared to conventional parent drugs (Harris et al., 2002; Petersen et al., 2016). In addition, PEGylated Doxil®/Caelyx®, due to its tendency to accumulate in the skin, still induces side effects, such as mucositis and dermal toxicity. At the same time, non-PEGylated Myocet® does not outperform Doxil®/Caelyx® in terms of half-life and tumor targeting, as the absence of a PEG coating results in more rapid elimination by the reticuloendothelial (RES) system (Aloss & Hamar, 2023; Gref et al., 2000; Van Vlerken et al., 2007). This non-superiority underscores the need for novel strategies to improve the therapeutic index of anthracyclines.

Preclinical data features the suitability of nanovesicles for anthracycline delivery, classifying drug carriers into 3 groups based on the composition of their hydrophobic membranes: liposomes with phospholipid membranes, polymersomes (PS) with synthetic block copolymer membranes, and niosomes (NSVs) with nonionic surfactant membranes (Fig. 4).

Table 1. Clinically approved nanomedicines for cancer diagnosis and treatment, as well as nanomedicines containing anthracyclines, are highlighted. Adapted from (L. Sun et al., 2023) and (Rodríguez et al., 2022).

Nanostructure	Product name®	Description	Application	Approval
Lipid-based NP	**Doxil/Caelyx**	PEGylated (stealth) liposomal doxorubicin	Ovarian cancer, Kaposi's sarcoma, Multiple myeloma	FDA (1995) EMA (1996)
	DaunoXome	Non-PEGylated liposomal daunorubicin	Kaposi's sarcoma	FDA (1996)
	Myocet	Non-PEGylated liposomal doxorubicin	Metastatic breast cancer (primary)	EMA (2000)
	Mepact	Non-PEGylated liposomal mifamurtide	Osteosarcoma	EMA (2009)
	Ameluz	5-aminolevulinic acid containing gel	Superficial and/or nodular basal cell carcinoma	EMA (2011)
	Marqibo	Non-PEGylated liposomal vincristine	Philadelphia chromosome-negative acute lymphoblastic leukemia	FDA (2012)
	Onivyde	PEGylated liposomal irinotecan	Pancreatic and colorectal cancers	FDA (2015)
	Vyxeos	Liposomal formulation of cytarbine and daunorubicin	Acute myelogenous leukemia	FDA (2017) EMA (2018)

Nanostructure	Product name®	Description	Application	Approval
Protein-drug conjugates	Oncaspar	Pegaspargase conjugated to L-asparaginase with mPEG, MSP, Na2HPO4, Heptahydrate, and NaCl	Acute lymphoblastic leukemia, chronic myelogenous leukemia	FDA (1994) EMA (2016)
	Ontak	Recombinant cytotoxic protein composed of diphtheria toxin fragments A and B (Met1-Thr387) His and human IL-2 (Ala1-Thr133)	Cutaneous T-cell lymphoma	FDA (1999)
	Eligard	Leuprorelin acetate bound to a polymeric matrix composed of PLGA, NMP, and LA	Prostate cancer	FDA (2002)
	Abraxane	Paclitaxel bound to albumin (active substance) in the form of a spherical nanoparticle	Breast cancer, non-small lung cancer, pancreatic cancer	FDA (2005) EMA (2008)
	Kadcyla	Trastuzumab covalently linked to DM1 via the stable thioether linker MCC	HER2-positive breast cancer	FDA (2013) EMA (2013)
	Pazenir	Paclitaxel formulated as albumin-bound nanoparticles	Breast cancer, metastatic adenocarcinoma of the pancreas, non-small cell lung cancer	EMA (2019)
Metallic NP	NanoTherm	Nanoparticles of superparamagnetic iron oxide coated with amino silane	Glioblastoma, prostate, and pancreatic cancers	EMA (2013)

2.2.2. Niosomes (NSVs)

NSVs are a promising alternative to liposomes for drug delivery, distinctively composed of nonionic surfactants (e.g., esters, ethers, and amides), cholesterol, and charge-inducing agents (Masjedi & Montahaei, 2021) (Fig. 4). The formation of bilayer vesicles rather than micelles depends on the hydrophilic-lipophilic balance (HLB) of the surfactant, the chemical structure of the involved components, and the critical packing parameter (CPP) (Uchegbu & Vyas, 1998). CPP is calculated by considering the volume of the hydrophobic group, the area of the hydrophilic head group, and the length of the lipophilic alkyl chain of the surfactant. If the CPP value is <0.5, micelles will form; if it is 0.5–1, spherical vesicles will form; and if it is >1, inverted micelles will form (Uchegbu & Vyas, 1998). Moreover, nonionic surfactants' size and chain length significantly influence drug encapsulation efficiency (EE), with larger and longer head groups exhibiting higher loading efficiency for hydrophilic drugs (Kumar & Rajeshwarrao, 2011).

The nonionic nature of surfactants offers benefits, including reduced toxicity and inhibition of P-glycoproteins, addressing drug efflux challenges from cancer cells, especially in the case of anthracycline treatment (Nielsen et al., 1996; Shtil et al., 2000). Incorporating cholesterol in NSVs delays the release and enhances the loading of hydrophilic drugs (Abd-Elbary et al., 2008; Yeo et al., 2017), while reducing cholesterol increases the EE for hydrophobic drugs, as it disrupts the membrane structure (S. Chen et al., 2019). These components enable NSVs to self-assemble and form a bilayer structure with a diameter ranging from 10 to 100 nm (Uchegbu & Vyas, 1998). Similar to liposomes, NSVs can effectively deliver a diverse range of drugs by encapsulating hydrophilic drugs in the aqueous lumen and hydrophobic drugs in the hydrophobic bilayer. The structural similarities between NSVs and liposomes result in comparable membrane thicknesses of approximately 3–5 nm for both nanovesicle structures (Ge et al., 2019).

In addition, NSVs offer several advantages over liposomes, including lower cost and more straightforward utilization (Ge et al., 2019; Witika et al., 2022). They are also more stable than liposomes, which are prone to oxidative degradation due to their phospholipid composition (Sankar et al., 2010). As liposomes, NSVs can be modified with PEG to achieve stealth properties, which enhance their stability in the bloodstream, prolong their circulation time, and protect encapsulated drugs from enzymatic degradation (Gref et al., 2000). They can be customized by surface functionalization, which involves the incorporation of specific affinity ligands, such as proteins, antibodies (ABs), and peptides (d'Avanzo et al., 2021; Witika et al., 2022). This allows targeting of the tumor microenvironment (TME) and specific cells. NSVs that respond to various stimuli can be created by incorporating particular structural components (such as functional groups) into vesicles, resulting in targeted drug-release properties (Momekova et al., 2021). However, as with every nanovesicle, some limitations

are associated with NSVs, such as aggregation, fusion, drug leakage, and shelf-life reduction due to drug hydrolysis (Bhardwaj et al., 2020).

NSVs have been explored as a potential DDS for multiple routes of administration, including the oral, parenteral, dermal/transdermal, ocular, and pulmonary (Masjedi & Montahaei, 2021). They have been studied for the delivery of DOX (Bragagni et al., 2012; Rogerson et al., 1988; Tavano et al., 2013) and DAU (Balasubramaniam et al., 2002).

As a result, NSVs are a promising platform for enhancing the therapeutic efficacy of anthracyclines and other drugs while minimizing their associated toxicities, making them a cost-effective and efficient alternative to liposomes.

2.2.3. Polymersomes (PS)

In addition to NSVs, polymeric NPs, also known as PS (D. E. Discher & Ahmed, 2006), show promise for enhanced cancer nanotherapeutics (Fig. 4) (Kamaly et al., 2012). PS can be prepared from natural polymers such as dextran, heparin, gelatin, and collagen, as well as synthetic polymers like PEG, polycaprolactone (PCL), polylactic acid (PLA), and poly(lactic-co-glycolic acid) (PLGA). Among these materials, PEG, PCL, and PLGA are Food and Drug Administration (FDA)-approved polymers for use in medicinal devices (Grossen et al., 2017; Health, 2023).

Amphiphilic diblock copolymers, similar to the nonionic surfactants used in NSVs or phospholipids in liposomes, comprise one hydrophobic and one hydrophilic block. This enables them to form bilayers in an aqueous solution, similar to NSVs and liposomes, but with greater versatility owing to the customizable chemistry of the block copolymers (D. E. Discher & Ahmed, 2006). The morphology of PS depends on the ratio of the water-soluble part to the total mass of the copolymer, which is represented by the "f" value determining the shape and size of the PS, with spherical micelles forming when $f > 50$ %, cylindrical micelles when $40\ \% > f > 50$ %, and spherical vesicles when $25\ \% > f > 40$ % (Blanazs et al., 2009; D. E. Discher & Ahmed, 2006; Du & O'Reilly, 2009). In addition, the molecular weight and structure of copolymers also affect the thickness of the membrane. The thicker hydrophobic membrane of diblock copolymers, ranging from 5–30 nm, compared to lipid bilayers (3–5 nm), not only enhances stability and permeability but also augments the loading capacity for hydrophobic drugs (Bermudez et al., 2002; Meng & Zhong, 2011). For instance, the EE of the hydrophobic drug PTX within the PS membrane is approximately 10-fold greater than that of liposomes (Ahmed, Pakunlu, Srinivas, et al., 2006). It is advantageous to encapsulate hydrophobic anthracyclines such as UTO in PS to achieve maximum drug loading into one nanocarrier to maximize the anticancer effect.

In addition to their improved stability and high loading capacity, there is another distinct advantage of PEG-PCL PS over liposomes (Grossen et al., 2017). Resilient polymeric bilayers containing high molecular weight components uniquely allow for incorporating a higher concentration of functionalized moieties

without compromising bilayer stability (L. Guan et al., 2015; Pawar et al., 2013; Thevenot et al., 2013). In contrast to liposomes limited to 4–6 % PEG-lipid incorporation for stability (Bradley et al., 1998), PEG-PCL PS are 100 % PEGylated, providing an effective barrier against opsonization and clearance (Alexis et al., 2008). This feature ensures prolonged circulation times compared with PEGylated liposomes (J. S. Lee & Feijen, 2012) and enhanced stability in aqueous solutions for several months (J. C. Lee et al., 2001; Sidorenko et al., 2024; Simón-Gracia, Hunt, Scodeller, Gaitzsch, Braun, et al., 2016).

Moreover, the considerable molecular weight of block copolymers results in the formation of highly entangled membranes that exhibit a high degree of resilience with mechanical properties similar to those of elastomers. This gives PS greater flexibility (Bermudez et al., 2002; B. M. Discher et al., 1999) and a superior ability for tissue penetration compared to vesicles self-assembled from lower molecular weight entities such as liposomes (Pegoraro et al., 2013).

To ensure bioavailability and controlled release of encapsulated drugs, PS have been made stimulus-responsive, thus enhancing their versatility (Li et al., 2010). They undergo physical or chemical alterations in response to external or internal signals, causing changes in their molecular structure, surface properties, solubility, and dissociation. Various stimuli, including ultrasound (Rapoport, 2004), magnetic fields (Oliveira et al., 2013), pH (Du et al., 2005; Jung et al., 2007; Simón-Gracia, Hunt, Scodeller, Gaitzsch, Braun, et al., 2016; Simón-Gracia, Hunt, Scodeller, Gaitzsch, Kotamraju, et al., 2016), temperature (H. Xu et al., 2009), and redox potential (Nahire et al., 2014), activate degradation and subsequent drug release from PS. In addition, PS have been used to deliver ABs (Canton et al., 2013; Massignani et al., 2010; Tian et al., 2015; L. Wang et al., 2012), antibiotics (Wayakanon et al., 2013), DNA (Lomas et al., 2007), and cytotoxic drugs (Nahire et al., 2014; Pegoraro et al., 2013; Simón-Gracia et al., 2021; Simón-Gracia, Hunt, Scodeller, Gaitzsch, Braun, et al., 2016, 2016), particularly anthracyclines (Ahmed, Pakunlu, Brannan, et al., 2006; Z. Pang et al., 2011).

As with liposomes and NSVs, PS can be further enhanced for early disease diagnosis by incorporating imaging molecules. For instance, PS for magnetic resonance imaging (MRI) (Pourtau et al., 2013) and radiolabeled PS for positron emission tomography (PET) imaging (Simón-Gracia et al., 2018) have already been developed for the early detection and targeting of solid tumors. PS functionalized with ligands are a more promising option for active delivery because of their ability to carry a high density of ligands without destabilizing the polymeric membrane (L. Guan et al., 2015).

Therefore, both NSVs and PS can improve the effectiveness of anthracycline delivery, offering an alternative to liposomes for drug delivery.

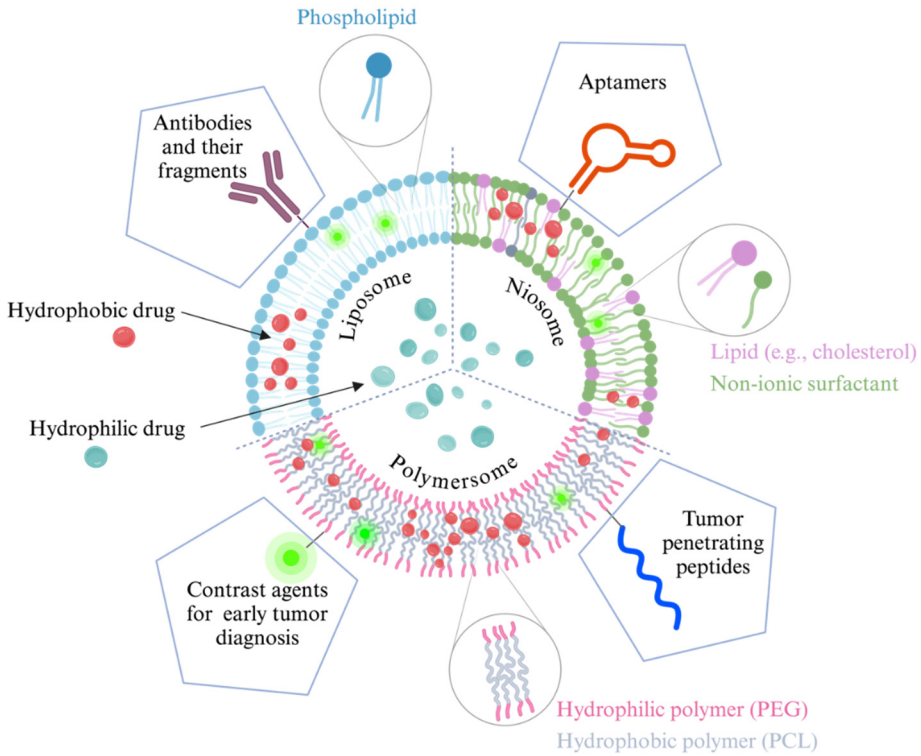

Figure 4. Schematic representation of multifunctional polymersomes (PS), niosomes (NSVs), and liposomes as nanovesicles. PS comprises amphiphilic block copolymers; NSV consists of nonionic surfactants with or without the addition of cholesterol; and liposomes composed of phospholipids are shown. The hydrophobic bilayer or membrane separates and protects the aqueous lumen of the nanovesicles from their surrounding environment. The chemical versatility of vesicles enables their functionalization with antibodies (ABs) or their fragments, imaging agents, aptamers, and tumor-oenetrating peptides (TPPs), as highlighted by polygons (Yoo et al., 2019). Hydrophilic molecules can be encapsulated in the aqueous lumen, whereas hydrophobic molecules can be simultaneously encapsulated in the hydrophobic membrane of nanovesicles. Cartoon adapted from (J. S. Lee & Feijen, 2012; Sánchez-Cerviño et al., 2023) and created using BioRender.com.

2.3. Passive drug delivery

Most of the clinically available nanodrugs rely on passive accumulation in tumors. The extended circulation time allows the drug-NPs to flow through the body, eventually reaching the abnormal and fenestrated tumor vasculature. Tumor blood vessels have a very poor lining of endothelial cells, leaving them with fenestrae of up to several hundred nm (Hobbs et al., 1998; Jain, 1994) through which the NPs can enter the tumor. In contrast, normal blood vessels have fenestrae not larger than 10 nm (Hobbs et al., 1998; Sarin, 2010). Due to the impaired lymphatic system of tumors, NPs can be retained longer in the tumor interstitium, giving them more time to reach the site of action in cancer cells. This phenomenon is known as the enhanced permeability and retention (EPR) effect (Maeda & Matsumura, 1986). However, a compromised lymphatic system limits the elimination of excess fluids entering from the leaky tumor blood vessels, thus creating high IFP in the tumor (Heldin et al., 2004; Jain & Stylianopoulos, 2010) and limiting the entrance of the NPs (Prabhakar et al., 2013). The dense tumor stroma and the ECM also restrict the diffusion of drug NPs into the tumor tissue (Miao et al., 2015). Moreover, not all tumor blood vessels are fenestrated (Hansen et al., 2015; Prabhakar et al., 2013; Wilhelm et al., 2016). Because of the significant inter- and intra-individual differences in tumor biology, the EPR effect is very heterogeneous (Danhier, 2016) and is primarily associated with animal tumor models, thus making EPR an unreliable drug delivery approach. In addition, passive targeting poses problems with the control of drug toxicity and side effects, as NP can end up in healthy organs with fenestrated endothelium linings, such as the spleen or liver (Gaumet et al., 2008).

Therefore, active targeting is required to overcome the limitations of passive tumor-homing mechanisms.

2.4. Enhancing drug delivery to tumors with tumor-homing peptides

Drug delivery can be enhanced through active or synaphic targeting (Ruoslahti et al., 2010) based on the differences between healthy and diseased tissues and the further development of tumor-targeting ligands. For instance, the vascular cells of each healthy tissue/organ have a specific set of cell surface molecules on the luminal side of the endothelial lining, also known as vascular or molecular ZIP codes (Ruoslahti, 2022). In cancer, this molecular signature differs from that of normal tissue, and molecules that are overexpressed in cancer can be targeted with various affinity ligands (Ruoslahti, 2002, 2004; Uhlen et al., 2017). The overexpression of such cell surface and ECM proteins is often involved in processes fundamental for cancer development and metastasis, such as angio- (Hanahan & Folkman, 1996) and lymphangiogenesis (Alitalo & Carmeliet, 2002). Targeting these tumor-specific markers provides opportunities for early

cancer detection, increased drug accumulation, and diminished drug resistance (Andrieu et al., 2019), ultimately leading to improved treatment outcomes.

Various molecules, such as ABs and their fragments, carbohydrates, aptamers, and peptides, have been used as affinity-targeting ligands (Yoo et al., 2019). ABs and their fragments have been widely used for precision targeting (Bregoli et al., 2016; Sivaram et al., 2018). Monoclonal ABs linked with cytotoxic drugs, known as antibody-drug conjugates (ADCs), hold promise for treating both solid and hematological cancers, as evidenced by the FDA approval of 11 ADCs (Tsuchikama et al., 2024). However, the use of ABs as targeting agents has certain limitations. Unlike smaller ligands, such as peptides and aptamers, these large proteins can trigger immune responses (Beck et al., 2017) and face challenges in crossing blood vessels to reach target cells within tumors (Z. Liu & Wu, 2008; Molema et al., 1997; Shockley et al., 1991; Thurber et al., 2008). Additionally, their high binding affinity may create an affinity site barrier that limits their penetration into tumors (Adams et al., 2001). In addition, on average, 1 AB can transport only 3–8 drug payloads, while a 100 nm liposome can encapsulate at least 10,000 small-molecule drugs (Hock et al., 2015; Huwyler et al., 1996; Lambert & Morris, 2017). Moreover, the development of monoclonal ABs is marked by complexity, high costs, and time-consuming procedures, making them a less favorable option (Knutson et al., 2016; Vadevoo et al., 2023; Yu et al., 2012).

Tumor-homing peptides are an appealing class of tumor-specific affinity ligands. Compared with ABs, the smaller size of peptides allows for better penetration into tissues and cells and decreased immunogenicity (McGregor, 2008; Ruoslahti, 2017; Teesalu et al., 2013). They often engage with conserved and functionally significant binding pockets on the surface of target molecules, resulting in frequent biological activity (Lingasamy & Teesalu, 2021). Recent developments in peptide synthesis technology have made it possible to automate and reduce costs during the manufacturing process. This is particularly important for clinical development and translation because large-scale AB manufacturing can be expensive. In addition, homing peptides can be engineered with various modifications to enhance target binding and stability, as well as to introduce functional groups for site-specific attachment to proteins, nanocarriers, cytotoxic drugs, radionuclides, and toxins (Araste et al., 2018; Fosgerau & Hoffmann, 2015; Scodeller & Asciutto, 2020; X. Sun et al., 2017). To avoid the affinity barrier phenomenon, NP decoration with peptides offers the advantage of both modulating and increasing the avidity of the target because of the multivalent representation of the low-affinity peptide on the NP surface (Montet et al., 2006), thus enhancing tumor penetration (Simón-Gracia et al., 2021).

Owing to these characteristics, peptides are considered promising candidates for the development of cancer diagnostics and treatments.

2.4.1. CendR peptides

Tumor-targeting peptides can be discovered through an *in vivo* phage display (Pasqualini & Ruoslahti, 1996; Teesalu et al., 2012, 2013). This peptide screening technology allows for unbiased and agnostic discovery of homing peptides specific to various pathologies such as tumors, wounds, inflammation, atherosclerotic plaques, and brain injuries (Augustin & Koh, 2017; Järvinen & Ruoslahti, 2010; Joyce et al., 2003; Mann et al., 2016; Ruoslahti, 2012; She et al., 2016). *In vivo* phage display has yielded peptides with targeting and homing capabilities and those with the ability to penetrate the tissue, which are classified as tumor-homing and-penetrating peptides (TPPs).

Fifteen years ago, a family of TPPs, known as C-end Rule or CendR peptides, was distinguished by a recognition motif R/KXXR/K (R – arginine, K – lysine, X – any amino acid), which requires C-terminal exposure for activity (Sugahara et al., 2009; Teesalu et al., 2009). The CendR receptor, neuropilin-1 (NRP-1), functions as a co-receptor for vascular endothelial growth factor (VEGF) family members, semaphorins, and various growth factors crucial in vascular biology and the progression of solid tumors (Djordjevic & Driscoll, 2013; Prud'homme & Glinka, 2012; Staton et al., 2007; Yaqoob et al., 2012). NRP-1, which is generally present on the surface of endothelial cells (Soker et al., 1998), is overexpressed in many types of cancers, such as melanoma (Straume & Akslen, 2003), breast (Stephenson et al., 2002), prostate cancer (Latil et al., 2000), leukemia (Karjalainen et al., 2011), glioblastoma (Nasarre et al., 2010), and gastric tumors (Sidorenko et al., 2024; Simón-Gracia, Hunt, Scodeller, Gaitzsch, Kotamraju, et al., 2016; Sugahara et al., 2015). These TPPs activate an endocytic transport pathway that is related to, but distinct from, macropinocytosis, and is only partially characterized (H. B. Pang et al., 2014). This process involves a sophisticated sequence of events, including binding to a primary tumor-specific receptor, proteolytic cleavage, and subsequent binding to a second receptor (Fig. 5). Interaction with NRP-1 triggers activation of the transport pathway (H. B. Pang et al., 2014; X. Sun et al., 2017), allowing deeper penetration into the tumor tissue. CendR motifs play versatile roles in biological and pathological processes, from modulating growth factor signaling to facilitating cellular entry of pathogenic viruses (Balistreri et al., 2021). Notably, the CendR peptide within VEGF-A165 has significant activity in cellular internalization and vascular leakage (Becker et al., 2005), and short peptides with CendR motifs show similar activity (Roth et al., 2016).

2.4.2. iRGD peptide

Integrins, consisting of 24 structurally related cell surface heterodimers, are essential for mediating cellular interactions with the ECM and facilitating cell-cell adhesion (Avraamides et al., 2008). These functions are necessary for tumor initiation, progression, and metastasis (M. Li et al., 2021). RGD-motif-containing peptides or peptidomimetics show a strong affinity for integrins, particularly αvβ3 (Ludwig et al., 2021; Vhora et al., 2015). iRGD (internalizing RGD; sequence CRGDKGPDC) is a prototypic TPP that is used to precisely guide anticancer drugs, imaging agents, and NPs to the tumor vasculature and then deep into the tumor parenchyma (Ruoslahti, 2017; Sidorenko et al., 2024; Simón-Gracia, Hunt, Scodeller, Gaitzsch, Kotamraju, et al., 2016; Sugahara et al., 2015; Teesalu et al., 2013). The targeted payload does not necessarily require a direct connection to the peptide. The peptide initiates a bulk transport system through its action, leading to a "bystander effect", which carries along any nearby compound present in the bloodstream (Sugahara et al., 2010). Initially, the peptide targets integrin $\alpha v\beta_3/\beta_5$ overexpressed in many tumor cells and tumor-associated endothelial cells via its RGD sequence (Ruoslahti, 2002; Sugahara et al., 2009). Subsequent proteolytic cleavage by proteases (Teesalu et al., 2013) displays the CRGDK/R sequence, an activated C-terminal CendR motif. The truncated peptide subsequently loses its affinity for integrin, while the CendR motif permits binding to NRP-1/2, which is a cell- and tissue-penetrating receptor overexpressed on malignant cells, such as those found in peritoneal and other solid tumors (Prud'homme & Glinka, 2012; Simón-Gracia, Hunt, Scodeller, Gaitzsch, Kotamraju, et al., 2016; Sugahara et al., 2015). Interaction between the CendR motif and NRP-1/2 activates the nutrient-dependent CendR pathway (H. B. Pang et al., 2014), which triggers the penetration of iRGD, conjugated, and coadministered cargo through the tumor vasculature into the tumor tissue (Sugahara et al., 2009, 2010).

The distinctive ability of iRGD to enhance the accumulation and distribution of both conjugated and coadministered cargoes within solid tumors makes it a promising candidate for the treatment of pancreatic ductal adenocarcinoma in clinical studies of iRGD-enhanced gemcitabine/Abraxane therapy (Buck et al., 2023; Dean et al., 2022). Its remarkable penetration into solid tumors is achieved not only through the vasculature but also locally and independently of circulation, expanding its applications to locoregional cancer therapy (Simón-Gracia, Hunt, Scodeller, Gaitzsch, Kotamraju, et al., 2016; Sugahara et al., 2015).

Preclinical animal studies have shown that iRGD can effectively improve the effectiveness of cytokines, kinase inhibitors, ABs, nucleic acid-based therapies, such as siRNA, and even cancer-fighting immune cells (Zuo et al., 2019). In addition, NPs decorated or coadministered with iRGD, like PTX-PS (Diaz Bessone et al., 2019; Simón-Gracia, Hunt, Scodeller, Gaitzsch, Kotamraju, et al., 2016), nanoworms (Kotamraju et al., 2016), and DOX-liposomes (Dai et al., 2015; Deng et al., 2017; Yan et al., 2017), have demonstrated the specific homing and penetrating activity of targeted NPs.

2.4.3. LinTT1 peptide

Due to hypoxic and nutrient-depleted stress conditions in tumors, some intracellular targets become displayed extracellularly. p32 (also known as gC1q receptor, p33, or hyaluronan binding protein 1 [HABP1]), primarily a mitochondrial protein, is extracellularly expressed in highly activated cells, such as tumor cells, tumor-associated endothelial cells, and tumor-associated macrophages (TAMs) (Fogal et al., 2008; Simón-Gracia et al., 2018). Many solid tumors originating from the breast (Y. B. Chen et al., 2009), lymphatics (Fogal et al., 2008), GI tract (Hunt et al., 2017), and brain (Agemy et al., 2013; Yenugonda et al., 2017) show a higher representation of p32 on the cell surface, making it a tumor-specific marker and highlighting its potential as a target for cancer diagnosis and therapeutic interventions (Fogal et al., 2008; Laakkonen et al., 2002; Paasonen et al., 2016).

TTPs like cyclic TT1 [sequence CKRGARSTC (Paasonen et al., 2016)] and its linear derivative, LinTT1 [sequence AKRGARSTA (S. Sharma, Kotamraju, et al., 2017)], are one of few p32-targeting peptides identified through *in vivo* phage display (Ruoslahti, 2017). After attaching to its primary target p32, it is further processed by cell surface-associated proteases, such as the tumor-associated protease urokinase-type plasminogen activator (uPA) (Braun et al., 2016), particularly at the second arginine residue (C/AKRGAR̲STC/A). This enzymatic cleavage exposes the CendR motif at the C-terminus of the peptide (KRGAR) (S. Sharma, Kotamraju, et al., 2017). Consequently, the cleaved peptide can engage with NRP-1/2, triggering the trans-tumor CendR transport pathway (Fig. 5) (H. B. Pang et al., 2014; Teesalu et al., 2009).

Another potential therapeutic target is p32-positive M2-type TAMs, which promote tumor growth (Lewis et al., 2016; G. Sharma et al., 2010). These cells play a crucial role in the progression of solid tumors and can also act as a slow-release reservoir for drugs encapsulated in polymeric NPs (Miller et al., 2015) and could be targeted with the TT1 peptide.

The targeting efficacy of LinTT1 and its therapeutic effectiveness have been assessed in preclinical studies, serving as ligands for iron oxide nanoworms carrying a pro-apoptotic effector peptide (Hunt et al., 2017; Säälik et al., 2019; S. Sharma, Kotamraju, et al., 2017), PTX-albumin NPs (Säälik et al., 2019), DOX-loaded liposomes (d'Avanzo et al., 2021), and PS for PET imaging of 4T1 breast tumors (Simón-Gracia et al., 2018).

Therefore, integrating potent anthracyclines into versatile and compatible nanocarriers such as NSVs and PS can significantly enhance drug efficacy. Moreover, functionalization or coadministration of these nanocarriers with CendR peptides is a strategic approach to advance their effectiveness further. This combined strategy promotes increased accumulation and facilitates the improved penetration of anthracycline-loaded NPs into tumors, offering promising possibilities for improved therapeutic outcomes.

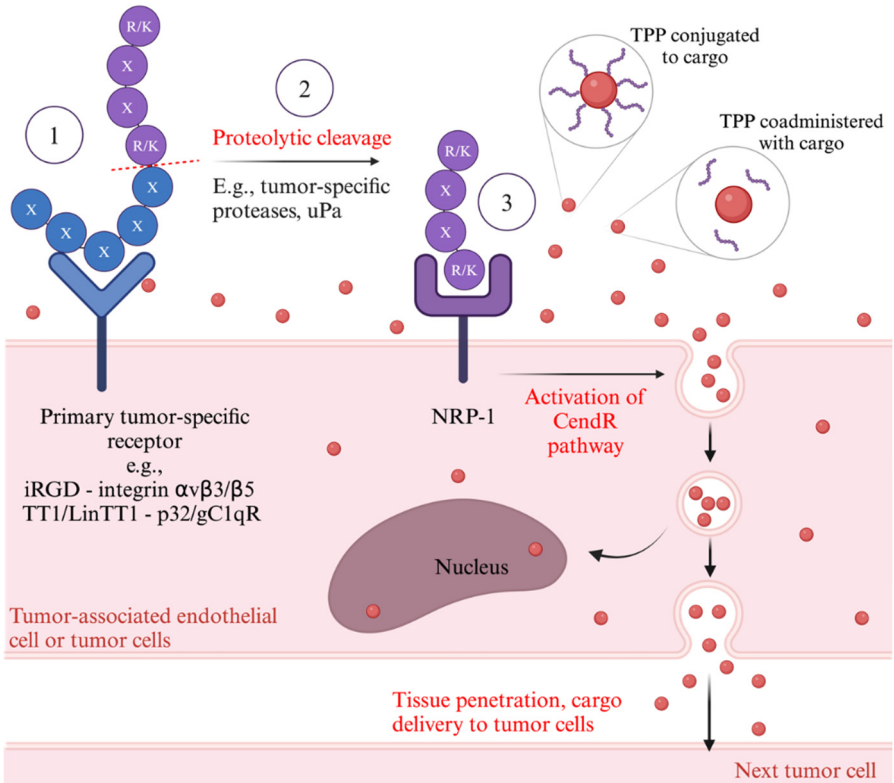

Figure 5. A tumor-penetrating peptide reveals a hidden CendR motif that facilitates tumor tissue penetration through a 3-step mechanism: (1) The peptide initially binds to a primary receptor overexpressed on the surface of tumor cells or tumor-associated endothelial cells, where iRGD recognizes αvβ3/β5 integrins and the TT1 family of peptides targets p32/gC1qR. (2) Protease cleavage then exposes the cryptic CendR element, R/KXXR/K, at the C-terminus (purple part of the peptide). (3) The exposed CendR element interacts with neuropilin-1 (NRP-1) to induce vascular and tissue permeability. The CendR pathway enhances tissue penetration of coadministered molecules (Sugahara et al., 2010) and cargo coupled to the peptide (Sugahara et al., 2009). Adapted from (Ruoslahti, 2017).

2.5. Modulation of tumor microenvironment for enhanced tumor targeting

Although TPPs help accumulate more anticancer drugs and imaging agents in the tumor tissue, the amount of potentially delivered drugs is proportional to the quantity and availability of ligands present in the TME (Hussain et al., 2014; Ruoslahti et al., 2010). TME plays a vital role in tumorigenesis, progression, and metastasis (Singh et al., 2016). Stress conditions, such as hypoxia, oxidative stress, nutrient deprivation, and inflammation, can activate adaptive compensatory mechanisms that result in the remodeling of the TME (Cortesi et al., 2023; Seebacher et al., 2021). Such remodeling can be utilized for therapeutic benefit. This concept involves using a second drug to target the molecular change or vulnerability induced by the initial therapeutic agent. Strategies employed to sensitize tumors for the second therapeutic include modulating the immune status of the tumor (e.g., use of cancer vaccines to render "cold," poorly infiltrated tumors into "hot" tumors receptive to cellular immunotherapies) (Kandalaft & Harari, 2021) and modulating the TME to amplify drug levels and distribution (Bookbinder et al., 2006; Zinger et al., 2019).

2.6. Targeting tumor blood vessels with vascular disrupting agent CA4P

Tumor blood vessels significantly affect the TME. They grow at an accelerated rate to satisfy the high nutrient demand required for the uncontrolled growth of tumor cells (Carmeliet & Jain, 2000). Due to fluctuating oxygen levels in tumors, the TME regulates angiogenesis, driven by processes activated by hypoxic stress conditions. Therefore, targeting established tumor-supplying blood vessels to disrupt tumor development and metastatic spread is an attractive strategy for anticancer therapy (Chaplin & Dougherty, 1999).

Vascular disrupting agents (VDAs) have demonstrated therapeutic potential and ability to modulate the TME by selectively and rapidly shutting down tumor blood vessels, resulting in secondary tumor cell death (Siemann, 2011; Siemann & Horsman, 2008). Among the most studied VDAs, combretastatin A-4 phosphate (CA4P, Fosbretabulin) (Pettit & Rhodes, 1998), a phosphorylated form of CA4 (Dark et al., 1997), has been clinically evaluated for the treatment of advanced solid tumors (Grisham et al., 2018; Mateon Therapeutics, 2018). The mechanism proposed for CA4P involves binding to the β-subunit of tubulin in endothelial cells, specifically at the colchicine-binding site. This binding causes the inhibition of tubulin polymerization, which results in G2/M cell cycle arrest with subsequent activation of apoptotic pathways (McLoughlin & O'Boyle, 2020), as well as the RhoA-GTPase and Rho kinase (ROCK)-dependent signaling cascade (Vincent et al., 2005). These events destroy endothelial cells, leading to blood vessel leakage and disruption, culminating in tumor necrosis in poorly perfused core regions (Galbraith et al., 2001; Kanthou & Tozer, 2002; Vincent et

al., 2005). In contrast, mature endothelial cells in normal blood vessels have a well-developed actin cytoskeleton that allows them to maintain their shape despite VDA binding (Siemann & Horsman, 2008).

Despite its impressive therapeutic activity, CA4P treatment leaves a layer of viable tumor cells in the periphery, contributing to tumor resistance to VDA treatment and regrowth (Liang et al., 2016; Salmon & Siemann, 2007; Tozer et al., 2005). Several clinical trials have demonstrated the limited antitumor activity of CA4P monotherapy in the treatment of solid tumors (Cooney et al., 2006; Dowlati et al., 2002; Rustin et al., 2003; Stevenson et al., 2003) driving its evaluation in combination with other anticancer drugs such as PTX, carboplatin, and antiangiogenic agents (Gill et al., 2019). Solid tumors are also resistant to non-traditional or synthetic VDAs, such as vascular-disrupting nanosystems (S. Sharma, Mann, et al., 2017). The use of iron oxide NPs coated with a tumor-homing peptide (CGKRK) fused to a pro-apoptotic peptide [$_{D}$(KLAKLAK)$_2$] in the treatment of breast tumors in mice has been found to increase the expression of angiogenesis-related genes and integrin β3 in treatment-resistant tumor blood vessels (S. Sharma, Mann, et al., 2017). Therefore, the iRGD peptide may be especially effective in targeting tumors following VDA treatment.

By employing secondary affinity ligand-guided therapies, it may be possible to target the molecular signatures that arise from VDA treatment and overcome drug resistance, leading to lasting therapeutic effects.

2.7. Summary of the literature

Cancer remains a global health challenge that demands continuous advancements in therapeutic strategies. Anthracyclines are vital components of cancer treatment because of their robust mechanisms of action. However, their efficacy is hampered by inherent limitations such as severe cardiotoxicity and MDR (Martins-Teixeira & Carvalho, 2020), underscoring the continuing demand for innovative and sophisticated anthracyclines that possess improved antitumor potency and efficacy, ultimately resulting in the development of improved analogs. This thesis aimed to develop and investigate the therapeutic potential of the novel anthracycline prodrug UTO, which exhibits reduced cardiotoxicity, enhanced potency, and increased tumor-selective cytotoxic activity (Simón-Gracia et al., 2021).

Developing drug-delivering NPs that specifically accumulate in tumors and reduce systemic toxicity is a promising solution (S.-D. Li & Huang, 2010; Maeda & Matsumura, 1986)to address these dose-limiting issues. These drug nanocarriers, particularly NPs composed of hydrophobic bilayers, such as NSVs and PS, offer opportunities to overcome challenges such as poor bioavailability, low tissue penetration, off-target toxicity (Wicki et al., 2015), and the possibility of delivering anthracyclines in a targeted and optimized manner. These nanocarriers possess a higher level of synthetic freedom that allows the customization of NPs to meet specific requirements, making them a promising solution for enhancing anthracycline delivery.

To enhance the selectivity and accumulation of NPs in the target tissue, they can be functionalized with ligands that have an affinity for the tumor tissue, such as ABs and tumor-homing peptides (Ruoslahti, 2017; Yoo et al., 2019). In addition, NPs can be engineered to contain drugs, targeting ligands, and agents that enable their tracking for early and accurate cancer diagnosis (Lammers et al., 2011).

Furthermore, manipulating the TME can serve as a strategy to sensitize and enhance tumor targeting. The emphasis on the VDA CA4P highlights its potential to disrupt tumor blood vessels and modulate the TME by upregulating angiogenesis-related molecular patterns, favoring further tumor targeting with TPPs to eliminate the VDA-resistant viable tumor rim. This presents an innovative approach to enhance therapeutic outcomes.

3. AIMS OF THE STUDY

This doctoral study aimed to develop novel TPP-targeted and anthracycline-loaded nanovesicles that selectively target, penetrate, and deliver antitumor and imaging agents to cancer cells while exhibiting specific penetration and tumor accumulation *in vivo*. The specific objectives are as follows:

1. Characterization of the targeting efficiency and cytotoxic impact of TPP peptide-functionalized NSVs loaded with DOX (TPP-DOX-NSVs) on receptor-positive prostate cancer cells, focusing on physicochemical properties and cellular studies.
2. Evaluation of the preclinical potential of UTO as a more potent anthracycline than DOX in a panel of cultured cancer cells. Further develop UTO-loaded polymersomes (UTO-PS), with and without TPP functionalization, emphasizing viability reduction in malignant cells and *in vivo* tumor homing capability.
3. Investigation of the tumor-sensitizing effects of the VDA CA4P and assessment of the therapeutic efficacy of UTO-PS combined with TPP iRGD in peritoneal carcinomatosis (PC) and breast cancer models.

This study focuses on NP functionalization, anthracycline encapsulation, and the synergistic effects of combining targeting peptides with therapeutic agents to enhance cancer treatment outcomes.

4.. MATERIALS AND METHODS

The methods used in this thesis have been thoroughly explained in the corresponding publications. This section summarizes the methodologies used in these studies.

4.1. Peptides (I, II, III)

The peptides used in these studies are listed in Table 2, including:

- FAM-Cys-Ahx-RPARPAR-OH (FAM-Cys-RPAR);
- FAM-Cys-Ahx-RRAAPRP-OH (scrambled RPAR peptide or FAM-Cys-scrRPAR);
- Ac-Cys-Ahx-RPARPAR-OH (Cys-RPAR);
- Ac-Cys-Ahx-AKRGARSTA-NH_2 (Cys-LinTT1);
- FAM-Cys-Ahx-AKRGARSTA-NH_2 (FAM-Cys-LinTT1);

where Cys is cysteine, FAM is 5-carboxyfluorescein, and Ahx is an aminohexanoic acid linker, were purchased from TAG Copenhagen, Denmark. CRGDKGPDC (with N-terminal acetylation and C-terminal amidation, featuring a C-C disulfide bond, iRGD) peptide was provided by Lisata Therapeutics, USA.

Table 2. Peptides used in this study.

Peptide	Amino acid sequence	Receptor(s)	Nanoparticle platform	Publication in thesis
RPAR	RPARPAR	NRP-1	NSVs, PS	I, II
scrRPAR	RRAAPRP	Control RPAR	NSVs	I
LinTT1	AKRGARSTA	p32, NRP-1	PS	II
iRGD	CRGDKGPDC	αv integrins, NRP-1	Coadministration with PS	III

4.2. Polymers and lipids (I, II, III)

Cholesterol and Tween 20 (Tw20) were acquired from Acros Organics, Belgium. 1,2-distearoyl-sn-glycero-3-phosphoethanolamine-N-[maleimide (polyethylene glycol)-2000] (ammonium salt) (DSPE-PEG_{2000}-Mal) was sourced from Avanti Polar, Suffolk, UK. The copolymers polyethylene glycol-polycaprolactone (PEG_{5000}-PCL_{10000}; Mw 5,000 and 10,000, respectively; referred to as PEG-PCL) and maleimide-PEG_{5000}-PCL_{10000} (Mal-PEG-PCL) were obtained from Advanced Polymer Materials Inc., Montreal, Canada.

For FAM-PEG-PCL synthesis, the copolymer Mal-PEG-PCL (20 mg) was dissolved in 300 µL of nitrogen-purged dimethylformamide (DMF), and 2 equivalents (eqs) of FAM-Cys were added. The mixture was stirred at room temperature (RT) for 2 hours, followed by stirring overnight at 4 °C. After dilution in 2 mL of deionized water, the solution underwent dialysis for 2 hours at RT and overnight at 4 °C against water, using a 10 kilodalton (kDa) dialysis cassette. The resulting suspension was freeze-dried to obtain a yellow powder.

4.3. Anthracyclines (I, II, III)

UTO synthesis is fully described in Publication II, and the synthesized prodrug was provided by ToxInvent LLC, Estonia. DOX hydrochloride (HCl) was purchased from Sigma-Aldrich, Germany.

4.4. Synthesis of NSVs (I)

NSVs were prepared using the thin-layer evaporation method, with modifications based on a previously established protocol (Di Francesco et al., 2021). Following hydration and extrusion, the surface of the resulting NSVs was functionalized with either FAM-Cys-RPAR or FAM-Cys-scrRPAR. This conjugation was achieved through the reaction between the thiol group in the peptide backbone and the Mal residues present on the nanovesicle surface (J. Guan et al., 2021). In cases where DOX incorporation was necessary, it was achieved through a remote loading procedure (Di Francesco et al., 2021). To ensure the purity of the nanovesicles and eliminate non-encapsulated DOX and nonreacted peptides, the particles were centrifuged in Amicon® Ultra centrifugal filters (molecular weight cut-off [MWCO] 100 kDa, 13,000 rpm, 5 min) and washed 5 times with fresh Hepes buffer (pH 7.4) before further investigations.

4.4.1. Characterization of NSVs (I)

The hydrodynamic size, polydispersity index (PDI), and zeta potential of the NSVs were measured using a Zetasizer Ultra (Malvern Instruments Ltd, Malvern, UK). Samples diluted in HEPES buffer solution or water were analyzed at 25 °C. Nanoparticle tracking analysis (NTA) was conducted with a ZetaView PMX 120 V4.1 instrument (Particle Metrix GmbH, Ammersee, Bavaria, Germany) and compared to dynamic light scattering (DLS). Transmission electron microscopy (TEM) was used to study the average diameter and shape of the nanocarriers.

The quantity of RPAR conjugated to NSVs was determined by measuring the fluorescence of the FAM group within the peptide backbone. The successful conjugation of RPAR peptide to DSPE-PEG_{2000}-Mal was further confirmed by 1H NMR analysis. The physical stability of RPAR-DOX-NSVs and DOX-NSVs (control) over time was assessed using Turbiscan Lab analysis and DLS for up to 4 weeks after appropriate storage at 4 °C.

4.4.2. Cell-free binding studies (I)

In a cell-free binding study, Ni-NTA magnetic agarose beads (Qiagen GmbH, Hilden, Germany) were coated with either the histidine-tagged recombinant b1b2 domain of NRP-1 or mutant NRP-1 b1b2 (containing an inactive CendR-binding pocket) (10 µg of protein/reaction) (Tobi et al., 2021). Coating was performed in binding buffer (tris buffer 50 mM, imidazole 5 mM, NaCl 150 mM, pH 7.0) for 1 hour at RT, followed by washing with buffer containing 0.1 % w/v serum albumin. Protein-coated beads were then incubated with FAM-RPAR-NSVs or FAM-scrRPAR-NSVs (lipid concentration 1.1×10^{-7} M) for 1 hour. After 3 washing cycles, bound NSVs were detached using elution buffer (tris buffer 50 mM, imidazole 400 mM, NaCl 150 mM, pH 7.0), and fluorescence was quantified using a Nanodrop 2000c spectrophotometer (Thermo Scientific Inc.).

4.4.3. DOX encapsulation efficiency in NSVs and drug release (I)

Following purification, the RPAR-DOX-NSVs and DOX-NSVs were lyophilized and disassembled with cooled absolute methanol (MeOH). The EE % of DOX inside the NSVs was quantified using an LS55 fluorometric spectrometer (PerkinElmer, USA) at 470 nm and 590 nm for absorption and emission wavelengths, respectively. EE % was determined by comparing the amount of encapsulated drug to the total amount added during NSV formation.

The amount of DOX entrapped inside the NSVs was calculated using an external DOX calibration curve in MeOH. The kinetic release of DOX was assessed using the dialysis bag method with Slize-A-Lyzed dialysis cassettes (10 kDa, Thermo Scientific Inc., USA) and HEPES buffer solution (pH 7.4) as the receiver medium. The release experiment spanned 72 hours, and samples were collected at various time points. The amount of DOX released from the RPAR-DOX-NSVs was calculated based on the external calibration curve prepared in the HEPES buffer.

4.4.4. Stability studies (I)

The physical stability of RPAR-DOX-NSVs in fetal bovine serum (FBS) and human plasma was assessed following a previously reported protocol with slight modifications (Di Francesco et al., 2021). Briefly, 200 µL of RPAR-DOX-NSVs were incubated with 1 mL of FBS (10 % v/v), human plasma (50 % v/v), or HEPES buffer (used as a negative control) at 37 °C under slow magnetic stirring for up to 72 hours. Samples were withdrawn at specified time points (15 min, 30 min, 45 min, and 1, 2, 4, 6, 8, 24, 48, and 72 hours) and analyzed using a Zetasizer Ultra (Malvern Panalytical, UK).

4.5. Synthesis of PS (II, III)

4.5.1. Synthesis of FAM-PS (II, III)

The FAM-PS were produced using the film hydration method, adapting a protocol optimized in previous studies (Simón-Gracia et al., 2018). First, 1 eq of FAM-PEG-PCL and 9 eq of PEG-PCL were dissolved in acetone. The resulting thin polymeric film on the inner surface of a glass vial (Sigma-Aldrich, Germany) was formed by evaporating acetone with nitrogen flow. The film-coated vial was hydrated with sterile phosphate-buffered saline (PBS) at pH 7.4, followed by a 30 s heating step in a 65 °C water bath and a 30 s sonication. This cycle was repeated until PS formation was confirmed, ensuring the absence of polymer aggregates in the suspension. The final polymer concentration in each sample was 10 mg/mL.

4.5.2. Synthesis of peptide-targeted PS (TPP-PS) (II)

TPP-PS were prepared using the film hydration method described in section 4.5.1. FAM-PEG-PCL, Mal-PEG-PCL, and PEG-PCL were mixed with acetone (5 mg total polymer) to optimize the RPARPAR peptide density on the PS surfaces. Different Mal-PEG-PCL percentages (0, 2, 5, 10, and 20 %) were used, with all PS samples containing 5 % FAM-PEG-PCL. Acetone was evaporated to form a thin polymeric film, which was hydrated with PBS (pH 7.4), sonicated, and heated until a PS were formed. The Cys-RPARPAR peptide was added, and the sample was sonicated, shaken, and incubated overnight at 4 °C. The final volume of the PS samples was 0.5 mL, with a total polymer concentration of 10 mg/mL.

For the FAM-labeled LinTT1-targeted PS (FAM-LinTT1-PS), 1 mg Mal-PEG-PCL and 4 mg PEG-PCL were used to form the polymeric film. PS were formed, and the FAM-Cys-LinTT1 peptide (4 eq to Mal-PEG-PCL) was used for conjugation. Similarly, FAM-Cys-RPAR (4 eq of Mal-PEG-PCL) was used for conjugation to obtain RPAR-PS. Non-targeted or empty PS were synthesized using only the PEG-PCL copolymer (total polymer concentration of 10 mg/mL).

The prepared PS were labeled with FAM either by using the FAM-linked peptide or by incorporating the FAM-PEG-PCL polymer into the PS structure.

4.5.3. Synthesis of DiR-labeled PS (DiR-PS) for biodistribution studies (II)

To label the PS with DiR dye for biodistribution assays, 25 µg of DiR (5 µL of a 5 mg/mL solution in acetone) was added to the polymers dissolved in acetone (total polymer amount of 5 mg). Acetone was evaporated to form a polymer/dye film, and PS were formed as described above. The final DiR content in the PS sample was 0.5 % w/w.

4.5.4. Anthracycline encapsulation in PS (II, III)

For UTO encapsulation in PS (UTO-PS), 50 nmol of UTO in 100 µL of acetone was added to the polymers dissolved in acetone (5 mg total). Acetone was evaporated to form a polymer/drug film, and PS was formed as described previously. For DOX encapsulation in PS, the polymeric film was hydrated with 1 mM DOX solution in PBS at pH 7.4, and PS were formed accordingly.

For combination treatment studies, UTO was dissolved in acetone and added to the PEG-PCL-containing acetone solution to achieve a final concentration of 100 µM UTO. The resulting UTO/polymer solution in acetone was evenly distributed among the glass vials, each containing 50 mg of PEG-CPL and 500 nmol of UTO. Acetone was evaporated to form a thin film of the polymer and drug within each vial, following the same procedure described above for UTO-PS formation. The vials were tightly sealed, shielded from light, and stored at -20 °C. Immediately before injecting UTO-PS, 5 mL of sterile PBS was added to each vial to ensure freshness. The dry form reduces issues related to the physical stability of the nanovesicles, including aggregation, fusion, and leakage. In addition, it provides advantages in terms of transportation, distribution, storage, and dosing.

4.5.5. Purification (II)

TPP-PS samples were purified by size-exclusion chromatography using a Sephadex 4 B gel with agarose beads. Elution was performed using PBS (pH 7.4). DiR-labeled PS were concentrated to 20 mg polymer/mL using Amicon Ultra centrifugal filters (MWCO 100 kDa).

4.5.6. Characterization of PS samples (II, III)

For the TEM, PS samples (0.5 mg/mL) were applied to copper grids for 1 min, stained with 0.75 % phosphotungstic acid (pH 7) for 20 s, air-dried, and examined using Tecnai 10 TEM (Philips, Netherlands). The average hydrodynamic diameter of the PS samples was determined by DLS using a Zetasizer Nano ZSP instrument (Malvern, USA). Measurements were performed at 1 mg/mL in PBS (pH 7.4), and the samples were scanned for 10 s at 22 °C with 10 runs per measurement. Zeta potential was determined with Zetasizer Nano ZSP (Malvern, USA) at 0.2 mg polymer/mL in 10 mM NaCl, conducting 50 runs per sample.

The encapsulated UTO and DOX were quantified using a Nanodrop 2000c UV-VIS spectrophotometer (Thermo Scientific, USA). UTO quantification involved preparing serial dilutions in MeOH: water (1:1), with absorbance measured at 490 nm. For DOX, serial dilutions in PBS were prepared by measuring absorbance at 490 nm. A linear trend line from the data gathered in MS Excel was used to evaluate UTO and DOX concentrations inside the PS, measured at 490 nm absorbance.

To ensure uniform DiR encapsulation, the absorbance of DiR was measured at 756 nm using a Nanodrop spectrophotometer.

4.5.7. Efficiency of the peptide conjugation to PS (II)

The percentage of FAM-PEG-PCL in the PS samples was determined by fluorometry. A calibration curve of FAM-Cys was prepared in dimethyl sulfoxide (DMSO) : PBS (1:1), and fluorescence at 480 nm/535 nm was measured using a Victor X5 Multilabel Microplate Reader (Perkin Elmer, USA). PS samples (25 µL) were mixed with 25 µL of MeOH, and fluorescence was measured to calculate the percentage of FAM-PEG-PCL in the PS composition.

To estimate the amount of peptide on the PS with the optimum peptide density, PS were formed using 20 % Mal-PEG-PCL and 80 % PEG-PCL. The FAM-Cys-RPAR peptide was conjugated to PS, as previously described. A standard curve of FAM-Cys-RPAR was prepared in PBS and fluorescence was measured at 480 nm/535 nm. PS functionalized with FAM-Cys-RPAR peptide (25 µL) were mixed with 25 µL of DMSO, and fluorescence was measured to calculate the percentage of FAM-RPAR-PEG-PCL in the PS composition. The FAM-PEG-PCL percentage in the PS composition was 4.9 ± 0.3, and the percentage of FAM-peptide-PEG-PCL relative to the total polymer was 6 %.

4.5.8. Drug release study from PS (II)

To investigate the cumulative release of UTO, UTO-PS in PBS (0.25 mL) were incubated for various durations (0, 1, 3, 24, and 48 hours) at 37 °C. Subsequently, the samples were centrifuged using Amicon Ultra centrifugal filters (MWCO 100 kDa) for 20 min at 6,000 g at RT. The fluorescence of the filtrates was measured at 485 nm/535 nm using a Victor X5 Multilabel Microplate Reader (Perkin Elmer, USA) to quantify the amount of UTO released.

Similar to the UTO release, DOX-PS were incubated for different durations (0, 1, 3, 24, and 48 hours) at 37 °C. Subsequently, the samples were centrifuged using Amicon Ultra centrifugal filters (MWCO 100 kDa, 0.5 mL) for 10 min at 14,000 g at RT, and the absorbance of the filtrate was measured at 490 nm using a Nanodrop spectrophotometer for the quantification of released DOX.

4.6. Cell culture (I, II, III)

The cell lines used in the present study are listed in Table 3. PPC-1 human primary prostate cancer, M21 human melanoma, MKN45P human gastric carcinoma cells (Koga et al., 2011), and MCF10CA1a human triple-negative breast cancer cells were cultured in Dulbecco's Modified Eagle Medium (DMEM) supplemented with 100 IU/mL streptomycin, penicillin, and 10 % FBS. The 22Rv1 prostate carcinoma epithelial cells were cultured in RPMI-1640 medium supplemented with the same supplements.

The cell culture conditions were maintained at 37 °C in a 5 % CO_2 incubator. Cells were detached using trypsin solution (TrypLE Express, Gibco, USA) or enzyme-free dissociation buffer (CellStripper, Fisher Scientific, USA) for binding studies. When seeding a certain number of cells, the cells were mixed

with 0.4 % Trypan Blue and counted using a Bio-Rad TC 10 automated cell counter (Bio-Rad, USA).

Table 3. Cell lines used in this thesis.

Cell line		Cell sruface receptor			Application	Publication in thesis
		αv integrins	p32	NRP-1		
PPC-1	Human prostate adenocarcinoma	+	+	+	*In vitro*	I, II
M21	Human melanoma	+	+	-	*In vitro*	I, II
22Rv1	Human prostate carcinoma epithelial cells	+	+	+	*In vitro*	I
U937	Human monoblast-like histiocytic lymphoma	+	+	+	*In vitro*	II
Jurkat E6.1	Human T-lymphocyte from acute T-cell leukemia	+	+	-	*In vitro*	II
A549	Human lung carcinoma	+	+	+	*In vitro*	II
HT-29	Human colorectal adenocarcinoma	+	+	+	*In vitro*	II
MCF10CA1a	Human triple-negative breast cancer (TNBC)	+	+	+	*In vivo* (nude mice)	II, III
MKN45P	Human gastric carcinoma	+	+	+	*In vivo* (nude mice)	III

4.6.1. Cellular uptake studies using fluorescence confocal microscopy (I, II)

PPC-1 cells and M21 cells (50,000 cells/well; 0.5 mL/well) were seeded in 24-well plates (Croning, Sigma-Aldrich) with coverslips (12 mm diameter, Marienfeld-Superior) and allowed to grow for 1 day in a 37 °C incubator with 5 % CO_2. Subsequently, the cells were exposed to FAM-RPAR-PS samples with varying quantities of peptide (1 mg/mL) or FAM-RPAR-NSVs and FAM-scrRPAR-NSVs at different lipid concentrations (0.25, 0.5, and 1 mg/mL) for 1 hour, followed by

3 washes with 1 mL of PBS. Afterward, the cells were fixed with 4 % paraformaldehyde (PFA) in PBS for 10 min at RT, stained with 1 µg/mL of 4′,6-diamidino-2-phenylindole fluorescent dye (DAPI) for 5 min at RT, and mounted on coverslips using 20 µL of mounting medium (Fluoromount-G; Electron Microscopy Sciences), which was then sealed with nail polish. A confocal microscope FV1200MPE (Olympus, Japan) equipped with UPlanSApo 60x/1.35na or 10x/0.4na objectives (Olympus, Japan) was employed for cell imaging, and the resulting images were analyzed using the Olympus FluoView Ver.4.2a Viewer program.

4.6.2. Cellular binding assessment by flow cytometry (I, II)

PPC-1 and M21 cells were seeded in 24-well plates at a density of 100,000 cells/well (0.5 mL/well) and allowed to grow for 24 hours. Subsequently, the cells were incubated with FAM-labelled PS samples (1 mg/mL) or FAM-RPAR-NSVs and FAM-scrRPAR-NSVs at lipid concentrations of 0.125, 0.25, and 0.5 mg/mL for 1 hour, followed by washing with PBS. The cells were then detached, transferred to 1.5 mL tubes, and subjected to 3 washes with medium before being resuspended in 0.3 mL of PBS. Flow cytometry (FC) analysis was performed using a BD Accuri C6 Plus flow cytometer (BD Biosciences), and the data were analyzed using the corresponding software.

The uptake rate of FAM-RPAR-NSVs was assessed in the presence of blocking and non-binding pocket NRP-1 ABs, mAb7E8 and mAb3E7, respectively. PPC-1 and M21 cells, prepared as previously described, were treated with mAb7E8 or mAb3E7 ABs at final concentrations of 0.01 and 0.02 mg/mL and incubated for 2 hours at 37 °C. The cells were then exposed to FAM-RPAR-NSVs or FAM-scrRPAR-NSVs for 1 hour. After the incubation period, the cells were washed, detached, and analyzed using FC, as described earlier.

4.6.3. *In vitro* cytotoxicity assay (I, II)

PPC-1, M21, and 22Rv1 cells (10,000 cells/well for PPC-1 and M21; 5000 cells/well for 22Rv1) were plated in 96-well plates and allowed to grow for 1 day. The diluted PS, NSV, and free DOX were prepared in PBS. Free UTO, dissolved in DMSO, was further diluted in PBS to maintain a final DMSO concentration below 0.1 % in the well. The samples were added to the cells and incubated for 30 min (for PS) or 1 hour (for NSVs), washed with 0.2 mL PBS, and a fresh medium was added. The cells were then cultured for an additional 24 (for PS) or 48 hours (for NSVs). Subsequently, cells were introduced to 0.1 mL of 3-(4,5-dimethylthiazol-2-yl)-2,5-diphenyltetrazolium bromide (MTT) reagent (5 mg/mL in PBS). After a 2 hour incubation in a 37 °C incubator with 5 % CO_2, the MTT reagent was aspirated, and the formazan crystals were dissolved in 0.1 mL of isopropanol. The absorbance was measured at 570 nm using a Tecan Sunrise microplate reader (Tecan, Switzerland).

Determining the half-maximal inhibitory concentration (IC50) values for UTO and DOX was outsourced to Selvita (Poland). Various cultured tumor cell

lines, including U937 (30,000 cells/well), Jurkat E6.1 (80,000 cells/well), A549 (2,000 cells/well), and HT-29 (6,000 cells/well), were seeded in 96-well plates and treated with UTO at 8 different concentrations in culture medium with FBS, for both 30 min and 90 min (3 wells per condition). Following treatment, cell cultures were maintained for an additional 24 and 72 hours for cells growing in suspension and adherent cells, respectively, at 37 °C in a humidified atmosphere containing 5 % CO_2. The solvent controls (H_2O or DMSO, 1 %) were included in the test. After incubation, the 3-(4,5-dimethylthiazol-2-yl)-5-(3-carboxymethoxyphenyl)-2-(4-sulfophenyl)-2H-tetrazolium/phenazine methosulfate (MTS/ PMS) reagent was added (1–2 hours, depending on the cell line), and the absorbance at 490 nm was recorded. A blank experiment to detect cell-free background absorbance was conducted in parallel.

4.7. *In vivo* experiments (II, III)

Animal experiments were conducted following protocols approved by the Estonian Ministry of Agriculture Committee of Animal Experimentation (projects #159 and #160). All mouse experiments were performed following the relevant guidelines and regulations, and the study is reported in compliance with the Animal Research: Reporting of In Vivo Experiments (ARRIVE) guidelines.

4.7.1. Tumor models (II, III)

For the TPP-DiR-PS biodistribution study, athymic nude female mice (Hsd/Athymic Fox1 nu Harlan; 7–8 weeks old) received injections of 2M MCF10CA1a cells in 50 µL PBS into the mammary gland. Tumors developed over approximately 24 days until they reached a volume of 350 mm^3. Tumor volume was calculated using the formula $V = (W^2 \times L)/2$, where V is the tumor volume, W is the tumor width, and L is the tumor length (Faustino-Rocha et al., 2013).

To induce orthotopic MKN45P tumors, athymic nude female mice (Hsd/Athymic Fox1 nu Harlan; 7–8 weeks old) received intraperitoneal (IP) injections of 1M MKN45P cells in 200 µL PBS, with tumors developing over 4–7 days. For MCF10CA1a tumor induction, the same nude mice were injected with 2M MCF10CA1a TNBC cells in 50 µL PBS into the mammary gland, and tumors developed over 14 days until they reached a volume of 40 mm^3.

4.7.2. Biodistribution of TPP-DiR-PS (II)

Mice with orthotopic MCF10CA1a tumors were IV injected with DiR-labeled PS (80 mg/kg), both targeted (LinTT1 or RPAR) and non-targeted. Anesthesia was induced using 3 % isoflurane blended with O_2 (1 mL/min). *In vivo* imaging was conducted at various time points (0, 1, 3, 6, 24, and 48 hours post-injection) using the IVIS Spectrum *In Vivo* Imaging System (PerkinElmer, US) with specified parameters. After imaging, animals were sacrificed by cardiac perfusion with 10 mL PBS, and tumors and organs were preserved in 4 % PFA in PBS at 4 °C.

DiR-PS signal in tumors was quantified using Living Image 4.5.2, and the tumor's area under the curve (AUC) was determined from *in vivo* quantification data.

For *ex vivo* analysis, MCF10CA1a tumor-bearing mice were IV injected with LinTT1-UTO-PS, UTO-PS, and free DOX at 5 mg of drug/kg. After 24 hours, mice were terminated, tumors were extracted, and immunofluorescence microscopy was performed as described in Section 4.7.5.

4.7.3. Receptor-modulating effects in TNBC breast tumors (III)

When MCF10CA1a tumors reached around 40 mm^3 in volume, immunodeficient mice were evenly divided into 2 groups. One group received daily IP injections of PBS, while the other received IP injections of CA4P every other day (100 mg/kg). On day 33 post-tumor induction, mice were sacrificed by perfusion with 10 mL of PBS. Organs and tumors were excised, fixed in a 4 % PFA solution, and processed into 10 µm-thick sections after embedding in optimal cutting temperature compound (OCT). An immunostaining protocol without heat-induced antigen retrieval (HIAR) was employed, as described in Section 4.7.5. The tumor sections were immunostained with anti-integrin β3, anti-NRP-1, and anti-CD31/mCD105 primary ABs. Following incubation with secondary ABs (goat anti-rabbit Alexa Fluor 647 and goat anti-rat Alexa Fluor 546) and DAPI staining, the samples were imaged using a fluorescence confocal microscope (LSM 710, Zeiss). Image analysis, including fluorescence signal quantification, was performed as described below.

4.7.4. FAM-PS homing to MKN45P tumors in combination with CA4P and iRGD (III)

The experimental design is shown in Fig. 6. Mice with orthotopic MKN45P tumors were randomly assigned into 2 groups for 7 alternate IP injections of CA4P and PBS as a control. CA4P was administered at 100 mg/kg and dissolved in a saline solution at a concentration of 5 mg/mL every other day. The control group received 500 µL of PBS daily. After a 14-day interval, tumor-bearing mice were administered IP injections of FAM-PS at a dose of approximately 160 mg/kg of polymer. This injection was performed with or without coadministration of iRGD, which was administered IP at a dose of 14 µmol/kg 15 min before FAM-PS injection. FAM-PS were allowed to circulate for 6 hours, after which the mice were sacrificed by perfusion with 10 mL of PBS. Tumors and organs were excised and preserved in a 4 % PFA solution in PBS at 4 °C. Immunofluorescence was chosen to quantify receptor expression and examine the spatial distribution of both receptors and FAM-PS, primarily due to FAM-PS's solubility in MeOH. As a result, PFA fixation was used to enable the staining and quantification of FAM-PS targeting in tumors. However, this fixation method imposed certain limitations on the subsequent evaluation of receptor expression. For FAM-PS homing quantification, immunofluorescence staining was performed on dissected tumor sections (20 µm) following the procedure described below, excluding the HIAR step.

Primary AB included rabbit anti-FAM/Oregon Green, while secondary staining was performed using goat anti-rabbit Alexa Fluor 647 AB for FAM signal amplification.

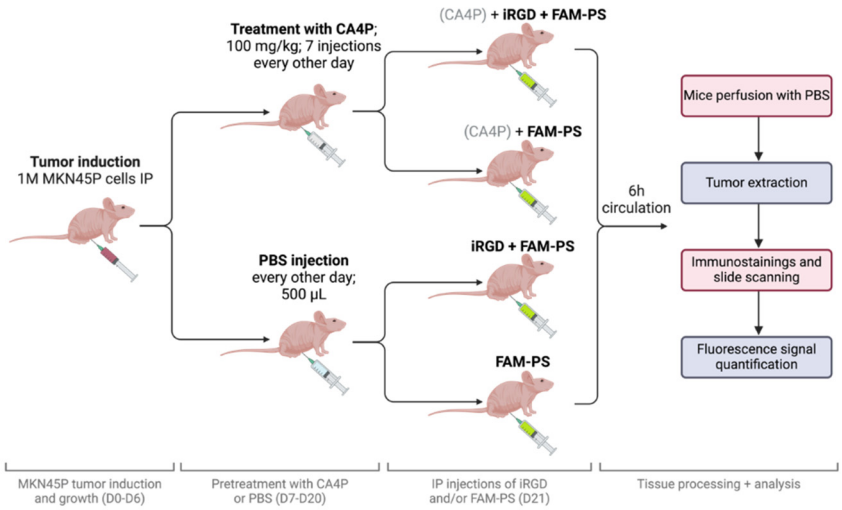

Figure 6. Schematic representation of the FAM-PS tumor-homing experiment (Fig. 18 and 19). Mice with peritoneal carcinomatosis (PC) were treated intraperitoneally (IP) with CA4P (100 mg/kg) or PBS every alternate day for 14 days. Subsequently, FAM-PS was coadministered with iRGD or PBS. After 6 hours of circulation, tumors were collected and subjected to immunostaining for further signal analyses. The fluorescence signals of integrin αv, NRP-1, and p32 were quantified in groups that received either CA4P (CA4P + iRGD + FAM-PS; CA4P + FAM-PS; n=6) or PBS (iRGD + FAM-PS; FAM-PS; n=6). For FAM-PS fluorescence signal quantification n=3. Created using BioRender.com.

4.7.5. Tissue immunofluorescence stainings (II, III)

The tissue processing for breast and peritoneal carcinomatosis (PC) tumors differed but shared key steps. For breast tumor tissues, PFA-fixed tissues were soaked in PBS for 1 hour, stored overnight at 4 °C in 15 % sucrose solution in PBS, and replaced with 30 % sucrose solution the next day. Cryosectioning into 10 µm sections was performed, followed by a 1 hour drying period at RT. The sections were then permeabilized with 0.2 % Triton X in PBS for 10 min, washed with PBST, and blocked with 5 % bovine serum albumin (BSA), 5 % FBS, and 5 % goat serum (GS) in PBST for 1 hour. Overnight incubation at 4 °C with primary ABs (rabbit anti-FAM, rat anti-mouse CD31, rat anti-mouse CD206, rabbit polyclonal anti-NRP-1, and rabbit anti-p32) in diluted blocking buffer (1/100 AB dilution) followed, with secondary AB (Alexa 647-conjugated goat

anti-rabbit IgG and Alexa 546-conjugated goat anti-rat IgG) applied at a 1/200 dilution. After washing with PBST and PBS, nuclei were stained with 1 µg/mL DAPI in PBS for 10 min. Stained slides were mounted and sealed, tissues were imaged using a fluorescence confocal microscope, and image analysis was conducted as previously described.

For PC tumors, PFA-fixed tissues were embedded in OCT, and 20 µm-thick sections were stored at -20 °C before staining. After 2 hours of air-drying at RT, the slides were washed 3 times with PBS (5 min each) and subjected to HIAR in a boiling solution. After cooling, the slides were washed thrice with PBST (5 min each). Tissue sections were permeabilized with PBS + 0.2 % Triton X-100 for 20 min at RT and blocked with 5 % BSA + 5 % GS + 50 nM glycine in PBST for 1 hour. Primary ABs (anti-integrin alpha V/CD51 and anti-NRP-1; dilution 1:200) were applied overnight at 4 °C. The next day, the slides were washed thrice with PBST (5 min each) and incubated with a secondary AB solution (goat anti-rabbit Alexa Fluor 546; dilution 1:500) for 1 hour at RT in the dark. After incubation, the slides were washed thrice with PBST (5 min each), counterstained with DAPI solution (1 mg/mL in PBS; dilution 1:500) for 5 min at RT, washed with PBS (5 min), and mounted. The stained tumors were scanned using an Aperio VERSA slide scanner (20x objective). Fluorescence signals from scans and confocal microscopy were analyzed using Fiji software (ImageJ 1.54f), normalizing the mean signal intensity to the DAPI signal. For quantification of FAM-positive area in tumor sections, images were processed to generate masks for DAPI and FAM signals. The areas of these masks were measured and converted into percentages to represent FAM-positive areas in the tumors. For FAM signal and distribution quantification n=3 mice per group, and for integrin and NRP-1 quantification n=6.

4.7.6. Drug combination treatment studies (III)

For the survival study, on day 6 after tumor induction, PC-bearing mice were divided into 6 groups (n=7 per group; PBS group n=10) and received different combinations of CA4P, iRGD, and UTO-PS for 20 consecutive days. From days 7–25 (only uneven days), CA4P (100 mg/kg) or PBS (500 µL) was administered every other day, and on days 8–26 (on even days), UTO-PS (1.4 mg/kg) with or without iRGD (14 µmol/kg) or PBS (500 µL) was injected every other day. The injections were terminated on the 27th day, and survival was monitored. Mice were euthanized if they had severe ascites, >20 % weight reduction, or severe behavioral changes (shivers, shaking, impaired movement, or severe cachexia).

A similar treatment study was conducted to evaluate tumor progression in terms of tumor weight and total tumor count. On day 4 after tumor induction, PC-bearing mice were divided into 6 groups (n=6). From days 4–21, CA4P (100 mg/kg) or PBS (500 µL) was administered every other day, and on days 5- 21, UTO-PS (1.4 mg/kg) with or without iRGD (4 µmol/kg) or PBS (500 µL) was injected every other day. On the 23rd day, all mice were euthanized by CO_2 inhalation, and tumors were extracted, weighed, and counted.

4.7.7. Toxicological studies (III)

Healthy 8-week-old female Balb/c mice were divided into 3 groups (n=3). Mice received IP injections of CA4P (100 mg/kg, 5 mg/mL solution in saline, 5 IP injections) or PBS (500 µL) every other day. On alternate days, the mice received IP injections of UTO-PS (1.4 mg/kg, 5 IP injections) with iRGD (14 µmol/kg; 5 IP injections) administered 15 min before UTO-PS injection. After 10 days of treatment, 2–3 mL of blood was collected from deeply anesthetized mice through retro-orbital bleeding into Lithium Heparin tubes (BD Vacutainer, no. 368494). The blood samples were centrifuged for 10 min at 1800 g at 4 °C, and plasma was analyzed for glucose (GLUC), creatinine (CREAT), and alanine aminotransferase (ALT) concentrations using a Cobas 6000 IT-MW machine (Roche Diagnostics Gmbh) and corresponding reagents (CREP2, REF 03263991 for CREAT; ALTLP, REF 04467388 for ALT). Tartu University Hospital conducted these measurements. After blood collection, heart tissues were removed from the treated mice, frozen at -80 °C, and used for subsequent histological analyses, as described below.

4.7.8. H&E stainings (III)

Paraffin-embedded tissue sections (2 µm) were stained using an ST 5020 device with the "Ready-to-Use hematoxylin and eosin (H&E) Staining System Leica ST Infinity" kit. The protocol included xylene treatment (3 times for 2 min, once for 1 min), dehydration with absolute and 80 % ethanol (1 min each), and sequential staining steps with specific durations. After staining, the sections were dehydrated (30 s, 30 s, 2 min), and xylene was cleared (2 times for 2 min). Stained heart sections were scanned using a Leica SCN400 slide scanner (20× objective lens), and the ImageScope x64 program was used for analysis. The Pathology Department of Tartu University Hospital conducted the H&E staining.

4.7.9. Statistical analyses (I, II, III)

GraphPad Prism (version 10) was used for all other statistical analyses, including Student's t-test, one-way analysis of variance (ANOVA), Fisher's LSD (Least Significant Difference), Kaplan–Meier survival curve plotting, and Gehan-Breslow-Wilcoxon test. A significance threshold of 0.05 was applied. The IC50 was determined using the log(inhibitor) versus response-variable slope (4 parameters) model in the same program.

5. RESULTS

5.1. Development of TPP-NSVs for effective internalization and DOX delivery to cancer cells

5.1.1. Functionalization of NSVs with RPAR and their characterization

Publication I

The aim of this research was to study the suitability and targeting effects of TPP in NSVs nanoplatforms to enhance the delivery and cytotoxicity of encapsulated DOX in receptor-positive cancer cells *in vitro*.

For that, we first synthesized NSVs targeted or not targeted with the RPAR peptide (RPAR-NSVs and NSVs) (Fig. 7). RPAR, with the sequence RPARPAR, is a prototypic CendR peptide capable of binding to and being internalized by cells that overexpress NRP-1 (Kadonosono et al., 2015; H. B. Pang et al., 2014; Teesalu et al., 2009). DLS showed that the average hydrodynamic diameters of RPAR-NSVs and non-targeted NSVs were approximately 155 and 121 nm, respectively (Fig. 7A). This size difference is likely due to RPAR peptide conjugation, which introduces an additional aqueous layer on the surface of the NPs (d'Avanzo et al., 2021). In addition, a positively charged RPAR peptide slightly increased the surface charge of NSVs from -47 to -37 mV. The low PDI values of <2 for both NSV samples indicate their homogenous and narrow size distribution, essential for the consistent and reproducible release of payloads over time (Danaei et al., 2018). TEM images confirmed the presence of homogenous spherical NPs (Fig. 7B), indicating that peptide conjugation did not alter the structures of the prepared NSVs.

A

Sample name	**RPAR-NSVs**	**NSVs**	**RPAR-DOX-NSVs**	**DOX-NSVs**
Size (nm)	155 ± 8	121 ± 5	164 ± 4	128 ± 7
Zeta potential (mV)	-37 ± 2	-47 ± 3.5	-38.7 ± 1.7	-45.3 ± 2.1
PDI	0.163 ± 0.01	0.145 ± 0.007	0.184 ± 0.009	0.158 ± 0.011
DOX EE (%)	-	-	44.2 ± 1.7	40.5 ± 2.6

B

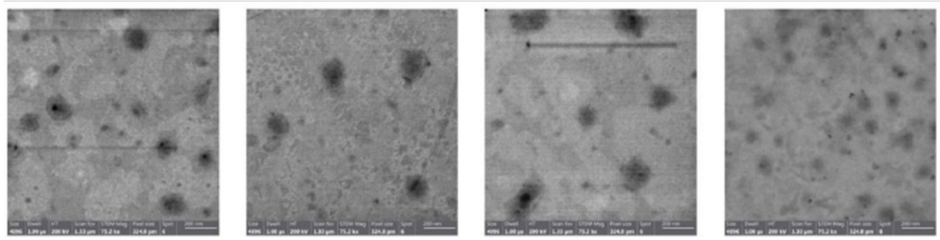

NSVs DOX-NSVs RPAR-NSVs RPAR-DOX-NSVs

C

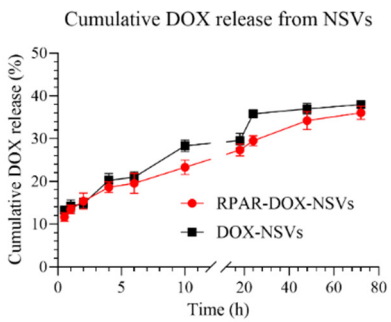

D

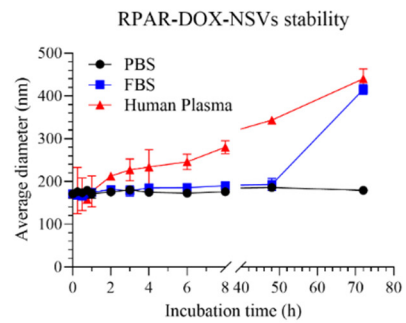

Figure 7. Physicochemical characterization and stability of niosomes (NSVs). (A) Physicochemical parameters, including average size (nm), zeta potential (mV), polydispersity index (PDI), and DOX encapsulation efficiency (EE %) with ± standard error of the mean (SEM) are presented for the prepared NSVs. (B) Transmission electron microscopy (TEM) images of NSVs, scale bar = 200 nm. (C) Cumulative DOX release profile from RPAR-DOX-NSVs and DOX-NSVs incubated in HEPES buffer (pH 7.4). (D) The stability of RPAR-DOX-NSVs was evaluated by assessing the change in average size (nm) in HEPES buffer, fetal bovine serum (FBS) (10 % v/v), and human plasma (50 % v/v) over 72 hours. n=3; error bars indicate ± SEM.

5.1.2. RPAR-NSVs selectively bind to their target protein NRP-1

Next, we tested the binding capabilities of the RPAR-targeted NSVs in different settings. First, we assessed the interaction between RPAR-NSVs and their respective receptor NRP-1 or mutant NRP-1 with an inactive CendR-binding pocket (mutNRP-1) in a cell-free system. In addition, we used NSVs targeted with scrambled RPAR peptide (scrRPAR-NSVs) as it lacks the required CendR motif for NRP-1 binding to serve as a negative control. As shown in Fig. 8A, RPAR-NSVs showed significantly higher binding to NRP-1-coated beads with an active CendR-binding pocket, whereas minor binding was observed with mutNRP-1-coated beads. Similarly, scrRPAR-NSVs showed negligible binding to both NRP-1 and mutNRP-1-coated beads, confirming the necessity of interaction between the CendR motif in the peptide and an active CendR-binding pocket in NRP-1 for binding. Additionally, the results demonstrate that RPAR on NSVs interacts with the CendR-binding pocket of the b1 domain of NRP-1, indicating that the peptide coated on NSVs is accessible for receptor interactions.

5.1.3. RPAR-NSVs selectively bind to cultured NRP-1$^+$ cells in a receptor-dependent manner

To test the cellular uptake of RPAR-NSVs, we used NRP-1 positive prostate (PPC-1) and NRP-1 negative human melanoma cancer cells (M21). PPC-1, known for NRP-1 overexpression (d'Avanzo et al., 2024; Simón-Gracia et al., 2021), showed significant RPAR-NSV uptake (approximately 100 % FAM-positive cells), whereas uptake of scrRPAR-NSVs was minimal (< 10 % FAM-positive cells) after 1 hour of incubation (Fig. 8C). Conversely, M21 cells exhibited similar uptake of both RPAR-NSVs and scrRPAR-NSVs, but much lower than that of PPC-1 cells (Fig. 8D), thus confirming that the peptide delivered and promoted receptor-specific uptake of RPAR-NSVs in PPC-1 cells.

In agreement with the FC data, confocal microscopy showed increasing intracellular fluorescence with increasing RPAR-NSV concentrations, indicating successful internalization at the lowest RPAR-NSV concentration of 0.25 mg/mL of lipid. Similarly, no uptake was observed in NRP-1-negative M21 cells treated with RPAR-NSVs or scrRPAR-NSVs (Fig. 8E), again emphasizing the critical role of the CendR motif in targeting NRP-1. To further verify that RPAR-NSV uptake was NRP-1-dependent, PPC-1 cells were first pretreated with monoclonal ABs specific to the NRP-1 b1 domain, either CendR-binding pocket blocking (mAb7E8) or non-blocking (mAB3E7) (Daly et al., 2020). Pre-incubation with CendR-blocking mAb7E8 at concentrations of 0.01 and 0.02 mg/mL resulted in less than 10 % intracellular uptake of RPAR-NSVs in NRP-1 positive PPC-1 cells (Fig. 8B). In contrast, pre-incubation with the same concentrations of non-blocking mAB3E7 AB resulted in approximately 80 % of treated cells internalization of RPAR-NSVs (Fig. 8B). These findings were consistent with those of FC (Fig. 8C), and confocal imaging (Fig. 8E) data, confirming the selectivity

of RPAR-NSVs for NRP-1 and their targeted uptake by cancer cells over-expressing the NRP-1 receptor on their surface.

These findings highlight the potential of RPAR-NSVs as a targeted drug delivery platform that offers selective binding and internalization in NRP-1 over-expressing cancer cells.

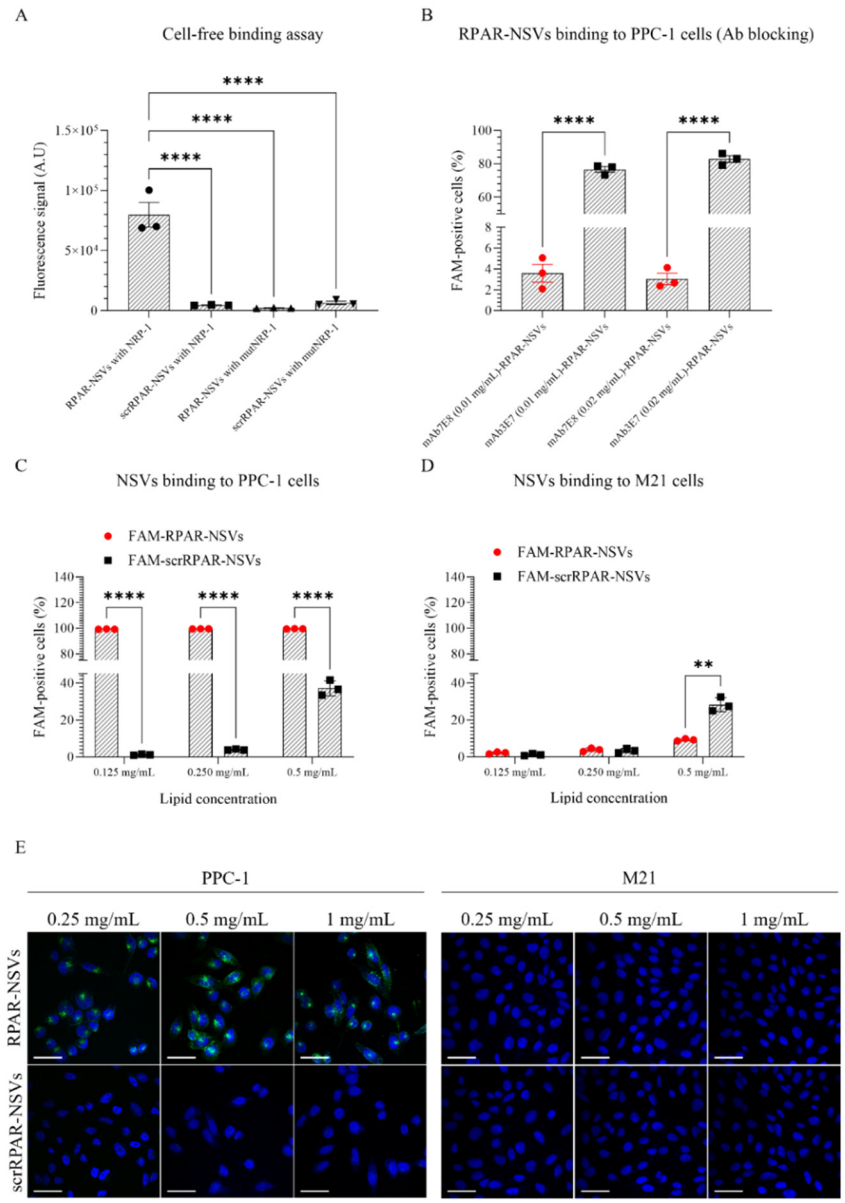

Figure 8. Evaluation of RPAR-NSV selectivity towards NRP-1 in cell-free and cell binding assays. (A) The cell-free binding assay showed significantly higher binding of

FAM-RPAR-NSVs to magnetic beads coated with NRP-1 than mutNRP-1. Quantification of RPAR-NSVs or scrRPAR-NSVs binding to NRP-1 was performed by flow cytometry (FC) after 1 hour of incubation. n=3; statistical analyses were performed using ANOVA; error bars indicate ± SEM; ****p<0.0001. (B) Uptake of RPAR-NSVs by NRP-1 positive PPC-1 cells. Cells were pretreated with an anti-NRP-1 AB blocking the CendR-binding pocket (mAb7E8) or non-blocking AB (mAb7E7) and incubated with RPAR-NSVs for 1 hour. Results, as the percentage of FAM-positive cells show significantly reduced intracellular RPAR-NSVs uptake in the presence of blocking mAb7E8 (0.01 and 0.02 mg/mL) compared to non-blocking mAb7E7. RPAR-specific internalization of RPAR-NSVs in PPC-1 (C) and M21 (D) cells treated with different lipid concentrations after 1 hour of incubation. Uptake was quantified by FC, and the results are represented as FAM-positive cells. n=3, Statistical analyses were performed using Student's t-test, error bars indicate ± SEM, **p<0.01, ****p<0.0001. (E) Representative confocal microscopy images of RPAR-NSV intracellular uptake by PPC-1 cells, but not by NRP-1-negative M21 cells, at 3 different NSV concentrations (0.25, 0.5, and 1 mg/mL). The cells were incubated with RPAR-NSVs or scrRPAR-NSVs for 1 hour. FAM (green), DAPI (blue). Scale bar = 50 μm.

5.1.4. Characterization and stability of RPAR-DOX-NSVs

To evaluate the potential of the RPAR-NSV platform for effective DOX loading and targeted delivery to cancer cells, we synthesized RPAR-DOX-NSVs and non-targeted DOX-NSVs. The physicochemical features of these formulations closely resembled those of their drug-free counterparts (RPAR-NSVs and NSVs), suggesting that DOX encapsulation did not disrupt the NSV structure (Fig. 7). Furthermore, DOX loading had negligible effects on the PDI, indicating a stable and narrowly distributed nanocarrier size during drug loading. This characteristic is essential for consistent and reliable payload release over time, addressing the storage challenges associated with liposomal DOX (Barenholz, 2012).

The DOX loading process was similar to that used for the synthesis of Doxil®/Caelyx® using the remote loading and pH gradient method. The EE % of DOX in RPAR-NSVs was approximately 41 %, and non-targeted DOX-NSVs showed a comparable loading of approximately 44 %. In neutral pH conditions, the cumulative release of DOX from the RPAR-NSVs and NSVs reached approximately 40 % after 72 hours (Fig. 7C). Importantly, the presence of the RPAR peptide on the NSV surfaces did not affect DOX release, as evidenced by the almost identical kinetic release profiles (Fig. 7C).

A protein corona can form when nanocarriers encounter biological fluids, altering their *in vivo* behavior and stability (Bashiri et al., n.d.; Gref et al., 2000). To assess this phenomenon, RPAR-DOX-NSVs were incubated with FBS and human plasma to simulate *in vitro* and *in vivo* conditions. During the first incubation hours, FBS induced minimal changes in particle size, while human plasma led to a slight increase (Fig. 7D). As incubation progressed (up to 72 hours), both FBS and human plasma substantially enlarged the particles, reaching approximately 420 nm.

These observations underscore the dynamic nature of the protein corona and its impact on nanocarrier stability in biological environments.

5.1.5. Cytotoxicity of RPAR-DOX-NSVs

Next, we tested the impact of RPAR-DOX-NSVs, non-targeted DOX-NSVs, and free DOX on NRP-1 positive PPC-1, 22Rv1, and NRP-1 negative M21 cell viability. The cells were treated for 1 hour with DOX-NSVs or free DOX at concentrations of 0.1, 0.5, 1, 5, and 10 μM, washed, and further incubated for 24 hours. In cytotoxicity assessments, RPAR-DOX-NSVs showed enhanced efficacy in NRP-1 positive PPC-1 cells, with a dose-dependent reduction in cell viability reaching approximately 55 % at 5 μM DOX (Fig 9A). This effect plateaued at higher concentrations, indicating possible CendR-binding site saturation. In addition, at a 10 μM concentration, RPAR-DOX-NSVs showed significantly higher potency than non-targeted DOX-NSVs in another NRP-1 positive cell line, 22Rv1 (Fig. 9C), thus broadening the applicability of tumor-specific peptide-mediated drug delivery. These results demonstrated that this potent anticancer effect was possible because of the specific targeting facilitated by the RPAR peptide. The greater cytotoxicity of free DOX in 22Rv1 cells compared to both RPAR-DOX-NSVs and DOX-NSVs (Fig. 9C) could be attributed to the higher sensitivity of cells to DOX relative to PPC-1 cells. Notably, the selectivity of RPAR-DOX-NSVs was further highlighted by their minimal impact on NRP-1 negative M21 cells viability (Fig. 9B). The observed cytotoxicity trends were consistent with those of the binding studies (Fig. 8), demonstrating the potential of RPAR-NSVs for specific and effective anthracycline delivery.

The comprehensive evaluation of RPAR-NSVs presented in this chapter supports their potential as a targeted drug delivery platform for hydrophilic anthracyclines, such as DOX, offering selective binding, efficient internalization, and controlled release in NRP-1 overexpressing cancer cells.

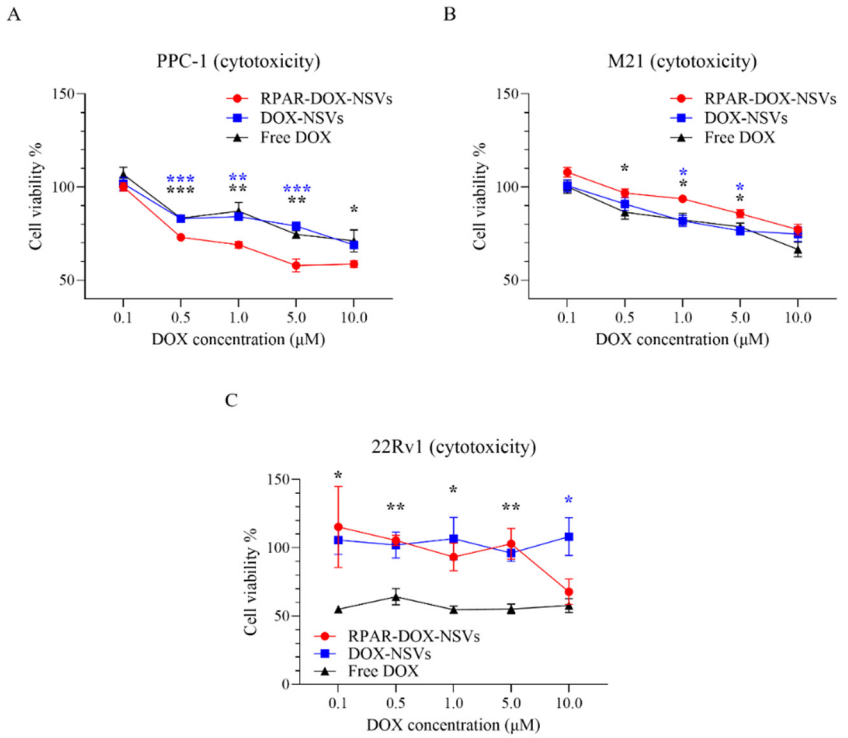

Figure 9. *In vitro* cytotoxic effects of NSVs on (A) PPC-1, (B) M21, and (C) 22Rv1 cells. The cytotoxicity of RPAR-DOX-NSVs, DOX-NSVs, and free DOX treatment (1 hour) was tested at different DOX concentrations (0.1, 0.5, 1, 5, and 10 μM). After incubation, the cells were washed to remove non-bound particles and cultured in a fresh medium for 24 hours. The non-treated cells served as a negative control (100 % viability). n=3; statistical analyses were performed using ANOVA; error bars indicate ± SEM, *p<0.05, **p<0.01, ***p<0.001, ****p<0.0001. Each asterisk corresponds to a representative sample, with the color of the asterisk matching the color of the sample it indicates. This color representation highlights the significance and depicts the difference between the RPAR-DOX-NSVs and their respective formulations.

5.2. UTO preclinical development as a nanocarrier payload for effective drug delivery *in vitro* and tumor homing *in vivo*

5.2.1. UTO is more potent than DOX in a panel of cultured cancer cells

Publication II

The study aimed to assess whether UTO is a more effective anthracycline than DOX across various cancer cell lines, thereby supporting the rationale for using advanced anthracyclines. It also investigated the potential of functionalizing PS with CendR peptides and further improving their targeting effects through peptide valency modulation. The goal was to develop a targeted delivery system for UTO to reduce cancer cell viability by optimizing its delivery and sequentially enhancing its anticancer efficacy.

To test the potency of UTO, we conducted comparative studies on its impact alongside DOX treatments on the viability of diverse cultured cell lines, including U937 monoblast-like human histiocytic lymphoma cells, Jurkat E6.1 human T-lymphocyte acute T-cell leukemia cells, A549 human lung carcinoma cells, and HT-29 human colorectal adenocarcinoma cells. Cytotoxicity was examined after 30 and 90 min of drug incubation, followed by a 24 hours culture for U937 and Jurkat E6.1 cells (in suspension) or a 72 hours culture for adherent A549 and HT-29 cells. As depicted in Fig. 10, UTO consistently demonstrated a more potent effect in reducing cell viability across all tested cell lines than DOX. Notably, the most significant disparity in half-maximal inhibitory concentration (IC50) values between UTO and DOX was observed for A549 cells, with UTO being approximately 16-fold more effective, whereas the most negligible difference was noted for HT-29 cells, with UTO being approximately 2-fold more effective.

These findings underscore the superior cytotoxic potency of UTO compared to DOX across a spectrum of cell lines.

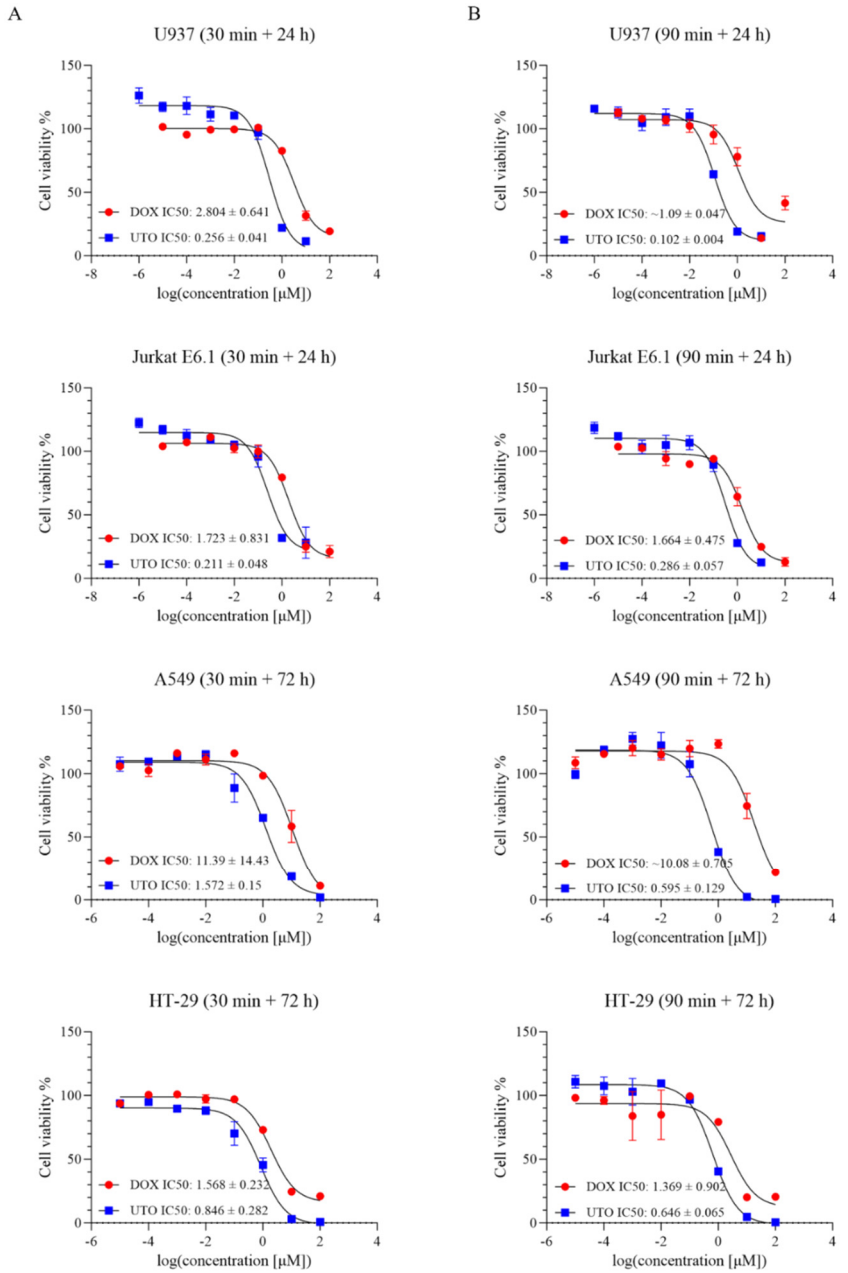

Figure 10. UTO cytotoxicity in cultured cancer cell lines. Viability of cancer cells incubated with the indicated concentrations of UTO and DOX for 30 (A) or 90 (B) min, followed by chase in a drug-free medium. IC50 (half-maximal inhibitory concentration in µM) was determined using a log(inhibitor) versus response–variable slope (4 parameters) model (GraphPad software (version 10.1.0). The SEM of IC50 is shown. The cells were incubated with anthracyclines, washed, and cultured for 24 hours (U937 and Jurkat E6.1 cells in suspension) or 72 hours (adherent A549 and HT-29 cells), followed

by the MTS viability assay. As controls, 1 % water or 1 % DMSO (solvents used to dissolve DOX and UTO, respectively) v/v in a cell culture medium was used. The MTS assay results were plotted as a curve of the percentage of viable cells (taking the viability of the non-treated control cells as 100 %) versus the log concentration of the tested sample. Error bars represent the ± SEM, n=3.

5.2.2. Enhancing PS targeting through peptide density optimization

To encapsulate the hydrophobic anthracycline prodrug UTO, we opted for PS because of their thicker hydrophobic membrane, allowing them to encapsulate larger quantities of hydrophobic drugs than NSVs or liposomes (Bermudez et al., 2002; Meng & Zhong, 2011). In addition, polymeric nanoplatforms offer higher synthetic freedom, which allows particles to be tailored for specific needs, especially when modifying their surfaces.

Optimizing ligand density on NP surfaces enhances cell targeting, with applications ranging from cell tracking to improved drug delivery (Fakhari et al., 2011; Kawano & Maitani, 2011). Despite limited data on the optimal ligand density, certain studies have identified optimal densities for specific NPs and targeting ligands, resulting in substantial enhancements in the target cell binding (Elias et al., 2013). Therefore, we optimized the RPAR peptide density on the PS surfaces for the best cellular uptake of our TPP-targeted DDS. Different RPAR peptide densities were achieved using various concentrations of Mal-PEG-PCL (0, 2, 5, 10, and 20 %) relative to the total copolymer, where peptide conjugation relies on thioether bond formation between the thiol group of the peptide cysteine and maleimide group of the copolymer (Simón-Gracia et al., 2018). Therefore, the number of surface maleimide groups determined the peptide density on the PS surface.

As shown in Fig. 11A and D (upper row), all PS samples contained uniform spherical polymeric vesicles of similar size. The hydrodynamic diameter and size distribution remained consistent across various PS samples (Fig. 11A and B). The average PS diameter was approximately 105 nm with a PDI of approximately 0.19 (Figure 11A and B). Similar to that observed with NSVs, the size of PS observed by TEM in Fig. 11D appeared to be smaller than 100 nm, which could be attributed to the measurement of dry PS, whereas DLS provided the diameter of solvated particles influenced by water molecules.

The binding of PS bearing different densities of RPAR on their surface was tested in an established *in vitro* system using PPC-1 and M21 cells. These cell lines were exposed to different RPAR-FAM-PS samples for 1 hour and FC was used to assess cell binding and internalization. As shown in Fig. 11C, specific binding to PPC-1 cells increased with higher peptide density on PS, with 20 % RPAR showing the highest uptake (approximately 100 % of cells were FAM-positive). In M21 cells, binding remained consistently low, irrespective of peptide density (Fig. 11C), confirming the significance of peptide-receptor interactions in cell binding and internalization.

A

Sample name	0 % Mal-PEG-PCL	2 % Mal-PEG-PCL	5 % Mal-PEG-PCL	10 % Mal-PEG-PCL	20 % Mal-PEG-PCL
Size (nm)	95 ± 47	105 ± 59	99 ± 50	108 ± 54	117 ± 70
Zeta potential (mV)	-1.5	-4.8	-4.0	-4.0	-2.4
PDI	0.186	0.214	0.194	0.171	0.188

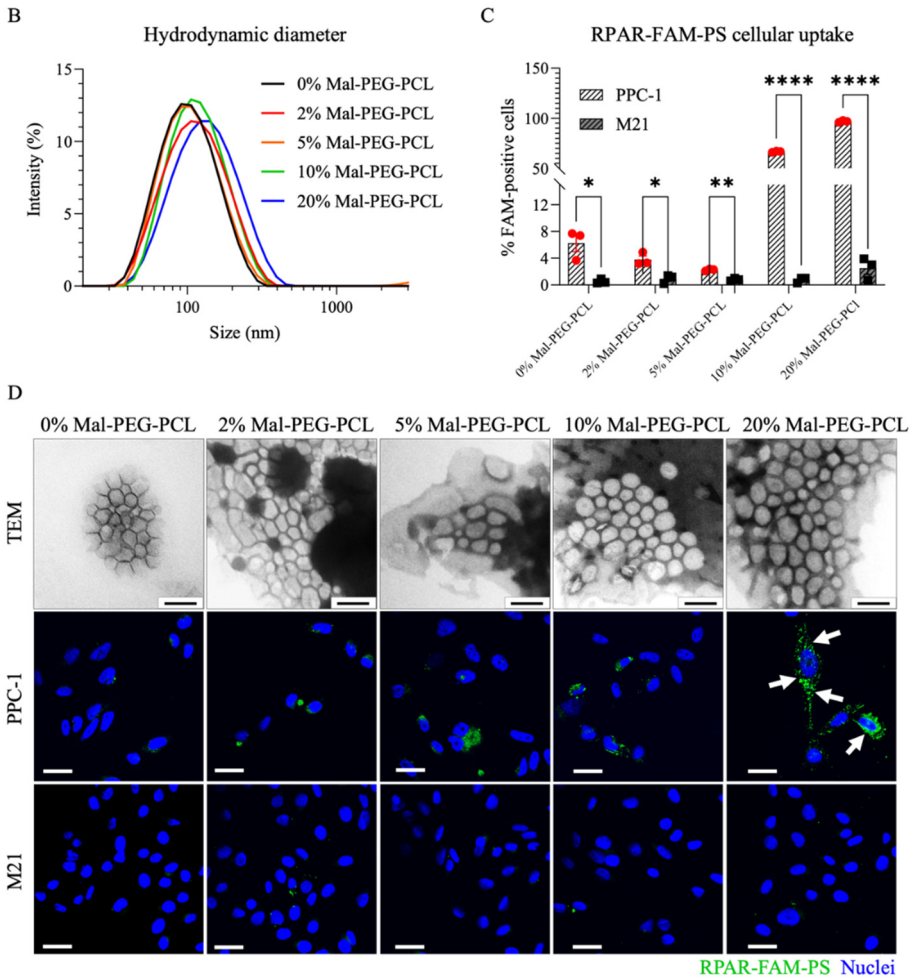

Figure 11. Optimization of peptide functionalization for peptide-guided delivery of PS. (A) Characterization of PS over a range of maleimide-PEG-PCL (Mal-PEG-PCL) percentages (0, 2, 5, 10, and 20 %) by assessing the average size, PDI, and Z-potential of the prepared PS formulations with ± SEM are presented. (B) The size distribution of prepared PS formulations was assessed using dynamic light scattering (DLS). (C) Binding of RPAR-FAM-PS to cultured PPC-1 and M21 cells. The attached cells were incubated with PS samples for 1 hour, washed, and detached, and FC was used to quantify the

binding of RPAR-FAM-PS to PPC-1 (NRP-1^{+}) and M21 (NRP1^{-}) cells. PS were prepared to incorporate the indicated percentages of Mal-PEG-PCL. The graph represents the percentage of FAM-positive cells. Non-treated cells served as controls. Statistical analyses were performed using the Student's t-test; n=3; error bars indicate ± SEM. (D) TEM images of the prepared PS formulations are shown in the upper panel; scale bar = 100 nm. The lower panel presents fluorescence confocal microscopy images of attached PPC-1 and M21 cells incubated with RPAR-FAM-PS samples for 1 hour. The PS were labeled with FAM (green signal), and the nuclei were stained with DAPI (blue signal). Scale bar = 50 mm.

The uptake of RPAR-FAM-PS by PPC-1 and M21 cells was further evaluated using fluorescence confocal microscopy. After 1 hour of incubation, the green signal of RPAR-FAM-PS was exclusively detected in the PPC-1 cells, with no observable uptake in the M21 cells (Fig. 11D). Consistent with the FC results, a significantly higher RPAR-FAM-PS signal was observed in PPC-1 cells when PS contained 20 % Mal-PEG-PCL. Moreover, RPAR-FAM-PS was predominantly located in the vesicular structures within the cytoplasm of PPC-1 cells, indicating effective cellular uptake.

Consequently, the PS were functionalized with 20 % peptide for further experiments.

5.2.3. DOX and UTO encapsulation into TPP-PS

Simultaneously with UTO encapsulation into the PS, we explored the encapsulation of DOX for comparative purposes within our PS. DLS measurements of RPAR-targeted and non-targeted DOX-PS indicated a similar size for both samples, with an average diameter of approximately 97 nm and a PDI of approx. 0.16 (Fig. 12 A and C). The DOX EE % was approximately 7 % (Fig. 12A).

For UTO-PS, the morphology observed by TEM (Fig. 12B) and the hydrodynamic diameter of UTO-loaded RPAR-functionalized PS (RPAR-UTO-PS), UTO-loaded non-targeted PS (UTO-PS), and non-loaded "empty" PS (PS) were similar (Fig. 12B). The zeta potential of PS was neutral, and the UTO EE % of approximately 80 % was significantly higher than the approximately 7 % observed for hydrophilic DOX (Fig. 12A).

We further investigated the drug release profiles of DOX-PS and UTO-PS over 72 hours at 37 °C. Fig. 12D illustrates that the drugs were well retained in the PS, considering the chemical properties of the encapsulated drug. UTO release consistently remained lower than DOX release, with less than 2 % of UTO released from the PS compared to a 10 % release from DOX-PS (Fig. 12D) at the 48 hour time point.

Considering the drug EE and release results, our findings demonstrated that PS are more suitable for encapsulating hydrophobic drugs such as UTO, and NSVs are more suitable for encapsulating hydrophilic drugs such as DOX.

A

	RPAR-UTO-PS	UTO-PS	PS	RPAR-DOX-PS	DOX-PS
Size (nm)	111 ± 62	87 ± 37	102 ± 34	89 ± 32	75 ± 20
Zeta potential (mV)	0.6	-1.1	-2.1	0.1	
PDI	0.211	0.155	0.092	0.179	0.139
Drug EE %	94	81	-	6	8

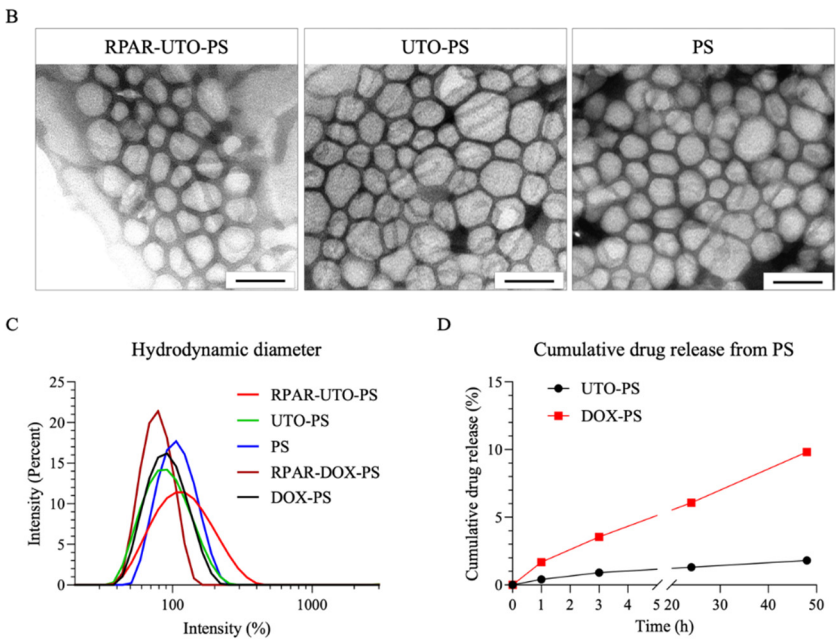

Figure 12. Physicochemical characterization and stability of different polymersome (PS) formulations. (A) Physicochemical parameters, including average size (nm), zeta potential (mV), polydispersity index (PDI), and DOX or UTO encapsulation efficiency (%) with ± SEM, are presented for the prepared PS. (B) TEM images of RPAR-UTO-PS, UTO-PS, and PS. Scale bar = 100 nm. (C) Size distribution of the prepared PS formulations, as assessed by DLS. (D) Cumulative DOX and UTO release profiles from DOX-PS and UTO-PS incubated in a PBS buffer (pH 7.4) over 48 hours.

5.2.4. RPAR-UTO-PS are more toxic in receptor-positive cancer cells

After optimizing the TPP-targeted PS nanoplatform for effective drug delivery to receptor-positive cancer cells, we conducted a comparative assessment of the effects of free UTO, free DOX, and RPAR-guided versus control UTO-PS on the viability of PPC-1 and M21 cells. The cells were treated for 30 min, followed by a 48 hours incubation in a fresh culture medium and an MTT viability assay. As expected, free UTO exhibited higher toxicity than free DOX in both cell lines (Fig. 13). The cytotoxic effect of UTO-PS on cultured cells depended on both targeting peptide functionalization and expression of the peptide receptor NRP-1. RPAR-UTO-PS (at 2 μM of UTO) demonstrated a significantly potentiated antiproliferative effect compared to non-targeted UTO-PS at the same drug loading (approximately 40 % vs. 70 % cell viability; Fig. 13A).

Therefore, our optimized TPP-PS platform efficiently delivers the more potent prodrug UTO to cancer cells, exhibiting higher efficacy in receptor-positive cancer cells compared to free DOX in a peptide-dependent manner.

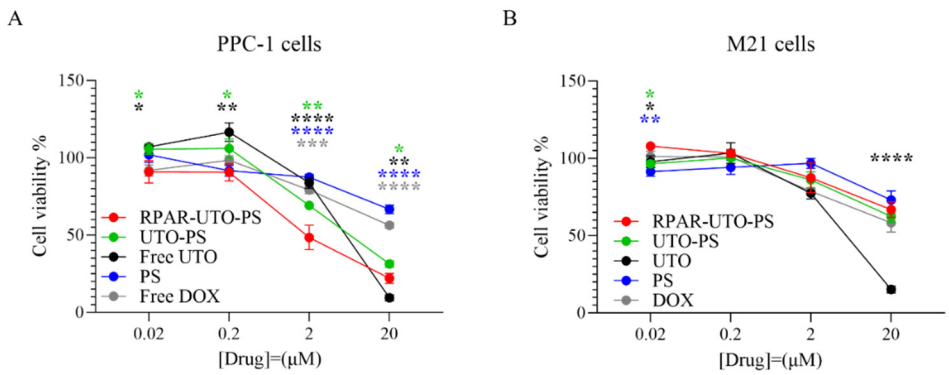

Figure 13. Effect of free and nano-encapsulated UTO (UTO-PS) on the viability of cultured cancer cells with different NRP-1 expression status. Percentage of viable PPC-1 (A) and M21 (B) cells after 30 min incubation with PS formulations at 0.02, 0.2, 2, and 20 μM of UTO and 48 hour follow-up incubation. Statistical analyses were performed using ANOVA; error bars indicate ± SEM; n=4, *p<0.05, **p<0.01, ***p<0.001, ****p<0.0001. Asterisks indicate significance when comparing RPAR-UTO-PS with the other formulations. Each asterisk corresponds to a representative sample, with the color of the asterisk matching the color of the sample it indicates.

5.2.5. TPP-PS home to orthotopic breast tumors *in vivo*

To evaluate TPP-PS tumor-targeting capabilities *in vivo*, LinTT1- or RPAR-targeted and non-targeted PS labeled with near-infrared DiR dye (LinTT1-DiR-PS, RPAR-DiR-PS, and DiR-PS) were used in orthotopic TNBC breast tumor-bearing mice. As shown in Fig. 14A-C, spherical nanovesicles with an average size of 116 nm were obtained. The encapsulation of hydrophobic DiR dye mimicking UTO's hydrophobic nature did not affect the PS structure, as the physicochemical parameters were similar to those of the previously synthesized PS samples (Fig. 11 and 12).

MCF10CA1a, a TNBC cancer cell line, overexpresses p32 protein on its surface, making it a suitable target for the LinTT1 CendR peptide (Agemy et al., 2013; Santner et al., 2001; S. Sharma, Kotamraju, et al., 2017; Simón-Gracia et al., 2018). LinTT1-DiR-PS, RPAR-DiR-PS, and DiR-PS were IV injected into mice with orthotopic MCF10CA1a breast tumors, and *in vivo* imaging was conducted at different time points. As shown in Fig. 14D, LinTT1 and RPAR functionalization enhanced tumor homing at early and late time points, whereas non-targeted DiR-PS became detectable only after 24 hours post-injection. The AUC in the tumor at 24 hours was approximately 40 % higher for LinTT1-DiR-PS than for non-targeted PS, and RPAR-DiR-PS also exhibited a higher AUC (approximately 26 % higher) (Fig. 14E). The observed high accumulation of both targeted and non-targeted PS in the liver, as indicated by arrowheads in Fig. 14D, can be attributed to the crucial role of RES organs, such as the liver and spleen, in the circulation of NPs (Longmire et al., 2008).

Tissue immunofluorescence microscopy analysis at 48 hours post-injection showed LinTT1-DiR-PS accumulation in the tumor parenchyma and colocalization with LinTT1's known receptors p32 and NRP-1 (Fig. 15A and C). LinTT1-DiR-PS also accumulated in M2 protumoral TAMs within the tumor (Fig. 15A, last column). Considering the known cardiotoxicity of free DOX, the presence of PS in the heart was also assessed. Notably, the heart showed a significantly lower LinTT1-DiR-PS signal than malignant tissue, indicating a potential reduction in cardiotoxicity (Fig 15A and B).

A

Sample name	DiR-PS	LinTT1-DiR-PS	RPAR-DiR-PS
Size (nm)	114 ± 41	111 ± 51	124 ± 61
Zeta potential (mV)	-1.0	-0.1	1.3
PDI	0.091	0.15	0.218

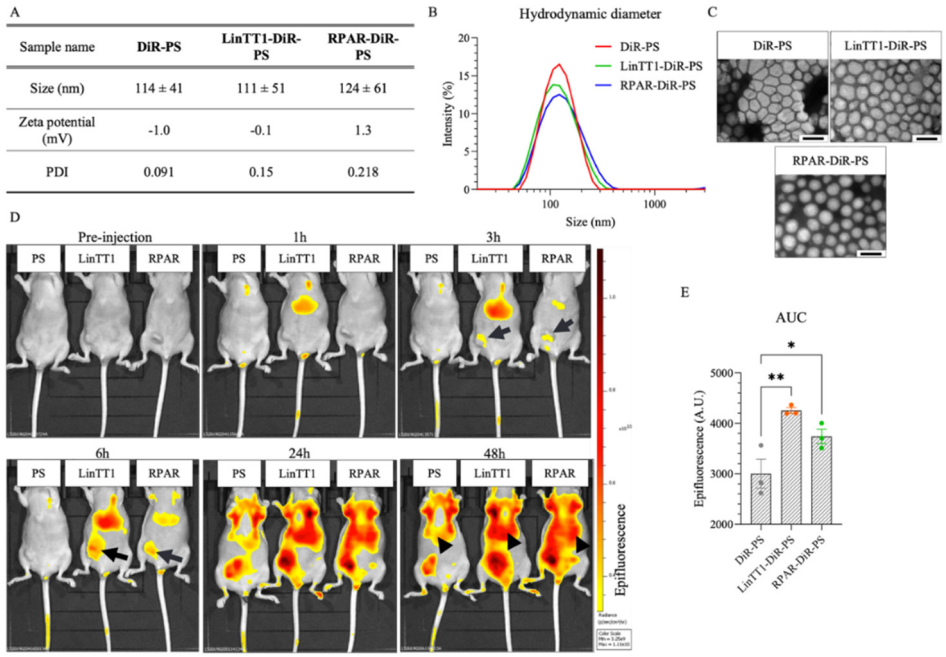

Figure 14. Systemic TPP-targeted PS home to orthotopic breast tumors. (A) Characterization of LinTT1-DiR-PS, RPAR-DiR-PS, and DiR-PS. The average size (nm), zeta potential (mV), and polydispersity index (PDI) were assessed for the prepared PS formulations. (B) The size distribution of the prepared PS formulations, as assessed by DLS with ± SEM, is presented. (C) TEM images of the prepared PS. Scale bar = 100 nm. (D) Live imaging of MCF10CA1a tumor-bearing mice injected with LinTT1-DiR-PS (LinTT1), RPAR-DiR-PS (RPAR), or non-targeted DiR-PS (PS) at the indicated time points after administration. The DiR-PS signal in the tumor is indicated by arrows and in the liver by arrowheads. (E) Area under the curve (AUC) in the tumors of LinTT1-DiR-PS, RPAR-DiR-PS, and DiR-PS up to 24 hours post-injection. n=3. Statistical analyses were performed using ANOVA; error bars indicate ± SEM. *p<0.05, **p<0.01.

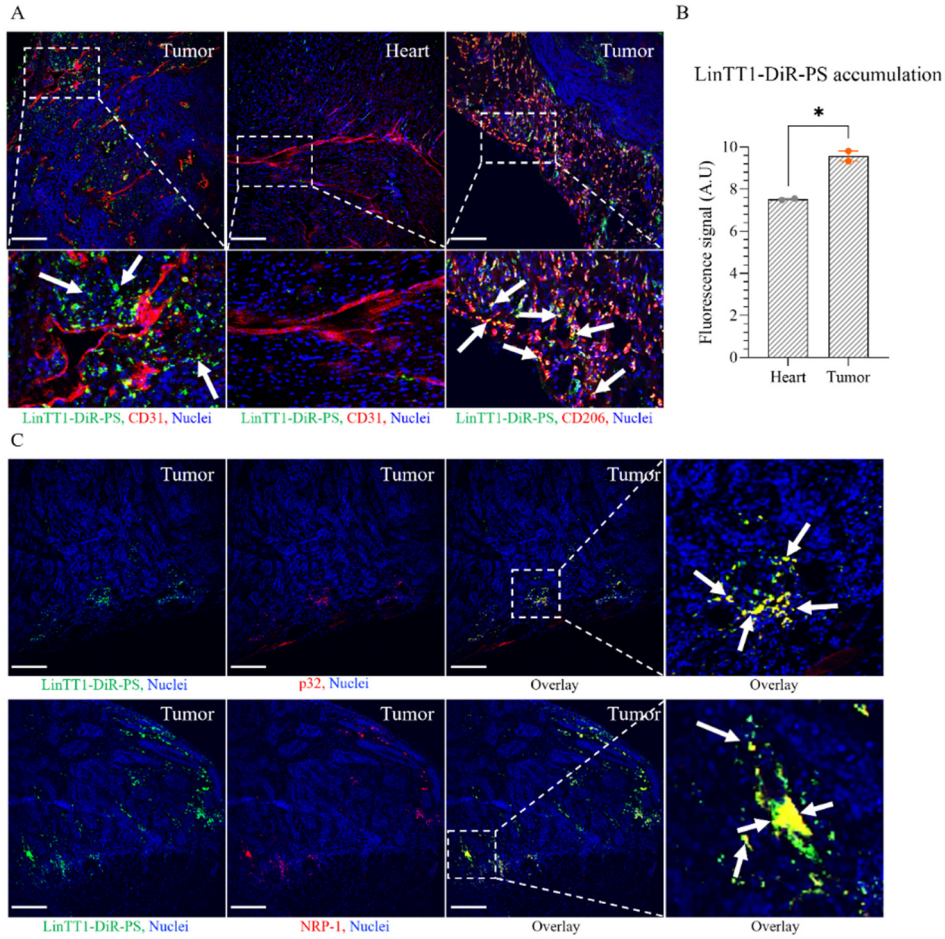

Figure 15. Tissue distribution of LinTT1-DiR-PS in MCF10CA1a tumor-bearing mice. (A) Confocal fluorescence imaging of the tumors and hearts of TNBC-bearing mice injected with LinTT1-DiR-PS. Tissues were extracted 48 hours post-injection of PS, sectioned, and immunostained for FAM, CD31, and CD206, and the nuclei were stained with DAPI. The green signal represents LinTT1-DiR-PS (FAM), the red signal represents blood vessels (CD31) or mannose receptor (CD206), and the blue signal represents nuclei (DAPI). Scale bar=200 µm. (B) LinTT1-DiR-PS signal quantification in the heart and tumor 48 hours post-injection, n=6 (different areas of the same section, n=2 mice per group). Statistical analyses were performed using the Student's t-test,*$p<0.05$. Error bars indicate ± SEM. (C) Colocalization of LinTT1-DiR-PS with NRP-1 or p32 proteins in the breast tumor tissues. The green signal represents LinTT1-DiR-PS (FAM), and the red represents NRP-1 or p32.

5.2.6. LinTT1-UTO-PS specifically deliver drug to breast tumors

After establishing the conditions for enhanced tumor accumulation of LinTT1-targeted PS, we investigated the ability of LinTT1-PS to precisely deliver UTO into breast tumors *in vivo*. LinTT1-targeted (LinTT1-UTO-PS) and non-targeted UTO-PS, as well as free DOX (as a surrogate for free UTO owing to its poor water solubility) (characteristics of prepared PS are shown in Fig. 16A and B) were injected IV into mice with orthotopic MCF10CA1a tumors. Figures 16C and D demonstrate an almost 10-fold higher tumor accumulation of UTO in mice injected with LinTT1-UTO-PS compared to other samples at 24 hour time point. The UTO signal colocalized with CD31-positive blood vessels, and with LinTT1-UTO-PS, some signal was observed in the perivascular space, suggesting drug extravasation into the tumor tissue (Figure 16C, inset). Importantly, no UTO signal was observed in the hearts of LinTT1-UTO-PS-treated mice (Figure 16C).

These observations suggest that encapsulating UTO in TPP-PS enhances the specific tumor accumulation of the drug.

A

Sample name	LinTT1-UTO-PS	UTO-PS
Size (nm)	79 ± 110	95 ± 109
Zeta potential (mV)	-6.5	-1.6
PDI	0.24	0.26

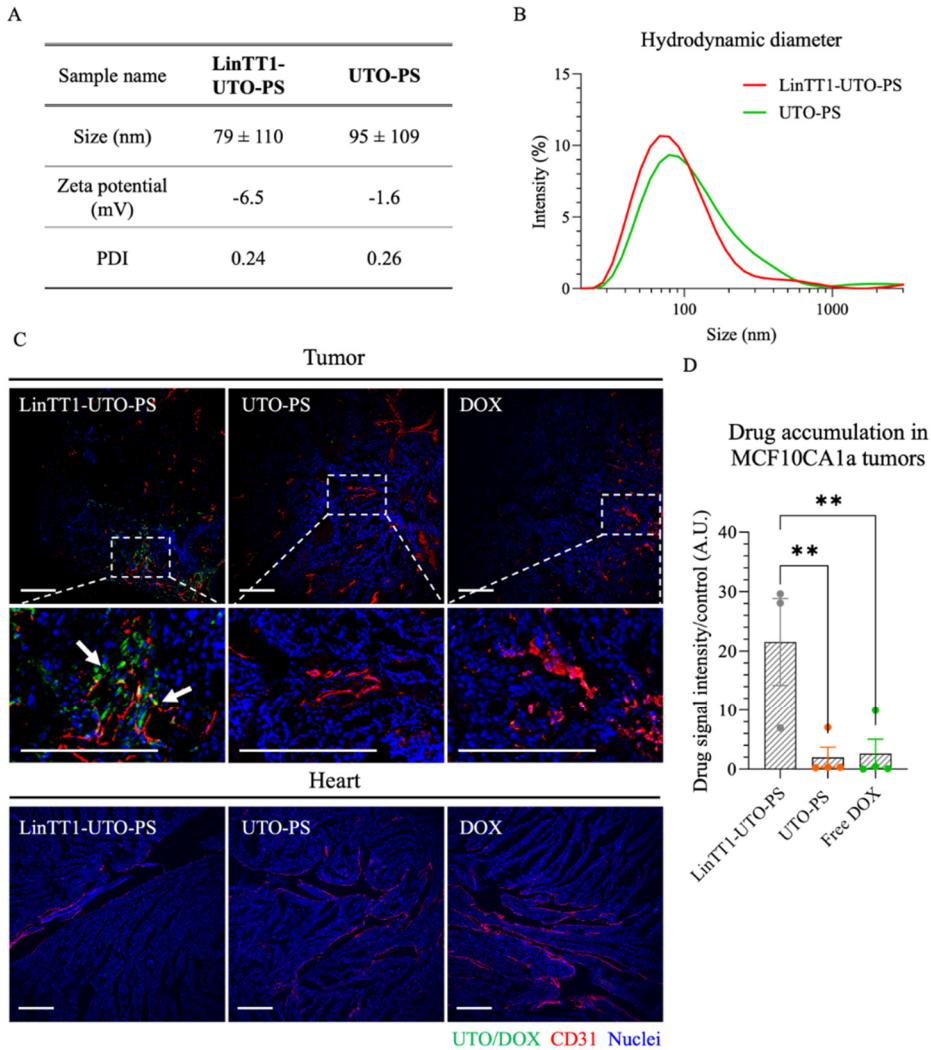

Figure 16. LinTT1-functionalized UTO-PS accumulated more than non-functionalized UTO-PS and free UTO in TNBC tumors but did not accumulate in the hearts of mice. (A) Characterization of LinTT1-UTO-PS and UTO-PS. The average size (nm), zeta potential (mV), and polydispersity index (PDI) with ± SEM were assessed for the prepared PS formulations. (B) Size distribution of the prepared PS formulations, as assessed by DLS. (C) Representative confocal fluorescence images of MCF10CA1a tumors and heart sections of mice injected with LinTT1-UTO-PS, UTO-PS, and free DOX. Samples were collected 24 hours post-injection, sectioned, immunostained for CD31, and stained with DAPI. Green: UTO or DOX; red: blood vessels (CD31); blue: nuclei (DAPI). Scale bar = 200 µm. (D) Quantification of the drug signal in tumors at 24 hours post-injection, normalized to the non-injected tumor. **p<0.001. Statistical analyses were performed using ANOVA. Error bars indicate ± SEM, n=3.

5.3. Evaluation of CA4P-induced molecular changes in TME for iRGD-enhanced secondary UTO-nanotherapy of peritoneal carcinomatosis

5.3.1. CA4P treatment enhances iRGD peptide receptor expression in breast and PC tumors

Publication III

This study aimed to test whether VDA-induced changes in the TME could sensitize tumors to targeted nanotherapy. Specifically, it evaluated the effect of VDA CA4P on iRGD peptide receptors, integrins, and NRP-1 in breast and peritoneal carcinomatosis (PC) xenografts. The primary goal was to determine if combining CA4P with UTO-PS and iRGD could enhance the efficacy and safety of PC treatment.

PC, the IP spread of cancer, poses a significant threat to patients with advanced abdominal neoplasms (Coccolini et al., 2013). IP administration of chemotherapeutics, including VDAs, has emerged as an effective treatment for PC (Harada et al., 2022; McCarty et al., 2004). Despite the pharmacokinetic advantages of the IP administration route, obstacles, such as IFP and ECM deposition, hinder drug penetration into peritoneal tumors (Carlier et al., 2017). Studies employing the iRGD peptide in combination with free DOX and PTX-PS have demonstrated enhanced intratumoral entry and therapeutic efficacy in PC lesions (Simón-Gracia, Hunt, Scodeller, Gaitzsch, Kotamraju, et al., 2016; Sugahara et al., 2015). These findings suggest that iRGD-based precision delivery strategies can amplify the therapeutic effect of IP cancer drugs and nanosystems. Moreover, investigations into treatment-resistant breast tumors have shown an overrepresentation of integrin-targeting RGD motifs when subjected to a vascular-disrupting nanosystem treatment (S. Sharma, Mann, et al., 2017). This discovery led us to explore whether VDA CA4P has the same impact on breast cancer models.

IP treatment with CA4P induced a molecular signature in tumor blood vessels, including significantly upregulated β3 integrins (2.4-fold increase) and NRP-1 (7.3-fold increase) in orthotopic MCF10CA1a tumors (Fig. 17). This upregulation indicated the potential for systemic iRGD-mediated targeting.

We next investigated whether such a phenomenon occurred in mice bearing the MKN45P PC model, known for its rapid abdominal dissemination (Miyagi et al., 2007). Consistent with the observations in TNBC breast tumors, IP CA4P treatment mildly upregulated the expression of αv integrins and NRP-1, particularly in the tumor periphery (Fig. 18). However, CA4P treatment did not affect the expression of p32 protein, a receptor for LyP-1 peptide (Laakkonen et al., 2002), and TT1/LinTT (Lin et al., 2014; Paasonen et al., 2016) TPPs.

These findings suggest that iRGD-based strategies can enhance the delivery of secondary therapeutics post-CA4P treatment.

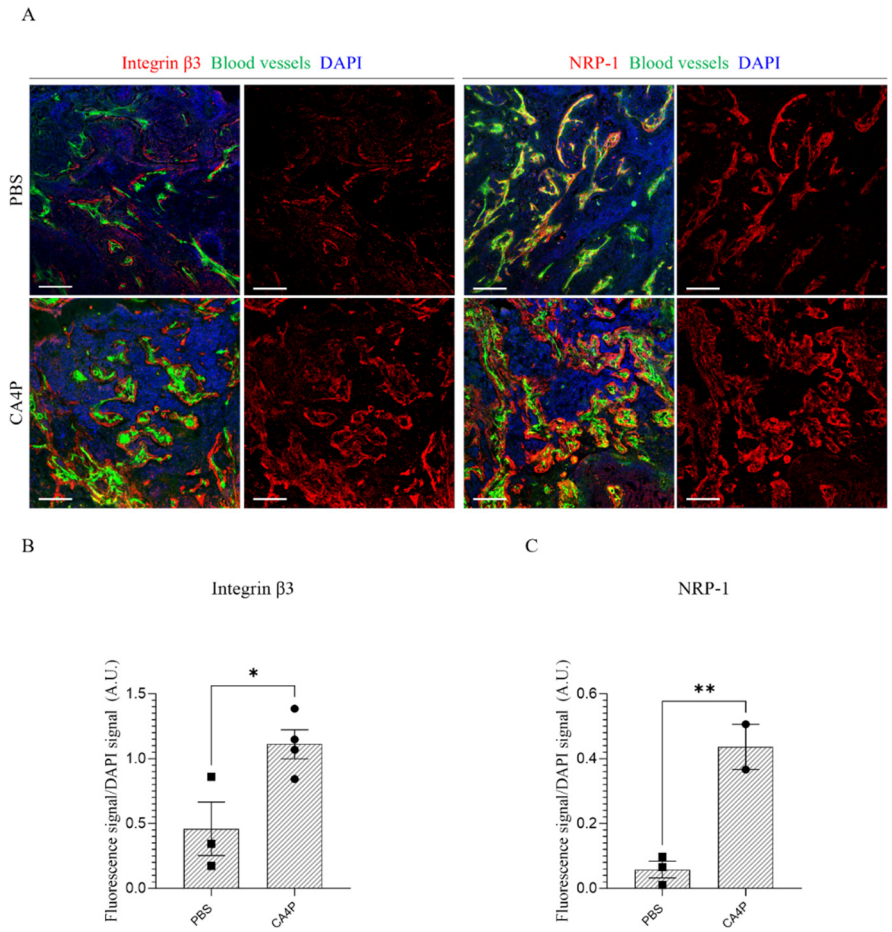

Figure 17. CA4P treatment upregulated the expression of β3 integrins and NRP-1 in MCF10CA1a breast tumors. (A) Representative confocal fluorescence images of tumors treated with CA4P or PBS. Tumors were collected on day 34 post-tumor induction, sectioned, and immunostained for the integrin β3 subunit, CD31/ CD105 (blood vessels), and NRP-1. The nuclei were counterstained with DAPI. Green, CD31 or CD105; red, integrin β3 or NRP-1; blue, nuclei (DAPI). Scale bar = 200 μm. Integrin β3 (B) and NRP-1 (C) fluorescence signals were normalized to the DAPI signal from the corresponding tumor sections and subsequently quantified. Statistical analysis was performed using the Student's t-test, *$p < 0.05$; **$p < 0.001$. Error bars: ± SEM; n=4 for the CA4P group quantification of integrin β3, n=2 for the quantification of NRP-1, and n=3 for the PBS group for both quantifications.

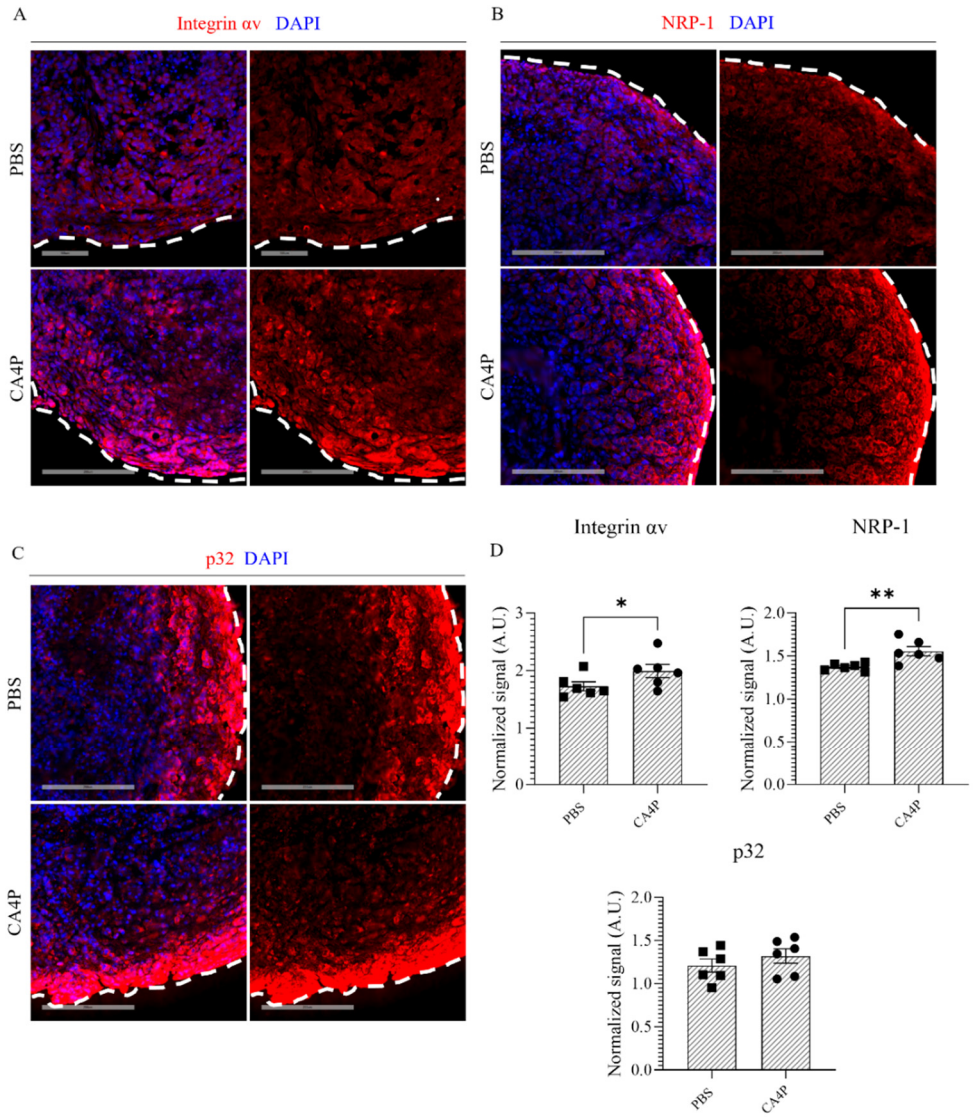

Figure 18. CA4P treatment upregulates the expression of αv integrins and NRP-1 in peritoneal tumors. MKN45P tumor-bearing mice were IP treated with CA4P (100 mg/kg, 7 IP injections every other day) and PBS, starting on day 7 after tumor induction. After treatment, the mice were perfused, and tumors were collected, sectioned, immunostained for (A) integrin αv subunit, (B) NRP-1, and (C) p32 (red), and counterstained with DAPI for the nuclei (blue). Scale bar = 200 µm, n=6. (D) Quantification of αv integrin, NRP-1, and p32 fluorescence signals normalized to the DAPI signal in CA4P treated and non-treated (PBS) tumors. Statistical analysis was performed using the Student's t-test; error bars indicate ± SEM; *p< 0.05, **p<0.01.

5.3.2. CA4P treatment sensitizes IP tumors to iRGD-potentiated nanoparticle delivery

Ongoing clinical development has explored iRGD's bystander effect as an adjunct to standard-of-care for pancreatic and other solid tumors (Buck et al., 2023; Dean et al., 2022). Our previous study showed that iRGD, when administered IP, enhances the accumulation and penetration of coinjected small-molecule drugs like DOX in PC tumors (Sugahara et al., 2015). We extended this to examine iRGD's impact on PS delivery to PC.

Using a mouse model of PC from MKN45P cells, we treated them with IP CA4P followed by IP injections of iRGD and FAM-labeled PS (FAM-PS; characterization is shown in Fig. 19A), alone or in combination. Biodistribution analyses after 6 hours demonstrated that after the coadministration of iRGD and FAM-PS, there was an approximately 2-fold increase in FAM-PS accumulation in PC lesions in mice pretreated with CA4P compared with other groups (Fig. 19B and C). In both CA4P-treated and control tumors, iRGD coadministration seemed to enhance tumor spreading of PS, as indicated by a diffuse signal in the tumor parenchyma (Fig. 19B). Notably, compared to the CA4P + FAM-PS group, mice treated with CA4P + iRGD + FAM-PS exhibited an approximately 3-fold increase in PS homing, emphasizing that iRGD enhances tumor accumulation and penetration of IP administered PS.

Quantification of the FAM-PS distribution in tumor tissue revealed that tumors treated with CA4P and targeted with iRGD exhibited the largest area of FAM-positive signal (Fig. 19D). This underscores the efficacy of sequential targeting, not only in facilitating a higher accumulation of potentially drug-loaded PS in the tumors but also in achieving a more even distribution of these particles within the tumor tissue. While VDAs are known to increase vascular permeability in tumors (Beauregard et al., 2001), the distribution of PS in CA4P-treated tumors without iRGD (CA4P + FAM-PS) was significantly lower than that in tumors injected with CA4P + iRGD + FAM-PS (30 % vs. 3 %, respectively). Thus, the iRGD peptide enhanced FAM-PS distribution in CA4P-treated tumors by almost 10-fold, addressing the challenge of the low penetrability and distribution of FAM-PS in tumors, which is a critical concern for effective drug delivery (El-Kareh & Secomb, 2004; Jain, 1994; Witkamp et al., 2001).

These findings underscore the applicability of a receptor amplification strategy, particularly in the case of PC tumors, for achieving an improved pharmacokinetic profile through sequential targeting.

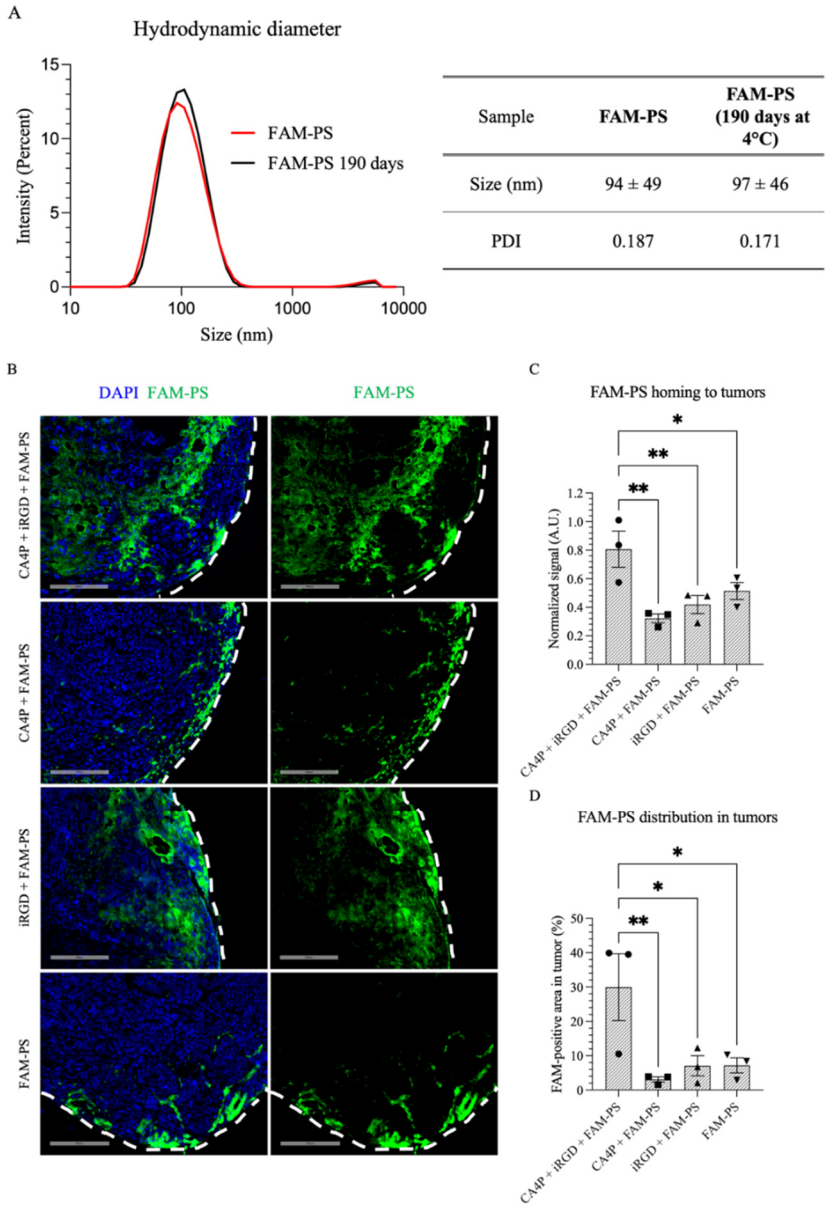

Sample	FAM-PS	FAM-PS (190 days at 4°C)
Size (nm)	94 ± 49	97 ± 46
PDI	0.187	0.171

Figure 19. CA4P sensitizes PC to iRGD-facilitated delivery of FAM-PS. (A) Characterization of FAM-PS immediately after synthesis and after 190 days of storage at 4 °C, showing PS stability. The size distribution, hydrodynamic diameter, and PDI values are also presented. (B) Representative slidescanner images of immunostained peritoneal tumors treated with CA4P or PBS. PC mice were treated with CA4P or PBS (CA4P, 100 mg/kg; 7 IP injections every alternate day) before administration of FAM-PS with iRGD or PBS. After 6 hours of circulation, tumors were collected, cryosectioned, immunostained for FAM-PS (FAM), and counterstained with DAPI. Green, FAM-PS (FAM); blue, nuclei (DAPI). Scale bar = 200 µm. (C) Quantification of the FAM-PS fluorescence

signal normalized to the DAPI signal in tumors. (D) Quantification of FAM-PS distribution in tumors by representing the percentage of FAM-signal-positive areas in the tumors. All tumors from the 3 different planes were used for analysis, with n=3 mice per group. Statistical analyses were performed using ANOVA. Error bars indicate ± SEM; *p<0.05, **p<0.001.

5.3.3. iRGD-enhanced secondary nanotherapy reduces peritoneal dissemination and improves the survival of mice with PC

We next conducted a survival study combining IP CA4P treatment with iRGD-enhanced nanotherapy (Fig. 20A). Despite its rapid impact on the tumor vasculature, CA4P monotherapy is ineffective in treating solid tumors (Chaplin et al., 1999; Horsman & Siemann, 2006). In our study, monotherapies of CA4P, UTO-PS, and their combination showed no significant survival extension compared with the control (Fig. 20B-D), emphasizing the need for enhanced therapeutic strategies. Both CA4P + iRGD + UTO-PS and iRGD + UTO-PS treatments improved survival by almost 5 days (Fig. 20E and F).

Due to limitations in the survival study design, hindering the assessment of tumor progression indicators, such as tumor weight and count, an additional treatment study was conducted. All mice were sacrificed on the same day, and the peritoneal tumors were extracted, weighed, and counted. While the survival differences among mice receiving iRGD combination therapies did not reach statistical significance, analysis of the tumor burden revealed that the CA4P + iRGD + UTO-PS combination treatment significantly decreased the overall tumor weight (Fig. 20H); this was the only treatment that resulted in a reduction in the number of tumor nodules (Fig. 20I). CA4P and UTO-PS monotherapies also reduced the total tumor weight. Still, they did not affect tumor dissemination (Fig. 20H). Interestingly, UTO-PS alone showed a significant reduction in tumor weight compared to CA4P + UTO-PS, hinting at the potential interference of CA4P with UTO-PS penetration, supported by biodistribution studies showing lower FAM-PS accumulation post-CA4P treatment (Fig. 19B and C). During treatment, mouse body weight decreased by 10–15 % in all groups owing to the progression of PC; however, the difference in body weight between the treated and control groups was not significant, suggesting that all mice tolerated the treatments without showing signs of systemic toxicity (Fig. 20G).

A

Treatment group	Days: 7, 9, 11, 13, 15, 17, 19, 21, 23, 25	Days: 8, 10, 12, 14, 16, 18, 20, 22, 24, 26
PBS (N=10)	PBS (500 µL)	PBS (500 µL)
CA4P + iRGD + UTO-PS (N=7)	CA4P (100 mg/kg)	iRGD (14 µmol/kg) + UTO-PS (1.4 mg/kg)
CA4P + UTO-PS (N=7)	CA4P (100 mg/kg)	UTO-PS (1 mg/kg)
CA4P (N=7)	CA4P (100 mg/kg)	PBS (500 µL)
UTO-PS (N=7)	PBS (500 µL)	UTO-PS (1 mg/kg)
iRGD + UTO-PS (N=7)	PBS (500 µL)	iRGD (14 µmol/kg) + UTO-PS (1.4 mg/kg)

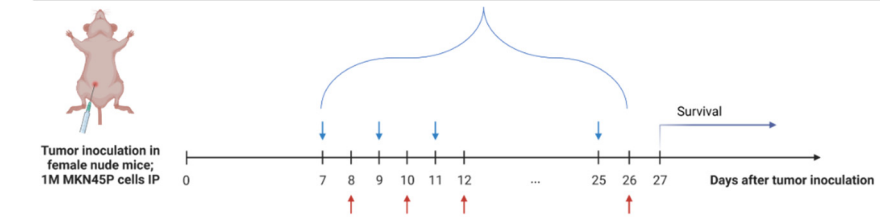

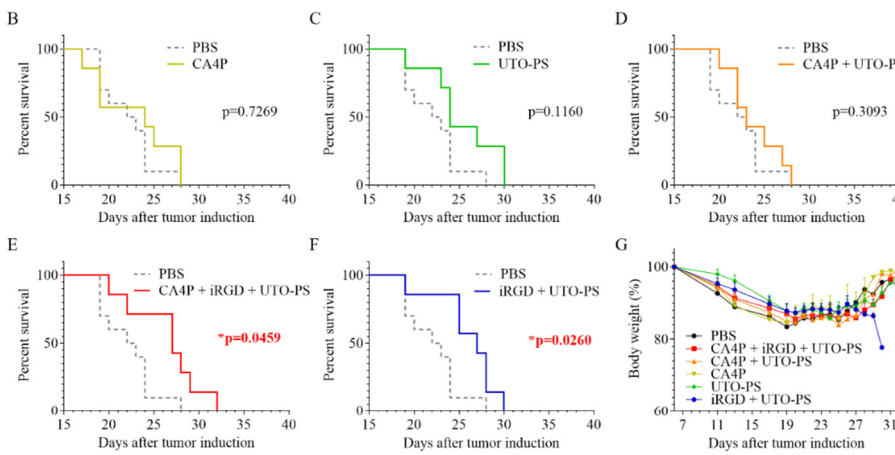

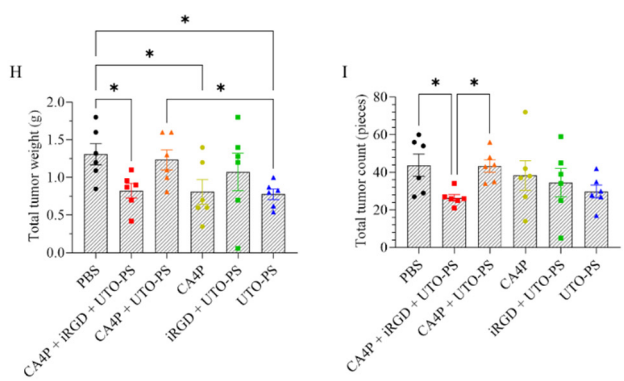

Figure 20. Combined therapy increased the survival of mice with disseminated gastric tumors without causing systemic toxicity. (A) Outline of treatment regimens. Immunodeficient mice with PC of gastric carcinoma origin were IP injected with combinations of the vascular disrupting agent CA4P (100 mg/kg, 10 IP injections every other day), tumor-penetrating peptide iRGD (14 µmol/kg, 10 IP injections every other day), and nano-

formulated UTO (UTO-PS) (1.4 mg/kg, 10 IP injections every other day). n=7 mice per group; PBS n=10. Survival curves of mice treated with CA4P (B), UTO-PS (C), CA4P + UTO-PS (D), CA4P + iRGD + UTO-PS (E), or iRGD + UTO-PS (F). Panels B-F show the graphs of the same treatment. Black dashed line, control group mice treated with PBS only; colored line, the group treated with the corresponding therapy. In an endpoint study, mice bearing PC were treated following the same regimen and sacrificed on the 23rd day after tumor induction. (G) The mice's body weight loss (%) was monitored throughout the treatment period to assess the systemic toxicity of the therapies. CA4P + iRGD + UTO-PS combination treatment significantly reduced tumor weight (H) and total tumor burden (I) (Panels A-G and H-I represent different treatments). Statistical comparisons were performed using the Gehan-Breslow-Wilcoxon test and ANOVA. Error bars indicate ± SEM; *$p < 0.05$.

5.3.4. Combination therapy of CA4P, iRGD, and UTO-PS does not induce overt toxicities

To confirm the safety of the therapies, we conducted toxicological studies in healthy mice that received 5 IP injections of CA4P, iRGD peptide, and UTO-PS. As shown in Fig. 21A, none of the treatments significantly affected the body weight of the mice, indicating their safety. The post-treatment levels of the hepatic and renal enzymes ALT, CREAT, and GLUC revealed no significant alterations in the CA4P + iRGD + UTO-PS or iRGD + UTO-PS groups compared to the control group (Fig. 21B-D). An approximately 40 % decrease in ALT after iRGD + UTO-PS treatment does not necessarily suggest hepatotoxicity, considering the established threshold for such toxicity is a ≥3-fold increase in ALT (Senior, 2012). These findings indicated no acute hepatic or renal toxicity or glucose-related metabolic dysfunction induced by the combination treatment.

Additionally, considering the dose-limiting cardiotoxicity associated with anthracycline-based chemotherapy (Levis et al., 2017; McGowan et al., 2017), we examined its effect on myocardial tissue, revealing negligible differences between the treatment and control groups (Fig. 21E).

In conclusion, toxicological assessments affirmed the safety of IP interventions, supporting the potential clinical applicability of CA4P, iRGD, and UTO-PS combination therapy for PC.

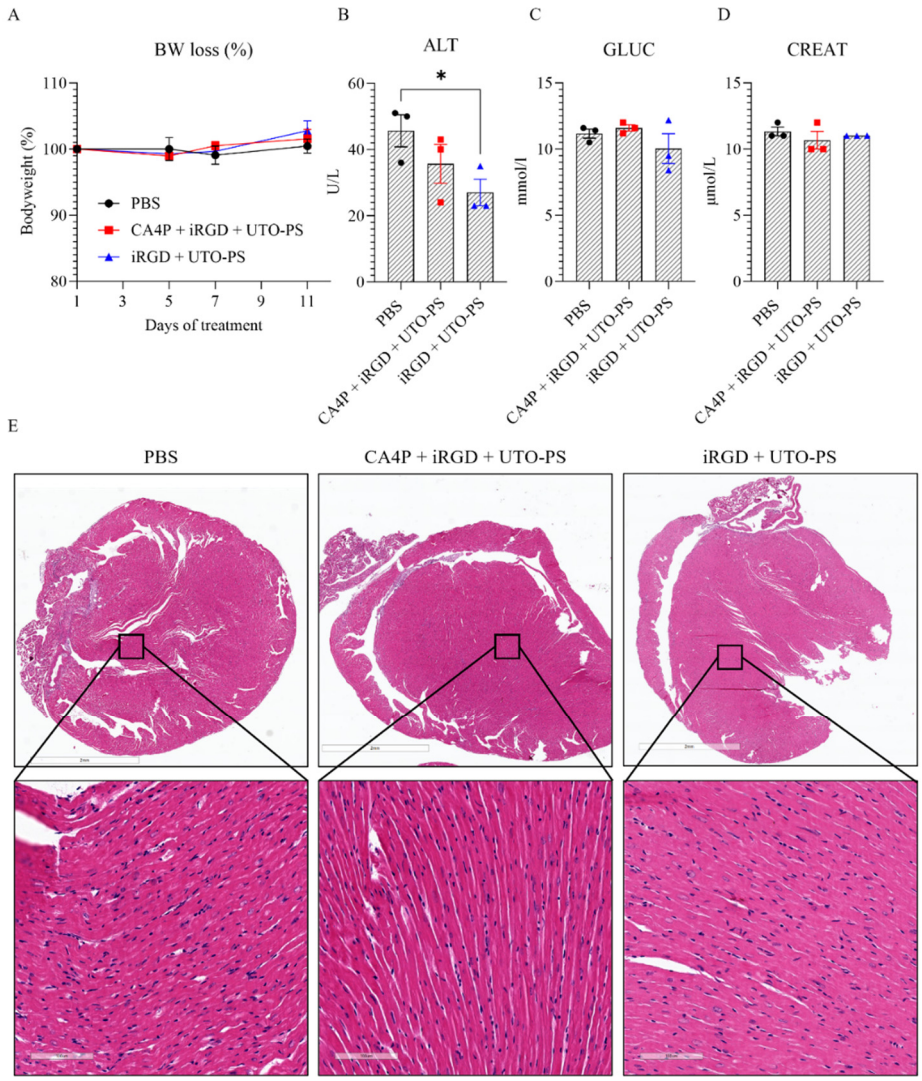

Figure 21. The combination therapy did not cause acute hepatic, renal, or cardiac toxicity. Healthy Balb/c mice received PBS or CA4P (100 mg/kg; 5 IP injections every other day) on one day, and iRGD (14 µmol/kg; 5 IP injections every other day) with UTO-PS (1.4 mg/kg UTO; 5 IP injections every other day) the other day for 10 days. (A) Body weight was monitored during treatment to assess systemic toxicity, and the percentage loss from initial body weight is shown. On the 11th day, blood was collected through retro-orbital bleeding and serum was tested for alanine transaminase (ALT) (B), glucose (GLUC) (C), and creatinine (CREAT) (D). n = 3. (E) Histological analysis of the extracted hearts treated with the same therapies. Scale bars = 2 mm in the upper row and 100 µm in the lower row. Representative images of 3 mice are shown. Statistical comparisons were performed using the ANOVA test. Error bars indicate ± SEM; *p<0.05.

6. DISCUSSION

6.1. Significance

Our study aimed to develop precise nanocarriers for anthracyclines, focusing on a widely clinically used anthracycline DOX and newly developed anthracycline prodrug UTO to enhance their antitumor activity. The introduction of the novel prodrug UTO aimed to reduce cardiotoxic effects and improve potency, addressing the challenges in traditional anthracycline chemotherapies. We investigated various nanovesicles, including NSVs and PS, to evaluate TPP-mediated affinity targeting, tumor accumulation, and antitumor efficacy. Our results demonstrate the efficient delivery of anthracyclines to cancer cells in a peptide-dependent manner. Furthermore, the strategic use of specific VDAs to sensitize solid tumors, such as breast and PC, for secondary precision nanotherapeutics significantly improves FAM-PS accumulation and distribution, and subsequently enhances antitumor efficacy while maintaining a safe toxicological profile.

6.2. Main findings

This research demonstrates improvement in precision nanotherapy with straightforward applications in cancer treatment. First, the developed RPAR-functionalized NSVs (RPAR-NSVs) showed selective binding to the NRP-1 receptor, leading to an increased uptake by NRP-1-positive prostate cancer cells. This targeted approach directly increased DOX anticancer efficacy in PPC-1 cells, demonstrating improved drug delivery and the suitability of this nanoplatform, which has better characteristics for DOX delivery compared to liposomes. In addition, we introduced UTO, a novel anthracycline with improved cell-killing activity compared to DOX. The specific challenges associated with UTO's hydrophobic nature were addressed by the encapsulation of UTO in peptide-guided, biocompatible, and biodegradable PS, which demonstrated selective internalization and effective killing of peptide receptor-positive cells, providing potential for targeted cancer therapy.

Furthermore, this study explored the molecular signatures in peritoneal tumors induced by VDA CA4P treatment, emphasizing their compatibility with iRGD tumor-homing peptide-potentiated nanotherapy. The improved outcomes observed in the combination therapy involving CA4P, iRGD, and UTO-PS for managing PC present a practical approach for more efficient and tolerable cancer treatment. These findings underscore the clinical potential of VDA-enhanced precision nanotherapy, laying a solid foundation for future advancements in cancer therapy.

6.2.1. Precision nanoplatform development for anthracycline delivery

To deliver anthracyclines to their site of action, we first optimized and developed potential drug delivery vehicles for precision therapy. NSVs and PS are particularly well-suited for encapsulating a sufficient amount of drugs (Yeo et al., 2017; J. Zhang et al., 2011). As both types of nanovesicles have hydrophobic membranes, it is possible to encapsulate both hydrophilic cargo inside the vesicles and hydrophobic cargo in the hydrophobic membrane. The thicker membrane in PS is advantageous for encapsulating hydrophobic drugs to carry more drugs per vesicle (Bermudez et al., 2002; Meng & Zhong, 2011). These nanovesicles, containing non-toxic, non-immunogenic, and biocompatible components, hold great promise for improving drug pharmacokinetics and biodistribution profiles.

Through careful optimization, we effectively developed a targeted delivery system employing TPP-functionalized PS and NSVs. The binding efficacy of these TPP-nanosystems was evaluated using PPC-1 and M21 cells based on previous studies and comparative literature focusing on these cell lines (d'Avanzo et al., 2024; Marchetti et al., 2023; Teesalu et al., 2009; Tobi et al., 2021; Willmore et al., 2016). PPC-1, derived from human primary prostate cancer cells (Brothman et al., 1989), exhibits high NRP-1 receptor expression (Simón-Gracia et al., 2021; Sugahara et al., 2009; Teesalu et al., 2009). Conversely, M21 cells derived from human melanoma cells (Cheresh & Spiro, 1987) lack NRP-1 expression (d'Avanzo et al., 2021; Simón-Gracia et al., 2021; Teesalu et al., 2009). These cell lines are valuable *in vitro* tools for demonstrating the specific binding and internalization of RPAR-targeted NPs to NRP-1-expressing cells.

The success of this targeted peptide-mediated delivery was evident, especially in receptor-positive PPC-1 cells, as confirmed through *in vitro* binding experiments. At the same time, cells lacking NRP-1 or those with a functionally blocked binding domain showed minimal interactions with the CendR peptide, leading to limited internalization.

Therefore, we developed TPP-targeted nanosystems, such as TPP-NSVs and TPP-PS, which demonstrated enhanced selective peptide-mediated delivery and internalization into receptor-positive cells *in vitro*, proving CendR-peptide-mediated binding and underlining the universality and suitability of these peptides for functionalization of different NP platforms.

6.2.2. Anthracyclines' anticancer activity is enhanced via TPP-targeted nanovesicles

Following the development of TPP-targeted nanovesicles, we proceeded with anthracycline encapsulation. NSVs were selected for DOX encapsulation because of their structural similarities to the clinically approved liposomes utilized for DOX delivery (Barenholz, 2012) and their improved physicochemical properties (Ge et al., 2019; Witika et al., 2022). The results showed that, compared to PS,

the NSVs platform was more appropriate for DOX encapsulation, exhibiting a significantly higher DOX EE of 40 % (Fig. 7A) (d'Avanzo et al., 2021), as opposed to the 7 % observed for PS (Fig. 12A) (Simón-Gracia et al., 2021). On the other hand, PS proved to be more suitable for encapsulating the novel hydrophobic prodrug UTO, which was designed to improve anticancer efficacy and reduce side effects (Simón-Gracia et al., 2021). Owing to its hydrophobic nature, PS achieved approximately 80–90 % (Fig. 12A) EE and favorable drug release kinetics, establishing its suitability as a nanocarrier for UTO (Simón-Gracia et al., 2021). However, the encapsulation and drug release kinetics of UTO within the NSVs platform remain to be determined.

To test the anticancer effect of TPP-targeted DOX-loaded NSVs (TPP-DOX-NSVs) and UTO-loaded PS (TPP-UTO-PS) *in vitro*, we performed cytotoxicity assays on receptor-positive PPC-1 and receptor-negative M21 cancer cells. In both scenarios, RPAR-targeted NPs carrying encapsulated anthracycline showed enhanced anticancer activity exclusively in receptor-positive cells, whereas receptor-negative cells were intact.

These findings confirm that TPP-targeted nanovesicles effectively amplify the anticancer effects of DOX and UTO by selectively directing the therapeutic payload to cancer cells. Notably, free UTO demonstrated superior anticancer activity compared with clinically used DOX at equivalent concentrations in a panel of cultured cancer cells. This result underscores the rationale behind the UTO synthesis.

Consequently, our focus shifted to evaluating the antitumor activity of UTO, given its proven heightened toxicity to cancer cells *in vitro*. Therefore, we opted to use PS for further *in vivo* studies.

6.2.3. *In vivo* tumor targeting with TPP-functionalized PS

In vivo imaging demonstrated the potential of CendR peptide-targeted PS for sensitive and specific TNBC breast tumor detection, proving their suitability for theranostic applications. LinTT1-guided nanocarriers, as shown in previous studies (Hunt et al., 2017; S. Sharma, Kotamraju, et al., 2017; Simón-Gracia et al., 2018), hold promise for the simultaneous detection and treatment of TNBC. The hydrophobic DiR dye used for *in vivo* imaging with its near-infrared properties facilitates whole-body imaging, benefiting from the deep-tissue penetration capabilities (Ntziachristos et al., 2003; Pansare et al., 2012) and minimal background interference (T. M. Liu et al., 2016). Therefore, encapsulating other hydrophobic near-infrared (NIR) dyes within peptide-targeted PEG-PCL PS opens new avenues for theranostic NPs for early and sensitive tumor detection.

LinTT1- and RPAR-targeted PS demonstrated notable tumor accumulation, highlighting the synergy between the tumor-homing peptides and PS properties. LinTT1 is a tumor-homing peptide that targets vascular docking sites and the tumor stroma, mainly through interaction with the p32 receptor overexpressed in malignant cells and activated macrophages (Fogal et al., 2008; Paasonen et al., 2016). The dual-targeting ability of LinTT1, which sequentially binds to both p32

and NRP-1 receptors, contributes to enhanced tumor specificity, outperforming RPAR, which targets only NRP-1. This dual targeting increases tumor tissue permeability and cargo internalization, providing potential advantages for therapeutic applications (Kadonosono et al., 2015; H. B. Pang et al., 2014; Teesalu et al., 2009). Functionalization with TPP further potentiated the accumulation of PS in MCF10CA1a breast tumors, with LinTT1 and RPAR targeting being more pronounced at earlier time points, potentially allowing early tumor detection (Fig. 14) (Simón-Gracia et al., 2018, 2021). In addition, the notably higher accumulation of LinTT1-PS in the tumor than in the heart implies a potential decrease in cardiotoxicity associated with anthracyclines (Fig. 15A and B) (Levis et al., 2017). In addition, using PS conjugated or coadministered with TPPs demonstrated increased breast and peritoneal tumor targeting via both IV and IP administration, highlighting that different administration routes can be chosen based on the specific tumor treatment strategy.

These findings highlight the efficacy of peptide-targeted PS for tumor diagnosis and theranostic applications and validate the suitability of TPP-PS for specific tumor delivery.

6.2.4. CA4P-induced receptor upregulation enables the enhancement of nanotherapy

This thesis explored the potential of utilizing VDA-induced molecular changes to prime tumors for homing peptide-guided nanotherapies to eliminate the VDA-resistant tumor rim (Liang et al., 2016). Collectively, these findings support the feasibility of the proposed approach.

First, the administration of CA4P increased the expression of integrins and NRP-1 receptors, which are targets of the tumor-penetrating peptide iRGD (Sugahara et al., 2009). Disruption of abnormal tumor blood vessels and subsequent necrosis likely induces significant molecular shifts. CA4P triggers a hypoxic response by activating more than 300 genes (Dachs et al., 2006; Semenza, 2014). This response plays a crucial role in angiogenesis, tumor development, and metastatic dissemination observed across various solid tumors, including breast (Bos et al., 2001) and gastric cancer (Miyake et al., 2013; Ucaryilmaz Metin & Ozcan, 2022). In solid tumors, αv integrins and NRP-1 are commonly expressed via hypoxia-inducible factor 1-alpha (HIF-1α)-dependent mechanisms that induce αvβ3 integrins and upregulate NRP-1 (Cowden Dahl et al., 2005; Fu et al., 2021).

Second, CA4P treatment in PC mice not only upregulated receptors but also significantly enhanced the accumulation and distribution of IP administered FAM-PS coadministered with the iRGD peptide (Fig. 19). This suggests a synergistic effect between VDA treatment and iRGD-guided nanotherapy, enhancing receptor accessibility and initiating a cascade for effective tumor penetration (H. B. Pang et al., 2014).

Finally, the therapeutic efficacy of CA4P in peritoneal dissemination was significantly improved with the complementary treatment of iRGD and UTO- PS, proving that it is well-tolerated and devoid of overt toxicities.

The study did not assess the effectiveness of DOX-PS in PC treatment for several reasons. First, as demonstrated above, PS were found to be not ideal for encapsulating DOX due to the low EE % of DOX in the PS (only 7 %). Second, the total UTO concentration used for the treatment was approximately 14 mg/kg, whereas free DOX has been previously used at a concentration of 28 mg/kg for treating mice with peritoneal carcinomatosis without any treatment benefit (Sugahara et al., 2015). Such low doses of free DOX, to be comparable with the concentration of UTO, have been shown to promote tumor growth, aggressiveness, and resistance (Verma & Vinayak, 2012).

The results emphasize the potential of sequential combination cancer therapies for enhanced disease control by targeting the molecular changes induced by the initial therapeutic agent. IP administration for iRGD and UTO-PS aligns with the clinical standard for PC, involving cytoreductive surgery (CRS) followed by IP chemotherapy (Young et al., 2022). IP administration increases drug residence time in the abdominal cavity, which is crucial for targeting PC lesions (Dakwar et al., 2017). The integration of CA4P-potentiated delivery, especially in combination with CRS, shows promise in eliminating microscopic tumor nodules left unresected after surgery, thereby reducing the risk of recurrence (Ceelen et al., 2007; Coffey et al., 2003). The coadministration mode of iRGD, which is currently being evaluated in phase I and II clinical studies on pancreatic cancer and other solid tumors (Buck et al., 2023; Dean et al., 2022), offers convenience and the potential to enhance standard therapies without limitations in delivery capacity (Hussain et al., 2014).

6.2.5. Safety assessment and clinical potential

Safety assessment of the therapeutic approach combining VDAs with TPP-guided nanotherapies provides a foundation for potential clinical applications. In our study, the combined treatment with CA4P, followed by iRGD-guided nanotherapy with UTO-PS, exhibited a well-tolerated pharmacodynamic profile without inducing overt hepatic, renal, or cardiac toxicities. The absence of acute cardiotoxicity, a significant concern associated with traditional anthracycline treatments (Levis et al., 2017), underscores the safety profile of our novel UTO-loaded nanocarrier. Notably, the controlled release of UTO from PS, remaining below 2 % over 48 hours (Simón-Gracia et al., 2021), further ensures the prevention of premature drug release, contributing to the overall safety and efficacy of the therapeutic strategy. In addition, the rationale for UTO synthesis has been developed to reduce off-side toxicity and cardiotoxicity.

Our work demonstrates that if rationally planned, novel therapeutic candidates can be developed to offer more efficacious treatment options.

6.2.6. Future directions

In this thesis, we systematically developed precision drug delivery vehicles designed for the targeted delivery of DOX and UTO in a preclinical setting. Our investigations focused explicitly on assessing the encapsulation of each drug in distinct types of nanovesicles, utilizing NSVs for DOX and PS for UTO encapsulation.

Given the ability of the evaluated nanoplatforms to encapsulate both hydrophobic and hydrophilic drugs, the next step is to test the coencapsulation of the more potent UTO anthracycline with another anticancer agents targeting a different therapeutic pathway, such as capecitabine (an oral prodrug of 5-fluorouracil; 5-FU) (G. Chen et al., 2017; Varshavsky-Yanovsky & Goldstein, 2020), irinotecan (Ishiguro et al., 2017), DOX or its derivatives (Barthel et al., 2016; Miles et al., 2018), antimicrobial peptides (Kelly et al., 2016), platinum-based agents (Moehler et al., 2017), or other, within NSVs and PS. This approach will likely provide a more robust synergistic cytotoxic effect, utilizing the diverse mechanisms by which each drug induces cancer cell death, as well as mitigating the possibility of MDR resistance development (Gilad et al., 2021; Keith et al., 2005; Mokhtari et al., 2017). Further enhancement of these potential synergistic effects is anticipated by incorporating the CendR peptides.

In this thesis, we opted for coadministration of iRGD together with UTO-PS and CA4P, the administration route that is currently being clinically evaluated in phase I and II trials (Buck et al., 2023; Dean et al., 2022). In follow-up studies, the conjugation of iRGD to NPs would offer the advantage of multivalent peptide presentation, potentially enhancing cellular transcytosis and tissue penetration by promoting receptor clustering. Multivalent presentation of targeting ligands can significantly increase ligand affinity through simultaneous engagement with multiple receptor-binding sites on the cell surface (Josan et al., 2011; Munoz et al., 2013). In addition, conjugating peptides onto NPs also allows for the incorporation of several types of different homing peptides, aiming to enhance the affinity and selectivity for cells expressing multiple target receptors. In the context of CA4P-potentiated delivery, additional peptides, such as PL1 (Lingasamy et al., 2019) and PL3 (Lingasamy et al., 2020) targeting Tenascin-C, LinTT1, and LyP-1 targeting cell surface p32 (Laakkonen et al., 2002; Paasonen et al., 2016), and mUNO binding to TAMs (Henze & Mazzone, 2016; Lepland et al., 2020) could be incorporated, further diversifying the targeting capabilities of the nanocarrier system. This multivalent approach is promising for improving the specificity and effectiveness of targeted drug delivery.

Despite the anticancer efficacy of our combination treatment, further optimization of the treatment schedule and dosage of CA4P is necessary to achieve optimal TME modulation and consequent anticancer effects. Preclinical data suggest that the potentiation of coadministered chemotherapy depends on the schedule of VDA used (Martinelli et al., 2007; Siemann et al., 2002). In addition, it is essential to conduct further investigations into the modulation of the TME by CA4P and its derivatives in other cancer models. This will enable full exploitation

of the ability of VDAs to modulate the TME and enhance the efficacy of combination cancer treatments.

Altogether, these findings highlight the promising therapeutic potential of combination therapy with CA4P, iRGD, and UTO-PS to achieve more efficient eradication of tumor lesions while minimizing cardiotoxic effects.

7. CONCLUSIONS

In this study, we have achieved significant results in developing precision-targeted nanoplatforms, specifically NSVs and PS, designed to effectively deliver anthracyclines – hydrophilic DOX and novel hydrophobic prodrug UTO. By incorporating the TPP, these nanocarriers were optimized to selectively target receptor-positive cancer cells, demonstrating enhanced drug delivery efficacy *in vitro*. Notably, our findings underscore the improved anticancer activity of UTO compared with DOX, establishing its potential as a potent and less cardiotoxic alternative. *In vivo* assessments showed that TPP-functionalized PS exhibited enhanced tumor accumulation, surpassing their non-targeted counterparts. The introduction of the vascular-disrupting agent CA4P-induced receptor upregulation in breast and peritoneal tumors (PC) has prompted the exploration of combination therapies. The synergistic administration of iRGD with UTO-PS significantly enhanced tumor homing and distribution post-CA4P treatment, reducing PC dissemination and improving survival in a preclinical PC model. Importantly, toxicological studies have affirmed the safety of these combination therapies, highlighting their potential for future clinical development.

Overall, this thesis advances precision cancer therapeutics, offering valuable insights into nanocarrier design, drug delivery strategies, and potential for improved treatment outcomes.

8. SUMMARY IN ESTONIAN

Uudse antratsükliiniga laetud nano-osakesed vähi täppisteraapiaks

Kasvajalised haigused on jätkuvalt globaalne terviseprobleem, mis nõuab uudsete terapeutiliste strateegiate arendamist ja kompleksset lähenemist ravile. Vähi keemiaravi puhul kasutatakse tsütotoksilisi ravimeid, et kahjustada maliigseid rakke ja takistada kasvaja kasvu ja levikut. Üheks enim kasutatud ja tõhusaimaks vähivastaste ravimite klassiks on antratsükliinid. Doksorubitsiin (DOX) on antratsükliin, mis on juba 50 aastat olnud kliinilises kasutuses erinevate soliidtuumorite ja hematoloogiliste vähkide, sealhulgas lümfoomi ja leukeemia ning rinna-, mao-, emaka-, munasarja-, põie- ja kopsuvähi raviks. Antratsükliinide rakendamisele vähiravis seavad piirangud kõrvalnähud nagu näiteks kardio-, hepato, ja neurotoksilisus. Seetõttu on akuutne vajadus innovatiivsete uue põlvkonna antratsükliinide järele, mis omaksid paremat kasvajavastast efektiivsust ja oleks vähemate kõrvalmõjudega.

Käesolevas töös uuriti uudse antratsükliini eelravimi Utorubitsiini (UTO) terapeutilist efektiivsust, kõrvalmõjusid ning nanoformulatsiooni mõju. Üheks võimaluseks kõrvalnähtude vähendamiseks on arendada ravimit tarnivaid nanokandjaid ehk nanopartikleid (NP-d), mis kogunevad selektiivselt kasvajatesse ja seetõttu vähendavad süsteemset toksilisust. Ravimite pakkimise abil nanokandjatesse (näiteks hüdrofoobse kaksikkihilise membraaniga ümbritsetud nanovesiikulid – niosoomid ja polümersoomid), on võimalik parandada ravimite biosaadavust, koepenetratsiooni ja kõrvaltoimed. NP-de selektiivsuse ja koedistributsiooni parandamiseks saab neid täppis-suunata kasvajakude "ära tundvate" afiinsusligandide, nagu näiteks antikehad või kasvajaid penetreerivad kullerpeptiidid (*tumor-penetrating peptides, TPP*), abil. Lisaks saab NP-sid disainida multifunktsionaalseteks, näiteks laadides afiinsussuunatud, ravimitega laetud, nanoosakesi täiendavalt diagnostiliste ühenditega, et võimaldada varajast ja täpset vähi diagnoosimist. Täppis-suunatud nanoravimite selektiivsust saab mõjutada läbi kasvaja mikrokeskkonna (*tumor microenvironment, TME*) manipuleerimise. Näiteks vähiveresooni destabiliseeriv ühend (VDA – *vascular disrupting agent*) CA4P moduleerib TME-d, suurendades angiogeneesiga seotud molekulaarseid mustreid, nii avades võimalusi edasiseks kasvajate sihtimiseks TPP-dega, et kõrvaldada VDA-teraapia suhtes resistentne maliigne kude.

Uurimistöö eesmärgid

Käesoleva doktoritöö käigus töötati välja ja testiti prekliiniliselt uusi TPP-dega sihitud ja antratsükliiniga laetud nanovesiikuleid, et tagada nende parem akumulatsioon ja efektiivsus soliidtuumorite mudelites *in vitro* ja *in vivo*.

Töö eesmärgid olid:

1. TPP-dega funktsionaliseeritud ja DOX-iga laetud NSV-de (TPP-DOX-NSVs) süntees, füüsikalis-keemiline iseloomustamine ja nanosakeste täppis-suunamise ja tsütotoksilise mõju iseloomustamine peptiidiretseptoreid ekspresseerivatel eesnäärmevähirakkudel *in vitro*.
2. Uudse antratsükliini UTO prekliinilise potentsiaali hindamine *in vit*ro ning UTO-ga laetud polümeersoomide (UTO-PS) arendamine *in vivo*.
3. CA4P, iRGD (kliinilises arenduses olev TPP) ja nanoformuleeritud UTO-PS kombineeritud terapeutilise efektiivsuse hindamine peritoneaalse kartsinomatoosi (*peritoneal carcinomatosis, PC*) ja hormoonretseptor-negatiivse rinnavähi (*triple-negative breast cancer, TNBC*) loommudelites.

Materjal ja metoodika

Doktoritöös kasutati üheksat erinevat patsientidelt pärinevat kasvajarakkude liini. Loomkatseteks kasutati atüümseid ja Balb/c-hiiri. Kõik loomkatsed kiideti heaks Eesti Põllumajandusministeeriumi vastava komisjoni poolt ning neile väljastati luba numbriga #159 ja #160. Töös kasutati erinevaid tuumorispetsiifilisi peptiide, nagu RPAR ja LinTT1 (ning erinevaid kontrollpeptiide nagu scrRPAR), mille konjugatsiooniks kasutati reaktsiooni peptiidide tioolrühma ja nanovesiikulite pinnal olevate maleimiidjääkide vahel. iRGD peptiidi kasutati konjugeerimata ehk vabal kujul. Nanoosakestena kasutati niosoome (NSV) ja polümersoome (PS). Nanoosakeste sünteesimiseks kasutati erinevaid meetodeid; mõlema nanoplatvormi puhul kasutati õhukese kihi aurustamismeetodit, kus niosoomide puhul kasutati kihi formeerumiskes amfifiilseid mitteioonseid surfaktante nagu lipiide ning polümersoomide puhul amfifiilseid polümeere. Mõlema nanosüsteemi puhul moodustusid sarnased, kaksikkihilise membraaniga nanovesiikulid, mida iseloomustati kasutades dünaamilist valgushajumist (DLS) ja transmissioonielektronmikroskoopiat. Rakuvabas süsteemis selektiivsuse hindamiseks kasutati Ni-NTA magnetilisi agaroosiosakesi, millele seondati rekombinantsed NRP-1 ja mutNRP-1 valgud. Fluorestsentsmärgisega nanoosakeste seondumine valkudele määrati fluorestsentsplaadilugejat kasutades. *In vitro* seondumiskatsed vähirakkudele viidi läbi voolutsütomeetria ja konfokaalmikroskoopia abil, kasutades sobivaid primaarseid ja sekundaarseid antikehi. Tsütotoksilisuse hindamiseks kasutati tetrasooliumil põhinevaid kolorimeetrilisi meetodeid. DOX osteti Sigma-Aldrich firmast ja UTO sünteesiti ToxInvent OÜ poolt. DOX laadimine nanoosakestesse viidi läbi kasutades õhukese filmi rehüdreerimise ravimit sisaldava füsioloogise lahusega. UTO laadimine toimus läbi ravimi ja polümeeri lahustamise orgaanilises lahustis ja hiljem õhukese ravimi-polümeeri kihi rehüdreerimise tavalise füsioloogilise lahusega. Ravimisisaldust nanoosakestes

mõõdeti kasutades spektrofotomeetriat. *In vivo* nanoosakeste biodistributsiooni katseteks indutseeriti hiirtes ortotoopsed rinna ja kõhuõõne kasvajad, süstides kasvajarakud kas piimanäärmesse või kõhuõõnde. Hiljem süstiti huvipakkuvaid nanosakesi kas intravenoosselt või intraperitoneaalselt ja seejärel teostati kasvajatest ja kontrollorganitest valmistatud koelõikudel immunohistokeemilised värvingud ja kuvamine konfokaalmikroskoopia ja slaidiskanneri abil. iRGD retseptorite ekspressiooni uurimiseks töödeldi katseloomi kõigepealt CA4P-ga, seejärel viidi läbi retseptorite immunohistokeemilised värvingud ja kuvamine. CA4P, iRGD ja UTO-polümersoomide kombinatsioonteraapia efektiivsuse hindamiseks viidi läbi eksperimentaalteraapia peritoneaalse kartsinomatoosi hiiremudelitel. Katse lõpus hinnati hiirte elulemust, kaalu, kasvajakoe kaalu ja kasvajanoodulite arvu. Eksperimentaalteraapia ohutust uuriti Tartu Ülikooli Kliinikumi laboris, viies läbi toksikoloogilised uuringud paneeli vereplasma markeritega ja kardiotoksilisuse hindamiseks kasutati hematoksüliini ja eosini värvinguid.

Doktoritöö tulemused ja järeldused

1. Doktoritöö keskendus uudsete täppis-suunatud nanoplatformide (niosoomid ja polümeersoomid) väljatöötamisele, mis võimaldavad paremat antratsükliinide (DOX ja UTO) kohaletoimetamist soliidtuumoritesse.
2. Nanoosakeste pinna katmine kasvajaid penetreeriva peptiididega (TPP) parandas oluliselt nende selektiivset akumulatsiooni kasvajarakkudes, eriti UTO-ga laetud nanoosakeste puhul, mis näitasid võrreldes DOX-ga märkimisväärset vähivastase aktiivsuse paranemist.
3. *In vivo* biodistributsiioni katsed näitasid, et TPP-funktsionaliseerimine parandas oluliselt polümeersoomide kogunemist soliidtuumoritesse.
4. Kasvaja veresooni destabiliseeriva ühendi CA4P kasutamine suurendas iRGD kullerpeptiidi retseptorite ekspressiooni rinnavähi ja peritoneaalse kartsinomatoosi kasvajates.
5. Eksperimentaalne kombinatsiooniteraapia prekliinilistes soliidtuumori mudelites kasutades CA4P, iRGD ja UTO-ga laetud PS (UTO-PS) vähendas peritoneaalse kartsinomatoosi levikut ja parandas hiirte elulemust.
6. Toksikoloogilised uuringud kinnitasid, et kombinatsiooniteraapia ravirežiim on ohutu ja ei põhjusta tõsiseid kõrvalmõjusid nagu hepato- ja kardiotoksilisus.

Kokkuvõtvalt näitavad käesoleva töö tulemused, et väljatöötatud nanokandjaid ja nende optimeeritud täppis-suunamisstrateegiaid saab kasutada efektiivsete vähiravimite disainimiseks ja arendamiseks.

9. REFERENCES

Abd-Elbary, A., El-laithy, H. M., & Tadros, M. I. (2008). Sucrose stearate-based proniosome-derived niosomes for the nebulisable delivery of cromolyn sodium. *International Journal of Pharmaceutics*, *357*(1), 189–198. https://doi.org/10.1016/j.ijpharm.2008.01.056

Adams, G. P., Schier, R., McCall, A. M., Simmons, H. H., Horak, E. M., Alpaugh, R. K., Marks, J. D., & Weiner, L. M. (2001). High affinity restricts the localization and tumor penetration of single-chain fv antibody molecules. *Cancer Research*, *61*(12), 4750–4755.

Agemy, L., Kotamraju, V. R., Friedmann-Morvinski, D., Sharma, S., Sugahara, K. N., & Ruoslahti, E. (2013). Proapoptotic peptide-mediated cancer therapy targeted to cell surface p32. *Molecular Therapy*, *21*(12), 2195–2204. https://doi.org/10.1038/mt.2013.191

Ahmed, F., Pakunlu, R. I., Brannan, A., Bates, F., Minko, T., & Discher, D. E. (2006). Biodegradable polymersomes loaded with both paclitaxel and doxorubicin permeate and shrink tumors, inducing apoptosis in proportion to accumulated drug. *Journal of Controlled Release*, *116*, 150–158. https://doi.org/10.1016/j.jconrel.2006.07.012

Ahmed, F., Pakunlu, R. I., Srinivas, G., Brannan, A., Bates, F., Klein, M. L., Minko, T., & Discher, D. E. (2006). Shrinkage of a rapidly growing tumor by drug-loaded polymersomes: pH-triggered release through copolymer degradation. *Molecular Pharmaceutics*, *3*(3), 340–350. https://doi.org/10.1021/mp050103u

Alexander, J., Cargill, R., Michelson, S. R., & Schwam, H. (1988). (Acyloxy)alkyl Carbamates as Novel Bioreversible Prodrugs for Amines: Increased Permeation through Biological Membranes. *Journal of Medicinal Chemistry*, *31*(2), 318–322. https://doi.org/10.1021/jm00397a008

Alexis, F., Pridgen, E., Molnar, L. K., & Farokhzad, O. C. (2008). Factors Affecting the Clearance and Biodistribution of Polymeric Nanoparticles. *Molecular Pharmaceutics*, *5*(4), 505–515. https://doi.org/10.1021/mp800051m

Alitalo, K., & Carmeliet, P. (2002). Molecular mechanisms of lymphangiogenesis in health and disease. *Cancer Cell*, *1*(3), 219–227. https://doi.org/10.1016/S1535-6108(02)00051-X

Allen, T. M., & Martin, F. J. (2004). Advantages of liposomal delivery systems for anthracyclines. *Seminars in Oncology*, *31*(6 Suppl 13), 5–15. https://doi.org/10.1053/j.seminoncol.2004.08.001

Aloss, K., & Hamar, P. (2023). Recent Preclinical and Clinical Progress in Liposomal Doxorubicin. *Pharmaceutics*, *15*(3), 893. https://doi.org/10.3390/pharmaceutics15030893

Andrieu, J., Re, F., Russo, L., & Nicotra, F. (2019). Phage-displayed peptides targeting specific tissues and organs. *Journal of Drug Targeting*, *27*(5–6), 555–565. https://doi.org/10.1080/1061186X.2018.1531419

Araste, F., Abnous, K., Hashemi, M., Taghdisi, S. M., Ramezani, M., & Alibolandi, M. (2018). Peptide-based targeted therapeutics: Focus on cancer treatment. *Journal of Controlled Release*, *292*, 141–162. https://doi.org/10.1016/j.jconrel.2018.11.004

Arcamone, F., Animati, F., Capranico, G., Lombardi, P., Pratesi, G., Manzini, S., Supino, R., & Zunino, F. (1997). New developments in antitumor anthracyclines. *Pharmacology & Therapeutics*, *76*(1–3), 117–124. https://doi.org/10.1016/s0163-7258(97)00096-x

Augustin, H. G., & Koh, G. Y. (2017). Organotypic vasculature: From descriptive heterogeneity to functional pathophysiology. *Science*, *357*(6353), eaal2379. https://doi.org/10.1126/science.aal2379

Avraamides, C. J., Garmy-Susini, B., & Varner, J. A. (2008). Integrins in angiogenesis and lymphangiogenesis. *Nature Reviews Cancer*, *8*(8). https://doi.org/10.1038/nrc2353

Balasubramaniam, A., Kumar, V. A., & Pillai, K. S. (2002). Formulation and in vivo evaluation of niosome-encapsulated daunorubicin hydrochloride. *Drug Development and Industrial Pharmacy*, *28*(10), 1181–1193. https://doi.org/10.1081/ddc-120015351

Balistreri, G., Yamauchi, Y., & Teesalu, T. (2021). A widespread viral entry mechanism: The C-end Rule motif–neuropilin receptor interaction. *Proceedings of the National Academy of Sciences of the United States of America*, *118*(49), e2112457118. https://doi.org/10.1073/pnas.2112457118

Barenholz, Y. (2001). Liposome application: Problems and prospects. *Current Opinion in Colloid & Interface Science*, *6*(1), 66–77. https://doi.org/10.1016/S1359-0294(00)00090-X

Barenholz, Y. (2012). Doxil®--the first FDA-approved nano-drug: Lessons learned. *Journal of Controlled Release: Official Journal of the Controlled Release Society*, *160*(2), 117–134. https://doi.org/10.1016/j.jconrel.2012.03.020

Barthel, B. L., Mooz, E. L., Wiener, L. E., Koch, G. G., & Koch, T. H. (2016). Correlation of in Situ Oxazolidine Formation with Highly Synergistic Cytotoxicity and DNA Cross-Linking in Cancer Cells from Combinations of Doxorubicin and Formaldehyde. *Journal of Medicinal Chemistry*, *59*(5), 2205–2221. https://doi.org/10.1021/acs.jmedchem.5b01956

Bashiri, G., Padilla, M. S., Swingle, K. L., Shepherd, S. J., Mitchell, M. J., & Wang, K. (n.d.). Nanoparticle protein corona: From structure and function to therapeutic targeting. *Lab on a Chip*, *23*(6), 1432–1466. https://doi.org/10.1039/d2lc00799a

Beauregard, D. A., Hill, S. A., Chaplin, D. J., & Brindle, K. M. (2001). The Susceptibility of Tumors to the Antivascular Drug Combretastatin A4 Phosphate Correlates with Vascular Permeability1. *Cancer Research*, *61*(18), 6811–6815.

Beck, A., Goetsch, L., Dumontet, C., & Corvaïa, N. (2017). Strategies and challenges for the next generation of antibody–drug conjugates. *Nature Reviews Drug Discovery*, *16*(5), Article 5. https://doi.org/10.1038/nrd.2016.268

Becker, P. M., Waltenberger, J., Yachechko, R., Mirzapoiazova, T., Sham, J. S. K., Lee, C. G., Elias, J. A., & Verin, A. D. (2005). Neuropilin-1 regulates vascular endothelial growth factor-mediated endothelial permeability. *Circulation Research*, *96*(12), 1257–1265. https://doi.org/10.1161/01.RES.0000171756.13554.49

Bermudez, H., Brannan, A. K., Hammer, D. A., Bates, F. S., & Discher, D. E. (2002). Molecular Weight Dependence of Polymersome Membrane Structure, Elasticity, and Stability. *Macromolecules*, *35*(21), 8203–8208. https://doi.org/10.1021/ma020669l

Bhardwaj, P., Tripathi, P., Gupta, R., & Pandey, S. (2020). Niosomes: A review on niosomal research in the last decade. *Journal of Drug Delivery Science and Technology*, *56*, 101581. https://doi.org/10.1016/j.jddst.2020.101581

Blanazs, A., Armes, S. P., & Ryan, A. J. (2009). Self-assembled block copolymer aggregates: From micelles to vesicles and their biological applications. *Macromolecular Rapid Communications*, *30*, 267–277. https://doi.org/10.1002/marc.200800713

Bookbinder, L. H., Hofer, A., Haller, M. F., Zepeda, M. L., Keller, G.-A., Lim, J. E., Edgington, T. S., Shepard, H. M., Patton, J. S., & Frost, G. I. (2006). A recombinant human enzyme for enhanced interstitial transport of therapeutics. *Journal of Controlled Release*, *114*(2), 230–241. https://doi.org/10.1016/j.jconrel.2006.05.027

Bos, R., Zhong, H., Hanrahan, C. F., Mommers, E. C. M., Semenza, G. L., Pinedo, H. M., Abeloff, M. D., Simons, J. W., van Diest, P. J., & van der Wall, E. (2001). Levels of

Hypoxia-Inducible Factor-1α During Breast Carcinogenesis. *JNCI: Journal of the National Cancer Institute*, *93*(4), 309–314. https://doi.org/10.1093/jnci/93.4.309

Bradley, A. J., Devine, D. V., Ansell, S. M., Janzen, J., & Brooks, D. E. (1998). Inhibition of liposome-induced complement activation by incorporated poly(ethylene glycol)-lipids. *Archives of Biochemistry and Biophysics*, *357*(2), 185–194. https://doi.org/10.1006/abbi.1998.0798

Bragagni, M., Mennini, N., Ghelardini, C., & Mura, P. (2012). Development and Characterization of Niosomal Formulations of Doxorubicin Aimed at Brain Targeting. *Journal of Pharmacy & Pharmaceutical Sciences*, *15*(1), Article 1. https://doi.org/10.18433/J3230M

Braun, G. B., Sugahara, K. N., Yu, O. M., Kotamraju, V. R., Mölder, T., Lowy, A. M., Ruoslahti, E., & Teesalu, T. (2016). Urokinase-controlled tumor penetrating peptide. *Journal of Controlled Release*, *232*, 188–195. https://doi.org/10.1016/j.jconrel.2016.04.027

Bregoli, L., Movia, D., Gavigan-Imedio, J. D., Lysaght, J., Reynolds, J., & Prina-Mello, A. (2016). Nanomedicine applied to translational oncology: A future perspective on cancer treatment. *Nanomedicine: Nanotechnology, Biology, and Medicine*, *12*, 81–103. https://doi.org/10.1016/j.nano.2015.08.006

Brothman, A. R., Lesho, L. J., Somers, K. D., Wright, G. L., & Merchant, D. J. (1989). Phenotypic and cytogenetic characterization of a cell line derived from primary prostatic carcinoma. *International Journal of Cancer*, *44*(5), 898–903. https://doi.org/10.1002/ijc.2910440525

Buck, K. K., Dean, A., & McSweeney, T. (2023). LSTA1 Potentiates Complete Response in Metastatic Gastroesophageal Adenocarcinoma. *Oncology & Cancer Case Reports*, *9*(6), 001–003.

Burgess, D. J., Doles, J., Zender, L., Xue, W., Ma, B., McCombie, W. R., Hannon, G. J., Lowe, S. W., & Hemann, M. T. (2008). Topoisomerase levels determine chemotherapy response in vitro and in vivo. *Proceedings of the National Academy of Sciences*, *105*(26), 9053–9058. https://doi.org/10.1073/pnas.0803513105

Canton, I., Massignani, M., Patikarnmonthon, N., Chierico, L., Robertson, J., Renshaw, S. A., Warren, N. J., Madsen, J. P., Armes, S. P., Lewis, A. L., & Battaglia, G. (2013). Fully synthetic polymer vesicles for intracellular delivery of antibodies in live cells. *FASEB Journal: Official Publication of the Federation of American Societies for Experimental Biology*, *27*(1), 98–108. https://doi.org/10.1096/fj.12-212183

Cappetta, D., De Angelis, A., Sapio, L., Prezioso, L., Illiano, M., Quaini, F., Rossi, F., Berrino, L., Naviglio, S., & Urbanek, K. (2017). Oxidative Stress and Cellular Response to Doxorubicin: A Common Factor in the Complex Milieu of Anthracycline Cardiotoxicity. *Oxidative Medicine and Cellular Longevity*, *2017*, e1521020. https://doi.org/10.1155/2017/1521020

Capranico, G., Zunino, F., Kohn, K. W., & Pommier, Y. (1990). Sequence-selective topoisomerase II inhibition by anthracycline derivatives in SV40 DNA: Relationship with DNA binding affinity and cytotoxicity. *Biochemistry*, *29*(2), 562–569. https://doi.org/10.1021/bi00454a033

Carlier, C., Mathys, A., De Jaeghere, E., Steuperaert, M., De Wever, O., & Ceelen, W. (2017). Tumour tissue transport after intraperitoneal anticancer drug delivery. *International Journal of Hyperthermia*, *33*(5), 534–542. https://doi.org/10.1080/ 02656736.2017.1312563

Carmeliet, P., & Jain, R. K. (2000). Angiogenesis in cancer and other diseases. *Nature*, *407*(6801), 249–257. https://doi.org/10.1038/35025220

Ceelen, W. P., Morris, S., Paraskeva, P., & Pattyn, P. (2007). Surgical trauma, minimal residual disease and locoregional cancer recurrence. *Cancer Treatment and Research*, *134*, 51–69. https://doi.org/10.1007/978-0-387-48993-3_4

Chaplin, D. J., & Dougherty, G. J. (1999). Tumour vasculature as a target fer cancer therapy. *British Journal of Cancer*, *80*(SUPPL. 1).

Chaplin, D. J., Pettit, G. R., & Hill, S. A. (1999). Anti-vascular approaches to solid tumour therapy: Evaluation of combretastatin A4 phosphate. *Anticancer Research*, *19*(1 A).

Chen, G., Guo, Z., Liu, M., Yao, G., Dong, J., Guo, J., & Ye, C. (2017). Clinical Value of Capecitabine-Based Combination Adjuvant Chemotherapy in Early Breast Cancer: A Meta-Analysis of Randomized Controlled Trials. *Oncology Research Featuring Preclinical and Clinical Cancer Therapeutics*, *25*(9), 1567–1578. https://doi.org/10.3727/096504017X14897173032733

Chen, S., Hanning, S., Falconer, J., Locke, M., & Wen, J. (2019). Recent advances in non-ionic surfactant vesicles (niosomes): Fabrication, characterization, pharmaceutical and cosmetic applications. *European Journal of Pharmaceutics and Biopharmaceutics*, *144*, 18–39. https://doi.org/10.1016/j.ejpb.2019.08.015

Chen, Y. B., Jiang, C. T., Zhang, G. Q., Wang, J. S., & Pang, D. (2009). Increased expression of hyaluronic acid binding protein 1 is correlated with poor prognosis in patients with breast cancer. *Journal of Surgical Oncology*, *100*, 382–286. https://doi.org/10.1002/jso.21329

Cheresh, D. A., & Spiro, R. C. (1987). Biosynthetic and functional properties of an Arg-Gly-Asp-directed receptor involved in human melanoma cell attachment to vitronectin, fibrinogen, and von Willebrand factor. *Journal of Biological Chemistry*, *262*(36), 17703–17711.

Chien, A. J., & Moasser, M. M. (2008). Cellular Mechanisms of Resistance to Anthracyclines and Taxanes in Cancer: Intrinsic and Acquired. *Seminars in Oncology*, *35*, S1–S14. https://doi.org/10.1053/j.seminoncol.2008.02.010

Coccolini, F., Gheza, F., Lotti, M., Virzì, S., Iusco, D., Ghermandi, C., Melotti, R., Baiocchi, G., Giulini, S. M., Ansaloni, L., & Catena, F. (2013). Peritoneal carcinomatosis. *World Journal of Gastroenterology : WJG*, *19*(41), 6979–6994. https://doi.org/10.3748/wjg.v19.i41.6979

Coffey, J., Wang, J., Smith, M., Bouchier-Hayes, D., Cotter, T., & Redmond, H. (2003). Excisional surgery for cancer cure: Therapy at a cost. *The Lancet Oncology*, *4*(12), 760–768. https://doi.org/10.1016/S1470-2045(03)01282-8

Cooney, M. M., Savvides, P., Agarwala, S., Wang, D., Flick, S., Bergant, S., Bhakta, S., Lavertu, P., Ortiz, J., & Remick, S. (2006). Phase II study of combretastatin A4 phosphate (CA4P) in patients with advanced anaplastic thyroid carcinoma (ATC). *Journal of Clinical Oncology*, *24*(18_suppl), 5580–5580. https://doi.org/10.1200/jco.2006.24.18_suppl.5580

Cortesi, M., Rossino, G., Chakrabarty, A., & Rossi, D. (2023). Editorial: Tumor adaptation to cellular stresses: mechanisms, biomarkers and therapeutic opportunities. *Frontiers in Medicine*, *10*. https://www.frontiersin.org/articles/10.3389/fmed.2023.1268976

Cowden Dahl, K. D., Robertson, S. E., Weaver, V. M., & Simon, M. C. (2005). Hypoxia-inducible Factor Regulates αvβ3 Integrin Cell Surface Expression. *Molecular Biology of the Cell*, *16*(4), 1901–1912. https://doi.org/10.1091/mbc.e04-12-1082

Cutts, S. M., Nudelman, A., Rephaeli, A., & Phillips, D. R. (2005). The power and potential of doxorubicin-DNA adducts. *IUBMB Life*, *57*(2), 73–81. https://doi.org/10.1080/15216540500079093

Cutts, S., Rephaeli, A., Nudelman, A., Ugarenko, M., & Phillips, D. (2015). Potential Therapeutic Advantages of Doxorubicin when Activated by Formaldehyde to Function as a DNA Adduct-Forming Agent. *Current Topics in Medicinal Chemistry*, *15*(14), 1409–1422. https://doi.org/10.2174/1568026615666150413154512

d'Avanzo, N., Sidorenko, V., Simón-Gracia, L., Rocchi, A., Ottonelli, I., Ruozi, B., Longo, F., Celia, C., & Teesalu, T. (2024). C-end rule peptide-guided niosomes for prostate cancer cell targeting. *Journal of Drug Delivery Science and Technology*, *91*, 105162. https://doi.org/10.1016/j.jddst.2023.105162

d'Avanzo, N., Torrieri, G., Figueiredo, P., Celia, C., Paolino, D., Correia, A., Moslova, K., Teesalu, T., Fresta, M., & Santos, H. A. (2021). LinTT1 peptide-functionalized liposomes for targeted breast cancer therapy. *International Journal of Pharmaceutics*, *597*, 120346. https://doi.org/10.1016/j.ijpharm.2021.120346

Dachs, G. U., Steele, A. J., Coralli, C., Kanthou, C., Brooks, A. C., Gunningham, S. P., Currie, M. J., Watson, A. I., Robinson, B. A., & Tozer, G. M. (2006). Anti-vascular agent Combretastatin A-4-P modulates Hypoxia Inducible Factor-1 and gene expression. *BMC Cancer*, *6*, 280. https://doi.org/10.1186/1471-2407-6-280

Dai, W., Fan, Y., Zhang, H., Wang, X., Zhang, Q., & Wang, X. (2015). A comprehensive study of iRGD-modified liposomes with improved chemotherapeutic efficacy on B16 melanoma. *Drug Delivery*, *22*(1), 10–20. https://doi.org/10.3109/10717544.2014.903580

Dakwar, G. R., Shariati, M., Willaert, W., Ceelen, W., De Smedt, S. C., & Remaut, K. (2017). Nanomedicine-based intraperitoneal therapy for the treatment of peritoneal carcinomatosis—Mission possible? *Advanced Drug Delivery Reviews*, *108*, 13–24. https://doi.org/10.1016/j.addr.2016.07.001

Daly, J. L., Simonetti, B., Klein, K., Chen, K.-E., Williamson, M. K., Antón-Plágaro, C., Shoemark, D. K., Simón-Gracia, L., Bauer, M., Hollandi, R., Greber, U. F., Horvath, P., Sessions, R. B., Helenius, A., Hiscox, J. A., Teesalu, T., Matthews, D. A., Davidson, A. D., Collins, B. M., … Yamauchi, Y. (2020). Neuropilin-1 is a host factor for SARS-CoV-2 infection. *Science*, *370*(6518), 861–865. https://doi.org/10.1126/science.abd3072

Danaei, M., Dehghankhold, M., Ataei, S., Hasanzadeh Davarani, F., Javanmard, R., Dokhani, A., Khorasani, S., & Mozafari, M. R. (2018). Impact of Particle Size and Polydispersity Index on the Clinical Applications of Lipidic Nanocarrier Systems. *Pharmaceutics*, *10*(2), 57. https://doi.org/10.3390/pharmaceutics10020057

Danhier, F. (2016). To exploit the tumor microenvironment: Since the EPR effect fails in the clinic, what is the future of nanomedicine? *Journal of Controlled Release*, *244*, 108–121. https://doi.org/10.1016/j.jconrel.2016.11.015

Dark, G. G., Hill, S. A., Prise, V. E., Tozer, G. M., Pettit, G. R., & Chaplin, D. J. (1997). Combretastatin A-4, an agent that displays potent and selective toxicity toward tumor vasculature. *Cancer Research*, *57*(10).

Dean, A., Gill, S., McGregor, M., Broadbridge, V., Järveläinen, H. A., & Price, T. (2022). Dual αV-integrin and neuropilin-1 targeting peptide CEND-1 plus nab-paclitaxel and gemcitabine for the treatment of metastatic pancreatic ductal adenocarcinoma: A first-in-human, open-label, multicentre, phase 1 study. *The Lancet. Gastroenterology & Hepatology*, *7*(10), 943–951. https://doi.org/10.1016/S2468-1253(22)00167-4

Deng, C., Zhang, Q., Fu, Y., Sun, X., Gong, T., & Zhang, Z. (2017). Coadministration of Oligomeric Hyaluronic Acid-Modified Liposomes with Tumor-Penetrating Peptide-iRGD Enhances the Antitumor Efficacy of Doxorubicin against Melanoma. *ACS*

Applied Materials & Interfaces, *9*(2), 1280–1292. https://doi.org/10.1021/acsami.6b13738

Di Francesco, M., Celia, C., Cristiano, M. C., d'Avanzo, N., Ruozi, B., Mircioiu, C., Cosco, D., Di Marzio, L., & Fresta, M. (2021). Doxorubicin Hydrochloride-Loaded Nonionic Surfactant Vesicles to Treat Metastatic and Non-Metastatic Breast Cancer. *ACS Omega*, *6*(4), 2973–2989. https://doi.org/10.1021/acsomega.0c05350

Diaz Bessone, M. I., Simón-Gracia, L., Scodeller, P., Ramirez, M. D. L. A., Lago Huvelle, M. A., Soler-Illia, G. J. A. A., & Simian, M. (2019). IRGD-guided tamoxifen polymersomes inhibit estrogen receptor transcriptional activity and decrease the number of breast cancer cells with self-renewing capacity. *Journal of Nanobiotechnology*, *17*(120). https://doi.org/10.1186/s12951-019-0553-4

Discher, B. M., Won, Y. Y., Ege, D. S., Lee, J. C. M., Bates, F. S., Discher, D. E., & Hammer, D. A. (1999). Polymersomes: Tough vesicles made from diblock copolymers. *Science*, *284*(5417), 1143–1146. https://doi.org/10.1126/science.284.5417.1143

Discher, D. E., & Ahmed, F. (2006). POLYMERSOMES. *Annual Review of Biomedical Engineering*, *8*(1), 323–341. https://doi.org/10.1146/annurev.bioeng.8.061505.095838

Djordjevic, S., & Driscoll, P. C. (2013). Targeting VEGF signalling via the neuropilin co-receptor. *Drug Discovery Today*, *18*(9–10), 447–455. https://doi.org/10.1016/j. drudis.2012.11.013

Dowlati, A., Robertson, K., Cooney, M., Petros, W. P., Stratford, M., Jesberger, J., Rafie, N., Overmoyer, B., Makkar, V., Stambler, B., Taylor, A., Waas, J., Lewin, J. S., McCrae, K. R., & Remick, S. C. (2002). A Phase I Pharmacokinetic and Translational Study of the Novel Vascular Targeting Agent Combretastatin A-4 Phosphate on a Single-Dose Intravenous Schedule in Patients with Advanced Cancer1. *Cancer Research*, *62*(12), 3408–3416.

Du, J., & O'Reilly, R. K. (2009). Advances and challenges in smart and functional polymer vesicles. *Soft Matter*, *5*, 3544–3561. https://doi.org/10.1039/b905635a

Du, J., Tang, Y., Lewis, A. L., & Armes, S. P. (2005). pH-sensitive vesicles based on a biocompatible zwitterionic diblock copolymer. *Journal of the American Chemical Society*, *127*(51), 17982–17983. https://doi.org/10.1021/ja056514l

Duncan, R., & Gaspar, R. (2011). Nanomedicine(s) under the Microscope. *Molecular Pharmaceutics*, *8*(6), 2101–2141. https://doi.org/10.1021/mp200394t

Edwardson, D. W., Narendrula, R., Chewchuk, S., Mispel-Beyer, K., Mapletoft, J. P. J., & Parissenti, A. M. (2015). Role of Drug Metabolism in the Cytotoxicity and Clinical Efficacy of Anthracyclines. *Current Drug Metabolism*, *16*(6), 412–426. https://doi.org/10.2174/1389200216888150915112039

Elias, D. R., Poloukhtine, A., Popik, V., & Tsourkas, A. (2013). Effect of ligand density, receptor density, and nanoparticle size on cell targeting. *Nanomedicine: Nanotechnology, Biology, and Medicine*, *9*(2), 194–201. https://doi.org/10.1016/j.nano.2012.05.015

El-Kareh, A. W., & Secomb, T. W. (2004). A Theoretical Model for Intraperitoneal Delivery of Cisplatin and the Effect of Hyperthermia on Drug Penetration Distance. *Neoplasia*, *6*(2), 117–127. https://doi.org/10.1593/neo.03205

Fakhari, A., Baoum, A., Siahaan, T. J., Le, K. B., & Berkland, C. (2011). Controlling ligand surface density optimizes nanoparticle binding to ICAM-1. *Journal of Pharmaceutical Sciences*, *100*, 1045–1056. https://doi.org/10.1002/jps.22342

Fassas, A., & Anagnostopoulos, A. (2005). The use of liposomal daunorubicin (DaunoXome) in acute myeloid leukemia. *Leukemia & Lymphoma*, *46*(6), 795–802. https://doi.org/10.1080/10428190500052438

Faustino-Rocha, A., Oliveira, P. A., Pinho-Oliveira, J., Teixeira-Guedes, C., Soares-Maia, R., Da Costa, R. G., Colaço, B., Pires, M. J., Colaço, J., Ferreira, R., & Ginja, M. (2013). Estimation of rat mammary tumor volume using caliper and ultrasonography measurements. *Lab Animal*, *42*, 217–224. https://doi.org/10.1038/laban.254

Fogal, V., Zhang, L., Krajewski, S., & Ruoslahti, E. (2008). Mitochondrial/cell-surface protein p32/gC1qR as a molecular target in tumor cells and tumor stroma. *Cancer Research*, *68*(17), 7210–7218. https://doi.org/10.1158/0008-5472.CAN-07-6752

Fosgerau, K., & Hoffmann, T. (2015). Peptide therapeutics: Current status and future directions. *Drug Discovery Today*, *20*(1), 122–128. https://doi.org/10.1016/j.drudis.2014.10.003

Fu, R., Du, W., Ding, Z., Wang, Y., Li, Y., Zhu, J., Zeng, Y., Zheng, Y., Liu, Z., & Huang, J. (2021). HIF-1α promoted vasculogenic mimicry formation in lung adenocarcinoma through NRP1 upregulation in the hypoxic tumor microenvironment. *Cell Death & Disease*, *12*(4), Article 4. https://doi.org/10.1038/s41419-021-03682-z

Galbraith, S. M., Chaplin, D. J., Lee, F., Stratford, M. R. L., Locke, R. J., Vojnovic, B., & Tozer, G. M. (2001). Effects of combretastatin A4 phosphate on endothelial cell morphology in vitro and relationship to tumour vascular targeting activity in vivo. *Anticancer Research*, *21*(1 A).

Gaumet, M., Vargas, A., Gurny, R., & Delie, F. (2008). Nanoparticles for drug delivery: The need for precision in reporting particle size parameters. *European Journal of Pharmaceutics and Biopharmaceutics*, *69*(1), 1–9. https://doi.org/10.1016/j.ejpb.2007.08.001

Ge, X., Wei, M., He, S., & Yuan, W.-E. (2019). Advances of Non-Ionic Surfactant Vesicles (Niosomes) and Their Application in Drug Delivery. *Pharmaceutics*, *11*(2), 55. https://doi.org/10.3390/pharmaceutics11020055

Gelderblom, H., Verweij, J., Nooter, K., & Sparreboom, A. (2001). Cremophor EL: The drawbacks and advantages of vehicle selection for drug formulation. *European Journal of Cancer*, *37*, 1590–1598. https://doi.org/10.1016/S0959-8049(01)00171-X

Gewirtz, D. (1999). A critical evaluation of the mechanisms of action proposed for the antitumor effects of the anthracycline antibiotics adriamycin and daunorubicin. *Biochemical Pharmacology*, *57*(7), 727–741. https://doi.org/10.1016/S0006-2952(98)00307-4

Gilad, Y., Gellerman, G., Lonard, D. M., & O'Malley, B. W. (2021). Drug Combination in Cancer Treatment—From Cocktails to Conjugated Combinations. *Cancers*, *13*(4), Article 4. https://doi.org/10.3390/cancers13040669

Gill, J. H., Rockley, K. L., De Santis, C., & Mohamed, A. K. (2019). Vascular Disrupting Agents in cancer treatment: Cardiovascular toxicity and implications for co-administration with other cancer chemotherapeutics. *Pharmacology & Therapeutics*, *202*, 18–31. https://doi.org/10.1016/j.pharmthera.2019.06.001

Gottesman, M. M. (2002). Mechanisms of Cancer Drug Resistance. *Annual Review of Medicine*, *53*(1), 615–627. https://doi.org/10.1146/annurev.med.53.082901.103929

Grantab, R. H., & Tannock, I. F. (2012). Penetration of anticancer drugs through tumour tissue as a function of cellular packing density and interstitial fluid pressure and its modification by bortezomib. *BMC Cancer*, *12*, 214–224. https://doi.org/10.1186/1471-2407-12-214

Gref, R., Lück, M., Quellec, P., Marchand, M., Dellacherie, E., Harnisch, S., Blunk, T., & Müller, R. H. (2000). "Stealth" corona-core nanoparticles surface modified by polyethylene glycol (PEG): Influences of the corona (PEG chain length and surface density) and of the core composition on phagocytic uptake and plasma protein

adsorption. *Colloids and Surfaces B: Biointerfaces*, *18*(3–4), 301–313. https://doi.org/10.1016/S0927-7765(99)00156-3

Grisham, R., Ky, B., Tewari, K. S., Chaplin, D. J., & Walker, J. (2018). Clinical trial experience with CA4P anticancer therapy: Focus on efficacy, cardiovascular adverse events, and hypertension management. *Gynecologic Oncology Research and Practice*, *5*, 1. https://doi.org/10.1186/s40661-017-0058-5

Grossen, P., Witzigmann, D., Sieber, S., & Huwyler, J. (2017). PEG-PCL-based nanomedicines: A biodegradable drug delivery system and its application. *Journal of Controlled Release*, *260*, 46–60. https://doi.org/10.1016/j.jconrel.2017.05.028

Guan, J., Guo, H., Tang, T., Wang, Y., Wei, Y., Seth, P., Li, Y., Dehm, S. M., Ruoslahti, E., & Pang, H.-B. (2021). iRGD-Liposomes Enhance Tumor Delivery and Therapeutic Efficacy of Antisense Oligonucleotide Drugs against Primary Prostate Cancer and Bone Metastasis. *Advanced Functional Materials*, *31*(24), 2100478. https://doi.org/10.1002/adfm.202100478

Guan, L., Rizzello, L., & Battaglia, G. (2015). Polymersomes and their applications in cancer delivery and therapy. *Nanomedicine*, *10*(17), 2757–2780. https://doi.org/10.2217/nnm.15.110

Hanada, M., Mizuno, S., Fukushima, A., Saito, Y., Noguchi, T., & Yamaoka, T. (1998). A new antitumor agent Amrubicin induces cell growth inhibition by stabilizing topoisomerase II-DNA complex. *Japanese Journal of Cancer Research*, *89*(11), 1229–1238. https://doi.org/10.1111/j.1349-7006.1998.tb00519.x

Hanahan, D., & Folkman, J. (1996). Patterns and Emerging Mechanisms of the Angiogenic Switch during Tumorigenesis. *Cell*, *86*(3), 353–364. https://doi.org/10.1016/S0092-8674(00)80108-7

Hansen, A. E., Petersen, A. L., Henriksen, J. R., Boerresen, B., Rasmussen, P., Elema, D. R., Rosenschöld, P. M. A., Kristensen, A. T., Kjær, A., & Andresen, T. L. (2015). Positron Emission Tomography Based Elucidation of the Enhanced Permeability and Retention Effect in Dogs with Cancer Using Copper-64 Liposomes. *ACS Nano*, *9*(7), 6985–6998. https://doi.org/10.1021/acsnano.5b01324

Harada, K., Yamashita, K., Iwatsuki, M., Baba, H., & Ajani, J. A. (2022). Intraperitoneal therapy for gastric cancer peritoneal carcinomatosis. *Expert Review of Clinical Pharmacology*, *15*(1), 43–49. https://doi.org/10.1080/17512433.2022.2044790

Harris, L., Batist, G., Belt, R., Rovira, D., Navari, R., Azarnia, N., Welles, L., & Winer, E. (2002). Liposome-encapsulated doxorubicin compared with conventional doxorubicin in a randomized multicenter trial as first-line therapy of metastatic breast carcinoma. *Cancer*, *94*(1), 25–36. https://doi.org/10.1002/cncr.10201

Health, C. for D. and R. (2023). Medical Device Material Safety Summaries. *FDA*. https://www.fda.gov/medical-devices/science-and-research-medical-devices/medical-device-material-safety-summaries

Henze, A.-T., & Mazzone, M. (2016). The impact of hypoxia on tumor-associated macrophages. *The Journal of Clinical Investigation*, *126*(10), 3672–3679. https://doi.org/10.1172/JCI84427

Hira, A., Watanabe, H., Maeda, Y., Yokoo, K., Sanematsu, E., Fujii, J., Sasaki, J., Hamada, A., & Saito, H. (2008). Role of P-glycoprotein in accumulation and cytotoxicity of amrubicin and amrubicinol in MDR1 gene-transfected LLC-PK1 cells and human A549 lung adenocarcinoma cells. *Biochemical Pharmacology*, *75*(4), 973–980. https://doi.org/10.1016/j.bcp.2007.10.023

Hobbs, S. K., Monsky, W. L., Yuan, F., Roberts, W. G., Griffith, L., Torchilin, V. P., & Jain, R. K. (1998). Regulation of transport pathways in tumor vessels: Role of tumor

type and microenvironment. *Proceedings of the National Academy of Sciences of the United States of America*, *95*(8), 4607–4612. Scopus. https://doi.org/10.1073/pnas.95.8.4607

Hock, M. B., Thudium, K. E., Carrasco-Triguero, M., & Schwabe, N. F. (2015). Immunogenicity of antibody drug conjugates: Bioanalytical methods and monitoring strategy for a novel therapeutic modality. *The AAPS Journal*, *17*(1), 35–43. https://doi.org/10.1208/s12248-014-9684-6

Hollingshead, L. M., & Faulds, D. (1991). Idarubicin. *Drugs*, *42*(4), 690–719. https://doi.org/10.2165/00003495-199142040-00010

Horsman, M. R., & Siemann, D. W. (2006). Pathophysiologic Effects of Vascular-Targeting Agents and the Implications for Combination with Conventional Therapies. *Cancer Research*, *66*(24), 11520–11539. https://doi.org/10.1158/0008-5472.CAN-06-2848

Hortobágyi, G. N. (1997). Anthracyclines in the Treatment of Cancer. *Drugs*, *54*(4), 1–7. https://doi.org/10.2165/00003495-199700544-00003

Hu, C.-M. J., & Zhang, L. (2009). Therapeutic nanoparticles to combat cancer drug resistance. *Current Drug Metabolism*, *10*(8), 836–841. https://doi.org/10.2174/138920009790274540

Hulst, M. B., Grocholski, T., Neefjes, J. J. C., Wezel, G. P. van, & Metsä-Ketelä, M. (2022). Anthracyclines: Biosynthesis, engineering and clinical applications. *Natural Product Reports*, *39*(4), 814–841. https://doi.org/10.1039/D1NP00059D

Hunt, H., Simón-Gracia, L., Tobi, A., Kotamraju, V. R., Sharma, S., Nigul, M., Sugahara, K. N., Ruoslahti, E., & Teesalu, T. (2017). Targeting of p32 in peritoneal carcinomatosis with intraperitoneal linTT1 peptide-guided pro-apoptotic nanoparticles. *Journal of Controlled Release: Official Journal of the Controlled Release Society*, *260*, 142–153. https://doi.org/10.1016/j.jconrel.2017.06.005

Hussain, S., Rodriguez-Fernandez, M., Braun, G. B., Doyle, F. J., & Ruoslahti, E. (2014). Quantity and accessibility for specific targeting of receptors in tumours. *Scientific Reports*, *4*(1), Article 1. https://doi.org/10.1038/srep05232

Huwyler, J., Wu, D., & Pardridge, W. M. (1996). Brain drug delivery of small molecules using immunoliposomes. *Proceedings of the National Academy of Sciences of the United States of America*, *93*(24), 14164–14169.

Ishiguro, H., Saji, S., Nomura, S., Tanaka, S., Ueno, T., Onoue, M., Iwata, H., Yamanaka, T., Sasaki, Y., & Toi, M. (2017). A phase I/II pharmacokinetics/pharmacodynamics study of irinotecan combined with S−1 for recurrent/metastatic breast cancer in patients with selected 1A1 genotypes (the JBCRG-M01 study). *Cancer Medicine*, *6*(12), 2909–2917. https://doi.org/10.1002/cam4.1258

Jain, R. K. (1994). Barriers to Drug Delivery in Solid Tumors. *Scientific American*, *271*(1), 58–65.

Jain, R. K. (1999). Transport of molecules, particles, and cells in solid tumors. *Annual Review of Biomedical Engineering*, *1*, 241–263. https://doi.org/10.1146/annurev.bioeng.1.1.241

Järvinen, T. A. H., & Ruoslahti, E. (2010). Target-seeking antifibrotic compound enhances wound healing and suppresses scar formation in mice. *Proceedings of the National Academy of Sciences of the United States of America*, *107*(50), 21671–21676. https://doi.org/10.1073/pnas.1016233107

Josan, J. S., Handl, H. L., Sankaranarayanan, R., Xu, L., Lynch, R. M., Vagner, J., Mash, E. A., Hruby, V. J., & Gillies, R. J. (2011). Cell-specific targeting by heterobivalent

ligands. *Bioconjugate Chemistry*, *22*(7), 1270–1278. https://doi.org/10.1021/bc1004284

Joyce, J. A., Laakkonen, P., Bernasconi, M., Bergers, G., Ruoslahti, E., & Hanahan, D. (2003). Stage-specific vascular markers revealed by phage display in a mouse model of pancreatic islet tumorigenesis. *Cancer Cell*, *4*(5), 393–403. https://doi.org/10.1016/s1535-6108(03)00271-x

Jung, J., Lee, I. H., Lee, E., Park, J., & Jon, S. (2007). pH-sensitive polymer nanospheres for use as a potential drug delivery vehicle. *Biomacromolecules*, *8*(11), 3401–3407. https://doi.org/10.1021/bm700517z

Kadonosono, T., Yamano, A., Goto, T., Tsubaki, T., Niibori, M., Kuchimaru, T., & Kizaka-Kondoh, S. (2015). Cell penetrating peptides improve tumor delivery of cargos through neuropilin-1-dependent extravasation. *Journal of Controlled Release*, *10*, 14–21. https://doi.org/10.1016/j.jconrel.2015.01.011

Kamaly, N., Xiao, Z., Valencia, P. M., Radovic-Moreno, A. F., & Farokhzad, O. C. (2012). Targeted polymeric therapeutic nanoparticles: Design, development and clinical translation. *Chemical Society Reviews*, *41*(7), 2971–3010. https://doi.org/10.1039/c2cs15344k

Kandalaft, L. E., & Harari, A. (2021). Vaccines as Priming Tools for T Cell Therapy for Epithelial Cancers. *Cancers*, *13*(22), 5819. https://doi.org/10.3390/cancers13225819

Kanthou, C., & Tozer, G. M. (2002). The tumor vascular targeting agent combretastatin A-4-phosphate induces reorganization of the actin cytoskeleton and early membrane blebbing in human endothelial cells. *Blood*, *99*(6). https://doi.org/10.1182/blood.V99.6.2060

Karjalainen, K., Jaalouk, D. E., Bueso-Ramos, C. E., Zurita, A. J., Kuniyasu, A., Eckhardt, B. L., Marini, F. C., Lichtiger, B., O'Brien, S., Kantarjian, H. M., Cortes, J. E., Koivunen, E., Arap, W., & Pasqualini, R. (2011). Targeting neuropilin-1 in human leukemia and lymphoma. *Blood*, *117*(3), 920–927. https://doi.org/10.1182/blood-2010-05-282921

Kawano, K., & Maitani, Y. (2011). Effects of Polyethylene Glycol Spacer Length and Ligand Density on Folate Receptor Targeting of Liposomal Doxorubicin In Vitro. *Journal of Drug Delivery*, *2011*, 1–6. https://doi.org/10.1155/2011/160967

Keith, C. T., Borisy, A. A., & Stockwell, B. R. (2005). Multicomponent therapeutics for networked systems. *Nature Reviews Drug Discovery*, *4*(1), 71–78. https://doi.org/10.1038/nrd1609

Kelly, G. J., Kia, A. F.-A., Hassan, F., O'Grady, S., Morgan, M. P., Creaven, B. S., McClean, S., Harmey, J. H., & Devocelle, M. (2016). Polymeric prodrug combination to exploit the therapeutic potential of antimicrobial peptides against cancer cells. *Organic & Biomolecular Chemistry*, *14*(39), 9278–9286. https://doi.org/10.1039/C6OB01815G

Knutson, S., Raja, E., Bomgarden, R., Nlend, M., Chen, A., Kalyanasundaram, R., & Desai, S. (2016). Development and evaluation of a fluorescent antibody-drug conjugate for molecular imaging and targeted therapy of pancreatic cancer. *PLoS ONE*, *11*(6), 1–25. https://doi.org/10.1371/journal.pone.0157762

Koga, A., Aoyagi, K., Imaizumi, T., Miyagi, M., & Shirouzu, K. (2011). Comparison between the gastric cancer cell line MKN-45 and the high-potential peritoneal dissemination gastric cancer cell line MKN-45P. *The Kurume Medical Journal*, *58*(3), 73–79. https://doi.org/10.2739/kurumemedj.58.73

Kotamraju, V. R., Sharma, S., Kolhar, P., Agemy, L., Pavlovich, J., & Ruoslahti, E. (2016). Increasing Tumor Accessibility with Conjugatable Disulfide-Bridged Tumor-Pene-

trating Peptides for Cancer Diagnosis and Treatment. *Breast Cancer : Basic and Clinical Research*, *9*(Suppl 2), 79–87. https://doi.org/10.4137/BCBCR.S29426

Krauss, A. C., Gao, X., Li, L., Manning, M. L., Patel, P., Fu, W., Janoria, K. G., Gieser, G., Bateman, D. A., Przepiorka, D., Shen, Y. L., Shord, S. S., Sheth, C. M., Banerjee, A., Liu, J., Goldberg, K. B., Farrell, A. T., Blumenthal, G. M., & Pazdur, R. (2019). FDA Approval Summary: (Daunorubicin and Cytarabine) Liposome for Injection for the Treatment of Adults with High-Risk Acute Myeloid Leukemia. *Clinical Cancer Research: An Official Journal of the American Association for Cancer Research*, *25*(9), 2685–2690. https://doi.org/10.1158/1078-0432.CCR-18-2990

Kumar, G. P., & Rajeshwarrao, P. (2011). Nonionic surfactant vesicular systems for effective drug delivery—An overview. *Acta Pharmaceutica Sinica B*, *1*(4), 208–219. https://doi.org/10.1016/j.apsb.2011.09.002

Kurata, T., Okamoto, I., Tamura, K., & Fukuoka, M. (2007). Amrubicin for non-small-cell lung cancer and small-cell lung cancer. *Investigational New Drugs*, *25*(5), 499–504. https://doi.org/10.1007/s10637-007-9069-0

Kwon, Y. (2016). Mechanism-based management for mucositis: Option for treating side effects without compromising the efficacy of cancer therapy. *OncoTargets and Therapy*, *9*, 2007–2016. https://doi.org/10.2147/OTT.S96899

Laakkonen, P., Porkka, K., Hoffman, J. A., & Ruoslahti, E. (2002). A tumor-homing peptide with a targeting specificity related to lymphatic vessels. *Nature Medicine*, *8*(7), Article 7. https://doi.org/10.1038/nm720

Lambert, J. M., & Morris, C. Q. (2017). Antibody–Drug Conjugates (ADCs) for Personalized Treatment of Solid Tumors: A Review. *Advances in Therapy*, *34*(5), 1015–1035. https://doi.org/10.1007/s12325-017-0519-6

Lammers, T., Aime, S., Hennink, W. E., Storm, G., & Kiessling, F. (2011). Theranostic nanomedicine. *Accounts of Chemical Research*, *44*, 1029–1038. https://doi.org/10.1021/ar200019c

Latil, A., Bièche, I., Pesche, S., Valéri, A., Fournier, G., Cussenot, O., & Lidereau, R. (2000). VEGF overexpression in clinically localized prostate tumors and neuropilin-1 overexpression in metastatic forms. *International Journal of Cancer*, *89*(2), 167–171.

Lee, J. C., Bermudez, H., Discher, B. M., Sheehan, M. A., Won, Y. Y., Bates, F. S., & Discher, D. E. (2001). Preparation, stability, and in vitro performance of vesicles made with diblock copolymers. *Biotechnology and Bioengineering*, *73*(2), 135–145. https://doi.org/10.1002/bit.1045

Lee, J. S., & Feijen, J. (2012). Polymersomes for drug delivery: Design, formation and characterization. *Journal of Controlled Release*, *161*, 473–483. https://doi.org/10.1016/j.jconrel.2011.10.005

Lepland, A., Asciutto, E. K., Malfanti, A., Simón-Gracia, L., Sidorenko, V., Vicent, M. J., Teesalu, T., & Scodeller, P. (2020). Targeting Pro-Tumoral Macrophages in Early Primary and Metastatic Breast Tumors with the CD206-Binding mUNO Peptide. *Molecular Pharmaceutics*, *17*(7), 2518–2531. https://doi.org/10.1021/acs.molpharmaceut.0c00226

Levis, B. E., Binkley, P. F., & Shapiro, C. L. (2017). Cardiotoxic effects of anthracycline-based therapy: What is the evidence and what are the potential harms? *The Lancet Oncology*, *18*, 445–456. https://doi.org/10.1016/S1470-2045(17)30535-1

Lewis, C. E., Harney, A. S., & Pollard, J. W. (2016). The Multifaceted Role of Perivascular Macrophages in Tumors. *Cancer Cell*, *30*(1), 18–25. https://doi.org/10.1016/j.ccell.2016.05.017

Li, M., Wang, Y., Li, M., Wu, X., Setrerrahmane, S., & Xu, H. (2021). Integrins as attractive targets for cancer therapeutics. *Acta Pharmaceutica Sinica B*, *11*(9), 2726–2737. https://doi.org/10.1016/j.apsb.2021.01.004

Li, S.-D., & Huang, L. (2010). Stealth nanoparticles: High density but sheddable PEG is a key for tumor targeting. *Journal of Controlled Release*, *145*(3), 178–181. https://doi.org/10.1016/j.jconrel.2010.03.016

Liang, W., Ni, Y., Yicheng Ni, Chen, F., & Chen, F. H. (2016). Tumor resistance to vascular disrupting agents: Mechanisms, imaging, and solutions. *Oncotarget*, *7*(13), 15444–15459. https://doi.org/10.18632/oncotarget.6999

Licht, T., Fiebig, H. H., Bross, K. J., Herrmann, F., Berger, D. P., Shoemaker, R., & Mertelsmann, R. (1991). Induction of multiple-drug resistance during anti-neoplastic chemotherapy in vitro. *International Journal of Cancer*, *49*(4), 630–637. https://doi.org/10.1002/ijc.2910490427

Lin, K. Y., Kwon, E. J., Lo, J. H., & Bhatia, S. N. (2014). Drug-induced amplification of nanoparticle targeting to tumors. *Nano Today*, *9*(5), 550–559. https://doi.org/10.1016/j.nantod.2014.09.001

Lingasamy, P., & Teesalu, T. (2021). Homing Peptides for Cancer Therapy. *Advances in Experimental Medicine and Biology*, *1295*, 29–48. https://doi.org/10.1007/978-3-030-58174-9_2

Lingasamy, P., Tobi, A., Haugas, M., Hunt, H., Paiste, P., Asser, T., Rätsep, T., Kotamraju, V. R., Bjerkvig, R., & Teesalu, T. (2019). Bi-specific tenascin-C and fibronectin targeted peptide for solid tumor delivery. *Biomaterials*, *219*, 119373. https://doi.org/10.1016/j.biomaterials.2019.119373

Lingasamy, P., Tobi, A., Kurm, K., Kopanchuk, S., Sudakov, A., Salumäe, M., Rätsep, T., Asser, T., Bjerkvig, R., & Teesalu, T. (2020). Tumor-penetrating peptide for systemic targeting of Tenascin-C. *Scientific Reports*, *10*, 5809. https://doi.org/10.1038/s41598-020-62760-y

Liu, T. M., Conde, J., Lipiński, T., Bednarkiewicz, A., & Huang, C. C. (2016). Revisiting the classification of NIR-absorbing/emitting nanomaterials for in vivo bioapplica tions. *NPG Asia Materials*, *8*(8), 1–25. https://doi.org/10.1038/am.2016.106

Liu, Z., & Wu, K. (2008). Peptides Homing to Tumor Vasculature: Imaging and Therapeutics for Cancer. *Recent Patents on Anti-Cancer Drug Discovery*, *3*(3), 202–208. https://doi.org/10.2174/157489208786242250

Lomas, H., Canton, I., MacNeil, S., Du, J., Armes, S. P., Ryan, A. J., Lewis, A. L., & Battaglia, G. (2007). Biomimetic pH Sensitive Polymersomes for Efficient DNA Encapsulation and Delivery. *Advanced Materials*, *19*(23), 4238–4243. https://doi.org/10.1002/adma.200700941

Longmire, M., Choyke, P. L., & Kobayashi, H. (2008). Clearance properties of nano-sized particles and molecules as imaging agents: Considerations and caveats. *Nanomedicine Lond.*, *3*(5), 703–717. https://doi.org/10.2217/17435889.3.5.703

Ludwig, B. S., Kessler, H., Kossatz, S., & Reuning, U. (2021). RGD-Binding Integrins Revisited: How Recently Discovered Functions and Novel Synthetic Ligands (Re-)Shape an Ever-Evolving Field. *Cancers*, *13*(7), 1711. https://doi.org/10.3390/cancers13071711

Ma, P., & Mumper, R. J. (2013). Anthracycline nano-delivery systems to overcome multiple drug resistance: A comprehensive review. *Nano Today*, *8*(3), 313–331. https://doi.org/10.1016/j.nantod.2013.04.006

Maeda, H., & Matsumura, Y. (1986). A new concept for macromolecular therapeutics in cancer chemotherapy: Mechanism of tumoritropic accumulation of proteins and the

antitumor agent SMANCS. *Cancer Research*, *46*, 6387–6392. https://doi.org/10.1021/bc100070g

Mann, A. P., Scodeller, P., Hussain, S., Joo, J., Kwon, E., Braun, G. B., Mölder, T., She, Z.-G., Kotamraju, V. R., Ranscht, B., Krajewski, S., Teesalu, T., Bhatia, S., Sailor, M. J., & Ruoslahti, E. (2016). A peptide for targeted, systemic delivery of imaging and therapeutic compounds into acute brain injuries. *Nature Communications*, *7*, 11980. https://doi.org/10.1038/ncomms11980

Marchetti, L., Simon-Gracia, L., Lico, C., Mancuso, M., Baschieri, S., Santi, L., & Teesalu, T. (2023). Targeting of Tomato Bushy Stunt Virus with a Genetically Fused C-End Rule Peptide. *Nanomaterials (Basel, Switzerland)*, *13*(8), 1428. https://doi.org/10.3390/nano13081428

Marinello, J., Delcuratolo, M., & Capranico, G. (2018). Anthracyclines as Topoisomerase II Poisons: From Early Studies to New Perspectives. *International Journal of Molecular Sciences*, *19*(11), 3480–3497. https://doi.org/10.3390/ijms19113480

Martinelli, M., Bonezzi, K., Riccardi, E., Kuhn, E., Frapolli, R., Zucchetti, M., Ryan, A. J., Taraboletti, G., & Giavazzi, R. (2007). Sequence dependent antitumour efficacy of the vascular disrupting agent ZD6126 in combination with paclitaxel. *British Journal of Cancer*, *97*(7), 888–894. https://doi.org/10.1038/sj.bjc.6603969

Martins-Teixeira, M. B., & Carvalho, I. (2020). Antitumour Anthracyclines: Progress and Perspectives. *ChemMedChem*, *15*(11), 933–948. https://doi.org/10.1002/cmdc.202000131

Masjedi, M., & Montahaei, T. (2021). An illustrated review on nonionic surfactant vesicles (niosomes) as an approach in modern drug delivery: Fabrication, characterization, pharmaceutical, and cosmetic applications. *Journal of Drug Delivery Science and Technology*, *61*, 102234. https://doi.org/10.1016/j.jddst.2020.102234

Massignani, M., Canton, I., Patikarnmonthon, N., Warren, N., Armes, S., Lewis, A., & Battaglia, G. (2010). Cellular delivery of antibodies: Effective targeted subcellular imaging and new therapeutic tool. *Nature Precedings*, 1–1. https://doi.org/10.1038/npre.2010.4427.1

Mateon Therapeutics. (2018). *FOCUS: A Multicenter, Multinational, Double-Blind, 2-Arm, Randomized, Phase 2/3, Study of Physician's Choice Chemotherapy ([PCC] Weekly Paclitaxel or Pegylated Liposomal Doxorubicin [PLD]) Plus Bevacizumab and CA4P Versus PCC Plus Bevacizumab and Placebo for Subjects With Platinum-Resistant, Recurrent Epithelial Ovarian, Primary Peritoneal or Fallopian Tube Cancer* (Clinical Trial Registration No. NCT02641639). clinicaltrials.gov. https://clinicaltrials.gov/ct2/show/NCT02641639

McCarty, M. F., Takeda, A., Stoeltzing, O., Liu, W., Fan, F., Reinmuth, N., Akagi, M., Bucana, C., Mansfield, P. F., Ryan, A., & Ellis, L. M. (2004). ZD6126 inhibits orthotopic growth and peritoneal carcinomatosis in a mouse model of human gastric cancer. *British Journal of Cancer*, *90*(3), 705–711. https://doi.org/10.1038/sj.bjc.6601490

McCoy, C. P., Brady, C., Cowley, J. F., McGlinchey, S. M., McGoldrick, N., Kinnear, D. J., Andrews, G. P., & Jones, D. S. (2010). Triggered drug delivery from biomaterials. *Expert Opinion on Drug Delivery*, *7*(5), 605–616. https://doi.org/10.1517/17425241003677731

McGowan, J. V., Chung, R., Maulik, A., Piotrowska, I., Walker, J. M., & Yellon, D. M. (2017). Anthracycline Chemotherapy and Cardiotoxicity. *Cardiovascular Drugs and Therapy*, *31*(1), 63–75. https://doi.org/10.1007/s10557-016-6711-0

McGregor, D. P. (2008). Discovering and improving novel peptide therapeutics. *Current Opinion in Pharmacology*, *8*(5), 616–619. https://doi.org/10.1016/j.coph.2008.06.002

McLoughlin, E. C., & O'Boyle, N. M. (2020). Colchicine-Binding Site Inhibitors from Chemistry to Clinic: A Review. *Pharmaceuticals*, *13*(1), Article 1. https://doi.org/10.3390/ph13010008

Meng, F., & Zhong, Z. (2011). Polymersomes spanning from nano- to microscales: Advanced vehicles for controlled drug delivery and robust vesicles for virus and cell mimicking. *Journal of Physical Chemistry Letters*, *2*(13), 1533–1539. https://doi.org/10.1021/jz200007h

Miao, L., Lin, C. M., & Huang, L. (2015). Stromal barriers and strategies for the delivery of nanomedicine to desmoplastic tumors. *Journal of Controlled Release*, *219*, 192–204. https://doi.org/10.1016/j.jconrel.2015.08.017

Miles, J. S., Sojourner, S. J., Whitmore, A. M., Freeny, D., Darling-Reed, S., & Flores-Rozas, H. (2018). Synergistic Effect of Endogenous and Exogenous Aldehydes on Doxorubicin Toxicity in Yeast. *BioMed Research International*, *2018*(1), 4938189. https://doi.org/10.1155/2018/4938189

Miller, M. A., Zheng, Y. R., Gadde, S., Pfirschke, C., Zope, H., Engblom, C., Kohler, R. H., Iwamoto, Y., Yang, K. S., Askevold, B., Kolishetti, N., Pittet, M., Lippard, S. J., Farokhzad, O. C., & Weissleder, R. (2015). Tumour-associated macrophages act as a slow-release reservoir of nano-therapeutic Pt(IV) pro-drug. *Nature Communications*, *6*, 8692–8705. https://doi.org/10.1038/ncomms9692

Minchinton, A. I., & Tannock, I. F. (2006). Drug penetration in solid tumours. *Nature Reviews Cancer*, *6*(8), Article 8. https://doi.org/10.1038/nrc1893

Minotti, G., Menna, P., Salvatorelli, E., Cairo, G., & Gianni, L. (2004). Anthracyclines: Molecular advances and pharmacologic developments in antitumor activity and cardiotoxicity. *Pharmacological Reviews*, *56*(2), 185–229. https://doi.org/10.1124/pr.56.2.6

Miyagi, M., Aoyagi, K., Kato, S., & Shirouzu, K. (2007). The TIMP-1 gene transferred through adenovirus mediation shows a suppressive effect on peritoneal metastases from gastric cancer. *International Journal of Clinical Oncology*, *12*(1), 17–24. https://doi.org/10.1007/s10147-006-0616-z

Miyake, S., Kitajima, Y., Nakamura, J., Kai, K., Yanagihara, K., Tanaka, T., Hiraki, M., Miyazaki, K., & Noshiro, H. (2013). HIF-1α is a crucial factor in the development of peritoneal dissemination via natural metastatic routes in scirrhous gastric cancer. *International Journal of Oncology*, *43*(5), 1431–1440. https://doi.org/10.3892/ijo.2013.2068

Moehler, M., Mahlberg, R., Heinemann, V., Obermannová, R., Kubala, E., Melichar, B., Weinmann, A., Scigalla, P., Tesařová, M., Janda, P., Hédouin-Biville, F., & Mansoor, W. (2017). Phase I study of orally administered S-1 in combination with epirubicin and oxaliplatin in patients with advanced solid tumors and chemotherapy-naïve advanced or metastatic esophagogastric cancer. *Gastric Cancer*, *20*(2), 358–367. https://doi.org/10.1007/s10120-016-0618-0

Mokhtari, R. B., Homayouni, T. S., Baluch, N., Morgatskaya, E., Kumar, S., Das, B., & Yeger, H. (2017). Combination therapy in combating cancer. *Oncotarget*, *8*(23), 38022–38043. https://doi.org/10.18632/oncotarget.16723

Molema, G., De Leij, L. F. M. H., & Meijer, D. K. F. (1997). Tumor vascular endothelium: Barrier or target in tumor directed drug delivery and immunotherapy. *Pharmaceutical Research*, *14*, 2–10. https://doi.org/10.1023/A:1012038930172

Momekova, D. B., Gugleva, V. E., & Petrov, P. D. (2021). Nanoarchitectonics of Multifunctional Niosomes for Advanced Drug Delivery. *ACS Omega*, *6*(49), 33265–33273. https://doi.org/10.1021/acsomega.1c05083

Mordente, A., Meucci, E., Silvestrini, A., Martorana, G. E., & Giardina, B. (2009). New developments in anthracycline-induced cardiotoxicity. *Current Medicinal Chemistry*, *16*(13), 1656–1672. https://doi.org/10.2174/092986709788186228

Morisada, S., Yanagi, Y., Kashiwazaki, Y., & Fukui, M. (1989). Toxicological Aspects of a Novel 9-Aminoanthracycline, SM-5887. *Japanese Journal of Cancer Research*, *80*(1), 77–82. https://doi.org/10.1111/j.1349-7006.1989.tb02248.x

Mross, K. (1991). New anthracycline derivatives: What for? *European Journal of Cancer (Oxford, England: 1990)*, *27*(12), 1542–1544. https://doi.org/10.1016/0277-5379(91)90409-7

Munoz, E. M., Correa, J., Riguera, R., & Fernandez-Megia, E. (2013). Real-time evaluation of binding mechanisms in multivalent interactions: A surface plasmon resonance kinetic approach. *Journal of the American Chemical Society*, *135*(16), 5966–5969. https://doi.org/10.1021/ja400951g

Nahire, R., Haldar, M. K., Paul, S., Ambre, A. H., Meghnani, V., Layek, B., Katti, K. S., Gange, K. N., Singh, J., Sarkar, K., & Mallik, S. (2014). Multifunctional polymersomes for cytosolic delivery of gemcitabine and doxorubicin to cancer cells. *Biomaterials*, *35*(24), 6482–6497. https://doi.org/10.1016/j.biomaterials.2014.04.026

Nasarre, C., Roth, M., Jacob, L., Roth, L., Koncina, E., Thien, A., Labourdette, G., Poulet, P., Hubert, P., Crémel, G., Roussel, G., Aunis, D., & Bagnard, D. (2010). Peptide-based interference of the transmembrane domain of neuropilin-1 inhibits glioma growth in vivo. *Oncogene*, *29*(16), 2381–2392. https://doi.org/10.1038/onc.2010.9

Nielsen, D., Maare, C., & Skovsgaard, T. (1996). Cellular resistance to anthracyclines. *General Pharmacology*, *27*(2), 251–255. https://doi.org/10.1016/0306-3623(95)02013-6

Ntziachristos, V., Bremer, C., & Weissleder, R. (2003). Fluorescence imaging with near-infrared light: New technological advances that enable in vivo molecular imaging. *European Radiology*, *13*, 195–208. https://doi.org/10.1007/s00330-002-1524-x

Okuda, S., Oh, Y., Tsuruda, H., Onoyama, K., Fujimi, S., & Fujishima, M. (1986). Adriamycin-induced nephropathy as a model of chronic progressive glomerular disease. *Kidney International*, *29*(2), 502–510. https://doi.org/10.1038/ki.1986.28

Oliveira, H., Pérez-Andrés, E., Thevenot, J., Sandre, O., Berra, E., & Lecommandoux, S. (2013). Magnetic field triggered drug release from polymersomes for cancer therapeutics. *Journal of Controlled Release*, *169*(3), 165–170. https://doi.org/10.1016/j.jconrel.2013.01.013

Paasonen, L., Sharma, S., Braun, G. B., Kotamraju, V. R., Chung, T. D. Y., She, Z.-G., Sugahara, K. N., Yliperttula, M., Wu, B., Pellecchia, M., Ruoslahti, E., & Teesalu, T. (2016). New p32/gC1qR Ligands for Targeted Tumor Drug Delivery. *Chembiochem: A European Journal of Chemical Biology*, *17*(7), 570–575. https://doi.org/10.1002/cbic.201500564

Pang, H. B., Braun, G. B., Friman, T., Aza-Blanc, P., Ruidiaz, M. E., Sugahara, K. N., Teesalu, T., & Ruoslahti, E. (2014). An endocytosis pathway initiated through neuropilin-1 and regulated by nutrient availability. *Nature Communications*, *5*, 4904–4916. https://doi.org/10.1038/ncomms5904

Pang, Z., Gao, H., Yu, Y., Guo, L., Chen, J., Pan, S., Ren, J., Wen, Z., & Jiang, X. (2011). Enhanced Intracellular Delivery and Chemotherapy for Glioma Rats by Transferrin-Conjugated Biodegradable Polymersomes Loaded with Doxorubicin. *Bioconjugate Chemistry*, *22*(6), 1171–1180. https://doi.org/10.1021/bc200062q

Pansare, V. J., Hejazi, S., Faenza, W. J., & Prud'Homme, R. K. (2012). Review of long-wavelength optical and NIR imaging materials: Contrast agents, fluorophores, and

multifunctional nano carriers. *Chemistry of Materials*, *24*, 812–827. https://doi.org/10.1021/cm2028367

Pasqualini, R., & Ruoslahti, E. (1996). Organ targeting in vivo using phage display peptide libraries. *Nature*, *380*, 364–366. https://doi.org/10.1038/380364a0

Pawar, P. V., Gohil, S. V., Jain, J. P., & Kumar, N. (2013). Functionalized polymersomes for biomedical applications. *Polymer Chemistry*, *4*(11), 3160–3176. https://doi.org/10.1039/C3PY00023K

Pegoraro, C., Cecchin, D., Gracia, L. S., Warren, N., Madsen, J., Armes, S. P., Lewis, A., Macneil, S., & Battaglia, G. (2013). Enhanced drug delivery to melanoma cells using PMPC-PDPA polymersomes. *Cancer Letters*, *334*(2), 328–337. https://doi.org/10.1016/j.canlet.2013.02.007

Petersen, G. H., Alzghari, S. K., Chee, W., Sankari, S. S., & La-Beck, N. M. (2016). Meta-analysis of clinical and preclinical studies comparing the anticancer efficacy of liposomal versus conventional non-liposomal doxorubicin. *Journal of Controlled Release: Official Journal of the Controlled Release Society*, *232*, 255–264. https://doi.org/10.1016/j.jconrel.2016.04.028

Pettit, G. R., & Rhodes, M. R. (1998). Antineoplastic agents 389. New syntheses of the combretastatin A-4 prodrug. *Anti-Cancer Drug Design*, *13*(3), 183–191.

Plosker, G. L., & Faulds, D. (1993). Epirubicin. *Drugs*, *45*(5), 788–856. https://doi.org/10.2165/00003495-199345050-00011

Pommier, Y. (1993). DNA topoisomerase I and II in cancer chemotherapy: Update and perspectives. *Cancer Chemotherapy and Pharmacology*, *32*(2), 103–108. https://doi.org/10.1007/BF00685611

Pommier, Y., Leo, E., Zhang, H., & Marchand, C. (2010). DNA topoisomerases and their poisoning by anticancer and antibacterial drugs. *Chemistry and Biology*, *17*, 421–433. https://doi.org/10.1016/j.chembiol.2010.04.012

Post, G. C., Barthel, B. L., Burkhart, D. J., Hagadorn, J. R., & Koch, T. H. (2005). Doxazolidine, a proposed active metabolite of doxorubicin that cross-links DNA. *Journal of Medicinal Chemistry*, *48*(24), 7648–7657. https://doi.org/10.1021/jm050678v

Pourtau, L., Oliveira, H., Thevenot, J., Wan, Y., Brisson, A. R., Sandre, O., Miraux, S., Thiaudiere, E., & Lecommandoux, S. (2013). Antibody-Functionalized Magnetic Polymersomes: In vivo Targeting and Imaging of Bone Metastases using High Resolution MRI. *Advanced Healthcare Materials*, *2*(11), 1420–1424. https://doi.org/10.1002/adhm.201300061

Prabhakar, U., Maeda, H., K. Jain, R., Sevick-Muraca, E. M., Zamboni, W., Farokhzad, O. C., Barry, S. T., Gabizon, A., Grodzinski, P., & Blakey, D. C. (2013). Challenges and key considerations of the enhanced permeability and retention effect for nanomedicine drug delivery in oncology. *Cancer Research*, *79*(8), 2412–2417. https://doi.org/10.1158/0008-5472.CAN-12-4561

Prud'homme, G. J., & Glinka, Y. (2012). Neuropilins are multifunctional coreceptors involved in tumor initiation, growth, metastasis and immunity. *Oncotarget*, *3*(9), 921–939. https://doi.org/10.18632/oncotarget.626

Rapoport, N. (2004). Combined cancer therapy by micellar-encapsulated drug and ultrasound. *International Journal of Pharmaceutics*, *277*(1–2), 155–162. https://doi.org/10.1016/j.ijpharm.2003.09.048

Reinert, K. E. (1983). Anthracycline-binding induced DNA stiffening, bending and elongation; stereochemical implications from viscometric investigations. *Nucleic Acids Research*, *11*(10), 3411–3430.

Rinehart, J. J., Lewis, R. P., & Balcerzak, S. P. (1974). Adriamycin cardiotoxicity in man. *Annals of Internal Medicine*, *81*(4), 475–478. https://doi.org/10.7326/0003-4819-81-4-475

Rodríguez, F., Caruana, P., De la Fuente, N., Español, P., Gámez, M., Balart, J., Llurba, E., Rovira, R., Ruiz, R., Martín-Lorente, C., Corchero, J. L., & Céspedes, M. V. (2022). Nano-Based Approved Pharmaceuticals for Cancer Treatment: Present and Future Challenges. *Biomolecules*, *12*(6), 784. https://doi.org/10.3390/biom12060784

Rogerson, A., Cummings, J., Willmott, N., & Florence, A. T. (1988). The distribution of doxorubicin in mice following administration in niosomes. *The Journal of Pharmacy and Pharmacology*, *40*(5), 337–342. https://doi.org/10.1111/j.2042-7158.1988.tb05263.x

Roth, L., Prahst, C., Ruckdeschel, T., Savant, S., Weström, S., Fantin, A., Riedel, M., Héroult, M., Ruhrberg, C., & Augustin, H. G. (2016). Neuropilin-1 mediates vascular permeability independently of vascular endothelial growth factor receptor-2 activation. *Science Signaling*, *9*(425), ra42. https://doi.org/10.1126/scisignal.aad3812

Ruoslahti, E. (2002). Specialization of tumour vasculature. *Nature Reviews Cancer*, *2*, 83–90. https://doi.org/10.1038/nrc724

Ruoslahti, E. (2004). Vascular zip codes in angiogenesis and metastasis. *Biochemical Society Transactions*, *32*, 397–402. https://doi.org/10.1042/bst0320397

Ruoslahti, E. (2012). Peptides as targeting elements and tissue penetration devices for nanoparticles. *Advanced Materials (Deerfield Beach, Fla.)*, *24*(28), 3747–3756. https://doi.org/10.1002/adma.201200454

Ruoslahti, E. (2017). Tumor penetrating peptides for improved drug delivery. *Advanced Drug Delivery Reviews*, *110–111*, 3–12. https://doi.org/10.1016/j.addr.2016.03.008

Ruoslahti, E. (2022). Molecular ZIP codes in targeted drug delivery. *Proceedings of the National Academy of Sciences of the United States of America*, *119*(28). https://doi.org/10.1073/pnas.2200183119

Ruoslahti, E., Bhatia, S. N., & Sailor, M. J. (2010). Targeting of drugs and nanoparticles to tumors. *The Journal of Cell Biology*, *188*(6), 759–768. https://doi.org/10.1083/jcb.200910104

Rustin, G. J. S., Galbraith, S. M., Anderson, H., Stratford, M., Folkes, L. K., Sena, L., Gumbrell, L., & Price, P. M. (2003). Phase I clinical trial of weekly combretastatin A4 phosphate: Clinical and pharmacokinetic results. *Journal of Clinical Oncology: Official Journal of the American Society of Clinical Oncology*, *21*(15), 2815–2822. https://doi.org/10.1200/JCO.2003.05.185

Säälik, P., Lingasamy, P., Toome, K., Mastandrea, I., Rousso-Noori, L., Tobi, A., Simón-Gracia, L., Hunt, H., Paiste, P., Kotamraju, V. R., Bergers, G., Asser, T., Rätsep, T., Ruoslahti, E., Bjerkvig, R., Friedmann-Morvinski, D., & Teesalu, T. (2019). Peptide-guided nanoparticles for glioblastoma targeting. *Journal of Controlled Release*, *308*, 109–118. https://doi.org/10.1016/J.JCONREL.2019.06.018

Salmon, B. A., & Siemann, D. W. (2007). Characterizing the Tumor Response to Treatment With Combretastatin A4 Phosphate. *International Journal of Radiation Oncology Biology Physics*, *68*(1). https://doi.org/10.1016/j.ijrobp.2006.12.051

Salvatorelli, E., Menna, P., Gonzalez Paz, O., Surapaneni, S., Aukerman, S. L., Chello, M., Covino, E., Sung, V., & Minotti, G. (2012). Pharmacokinetic Characterization of Amrubicin Cardiac Safety in an Ex Vivo Human Myocardial Strip Model. II. Amrubicin Shows Metabolic Advantages over Doxorubicin and Epirubicin. *Journal of Pharmacology and Experimental Therapeutics*, *341*(2), 474–483. https://doi.org/10.1124/jpet.111.190264

Sánchez-Cerviño, M. C., Fuioaga, C. P., Atanase, L. I., Abraham, G. A., & Rivero, G. (2023). Electrohydrodynamic Techniques for the Manufacture and/or Immobilization of Vesicles. *Polymers*, *15*(4), Article 4. https://doi.org/10.3390/polym15040795

Sankar, V., Ruckmani, K., Durga, S., & Jailani, S. (2010). Proniosomes as drug carriers. *Pakistan Journal of Pharmaceutical Sciences*, *23*(1), 103–107.

Santner, S. J., Dawson, P. J., Tait, L., Soule, H. D., Eliason, J., Mohamed, A. N., Wolman, S. R., Heppner, G. H., & Miller, F. R. (2001). Malignant MCF10CA1 cell lines derived from premalignant human breast epithelial MCF10AT cells. *Breast Cancer Research and Treatment*, *65*(2), 101–110. https://doi.org/10.1023/A:1006461422273

Sarin, H. (2010). Physiologic upper limits of pore size of different blood capillary types and another perspective on the dual pore theory of microvascular permeability. *Journal of Angiogenesis Research*, *2*(14). https://doi.org/10.1186/2040-2384-2-14

Scodeller, P., & Asciutto, E. K. (2020). Targeting Tumors Using Peptides. *Molecules*, *25*(4), Article 4. https://doi.org/10.3390/molecules25040808

Scodeller, P., Simón-Gracia, L., Kopanchuk, S., Tobi, A., Kilk, K., Säälik, P., Kurm, K., Squadrito, M. L., Kotamraju, V. R., Rinken, A., De Palma, M., Ruoslahti, E., & Teesalu, T. (2017). Precision Targeting of Tumor Macrophages with a CD206 Binding Peptide. *Scientific Reports*, *7*, 14655–14666. https://doi.org/10.1038/s41598-017-14709-x

Seebacher, N. A., Krchniakova, M., Stacy, A. E., Skoda, J., & Jansson, P. J. (2021). Tumour Microenvironment Stress Promotes the Development of Drug Resistance. *Antioxidants*, *10*(11), 1801. https://doi.org/10.3390/antiox10111801

Semenza, G. L. (2014). Oxygen sensing, hypoxia-inducible factors, and disease pathophysiology. *Annual Review of Pathology*, *9*, 47–71. https://doi.org/10.1146/annurev-pathol-012513-104720

Senior, J. R. (2012). Alanine aminotransferase: A clinical and regulatory tool for detecting liver injury-past, present, and future. *Clinical Pharmacology and Therapeutics*, *92*(3), 332–339. https://doi.org/10.1038/clpt.2012.108

Sharma, G., Karmali, P., Ramirez, M., Xie, H., Kotamraju, V. R., Ruoslahti, E., & Smith, J. (2010). Targeting tumor associated macrophages using clodronate-loaded PLGA nanoparticles. *Nanotechnology*, *3*, 382–385.

Sharma, S., Kotamraju, V. R., Mölder, T., Tobi, A., Teesalu, T., & Ruoslahti, E. (2017). Tumor-Penetrating Nanosystem Strongly Suppresses Breast Tumor Growth. *Nano Letters*, *17*(3), 1356–1364. https://doi.org/10.1021/acs.nanolett.6b03815

Sharma, S., Mann, A. P., Mölder, T., Kotamraju, V. R., Mattrey, R., Teesalu, T., & Ruoslahti, E. (2017). Vascular changes in tumors resistant to a vascular disrupting nanoparticle treatment. *Journal of Controlled Release : Official Journal of the Controlled Release Society*, *268*, 49–56. https://doi.org/10.1016/J.JCONREL.2017.10.006

She, Z.-G., Hamzah, J., Kotamraju, V. R., Pang, H.-B., Jansen, S., & Ruoslahti, E. (2016). Plaque-penetrating peptide inhibits development of hypoxic atherosclerotic plaque. *Journal of Controlled Release: Official Journal of the Controlled Release Society*, *238*, 212–220. https://doi.org/10.1016/j.jconrel.2016.07.020

Shimomura, T., Fujiwara, H., Ikawa, S., Kigawa, J., & Terakawa, N. (1998). Effects of Taxol on blood cells. *The Lancet*, *352*, 541–542. https://doi.org/10.1016/S0140-6736(05)79249-7

Shockley, T. R., Lin, K., Nagi, J. A., Tompkins, R. G., Dvorak, H. F., & Yarmush, M. L. (1991). Penetration of Tumor Tissue by Antibodies and Other Immunoproteins. *Annals of the New York Academy of Sciences*, *618*, 367–382. https://doi.org/10.1111/j.1749-6632.1991.tb27257.x

Shtil, A. A., Grinchuk, T. M., Tee, L., Mechetner, E. B., & Ignatova, T. N. (2000). Over-expression of P-glycoprotein is associated with a decreased mitochondrial trans-membrane potential in doxorubicin-selected K562 human leukemia cells. *International Journal of Oncology*, *17*(2), 387–392. https://doi.org/10.3892/ijo.17.2.387

Sidorenko, V., Scodeller, P., Uustare, A., Ogibalov, I., Tasa, A., Tshubrik, O., Salumäe, L., Sugahara, K. N., Simón-Gracia, L., & Teesalu, T. (2024). Targeting vascular disrupting agent-treated tumor microenvironment with tissue-penetrating nanotherapy. *Scientific Reports*, *14*, 17513. https://doi.org/10.1038/s41598-024-64610-7

Siemann, D. W. (2011). The unique characteristics of tumor vasculature and preclinical evidence for its selective disruption by Tumor-Vascular Disrupting Agents. *Cancer Treatment Reviews*, *37*(1). https://doi.org/10.1016/j.ctrv.2010.05.001

Siemann, D. W., & Horsman, M. R. (2008). Small-Molecule Vascular Disrupting Agents in Cancer Therapy. In B. A. Teicher & L. M. Ellis (Eds.), *Antiangiogenic Agents in Cancer Therapy* (pp. 297–310). Humana Press. https://doi.org/10.1007/978-1-59745-184-0_17

Siemann, D. W., Mercer, E., Lepler, S., & Rojiani, A. M. (2002). Vascular targeting agents enhance chemotherapeutic agent activities in solid tumor therapy. *International Journal of Cancer*, *99*(1), 1–6. https://doi.org/10.1002/ijc.10316

Simón-Gracia, L., Hunt, H., Scodeller, P. D., Gaitzsch, J., Braun, G. B., Willmore, A.-M. A., Ruoslahti, E., Battaglia, G., & Teesalu, T. (2016). Paclitaxel-Loaded Polymersomes for Enhanced Intraperitoneal Chemotherapy. *Molecular Cancer Therapeutics*, *15*(4), 670–679. https://doi.org/10.1158/1535-7163.MCT-15-0713-T

Simón-Gracia, L., Hunt, H., Scodeller, P., Gaitzsch, J., Kotamraju, V. R., Sugahara, K. N., Tammik, O., Ruoslahti, E., Battaglia, G., & Teesalu, T. (2016). iRGD peptide conjugation potentiates intraperitoneal tumor delivery of paclitaxel with polymersomes. *Biomaterials*, *104*, 247–257. https://doi.org/10.1016/j.biomaterials.2016.07.023

Simón-Gracia, L., Scodeller, P., Fuentes, S. S., Vallejo, V. G., Ríos, X., San Sebastián, E., Sidorenko, V., Di Silvio, D., Suck, M., De Lorenzi, F., Rizzo, L. Y., von Stillfried, S., Kilk, K., Lammers, T., Moya, S. E., & Teesalu, T. (2018). Application of polymersomes engineered to target p32 protein for detection of small breast tumors in mice. *Oncotarget*, *9*(27), 18682–18697. https://doi.org/10.18632/oncotarget.24588

Simón-Gracia, L., Sidorenko, V., Uustare, A., Ogibalov, I., Tasa, A., Tshubrik, O., & Teesalu, T. (2021). Novel Anthracycline Utorubicin for Cancer Therapy. *Angewandte Chemie*, *60*(31), 17018–17027. https://doi.org/10.1002/anie.202016421

Singh, S. R., Rameshwar, P., & Siegel, P. (2016). Targeting tumor microenvironment in cancer therapy. *Cancer Letters*, *380*(1), 203–204. https://doi.org/10.1016/j.canlet.2016.04.009

Sivaram, A. J., Wardiana, A., Howard, C. B., Mahler, S. M., & Thurecht, K. J. (2018). Recent Advances in the Generation of Antibody-Nanomaterial Conjugates. *Advanced Healthcare Materials*, *7*(1). https://doi.org/10.1002/adhm.201700607

Soker, S., Takashima, S., Miao, H. Q., Neufeld, G., & Klagsbrun, M. (1998). Neuropilin-1 is expressed by endothelial and tumor cells as an isoform- specific receptor for vascular endothelial growth factor. *Cell*, *92*, 735–745. https://doi.org/10.1016/S0092-8674(00)81402-6

Solmaz, U., Mat, E., Dereli, M. L., Turan, V., Peker, N., Tosun, G., Dogan, A., Adiyeke, M., Ozdemir, A., Gungorduk, K., Sanci, M., & Yildirim, Y. (2015). Does neoadjuvant chemotherapy plus cytoreductive surgery improve survival rates in patients with advanced epithelial ovarian cancer compared with cytoreductive surgery alone? *Journal of B.U.ON.*, *20*(3), 847–854.

Staton, C. A., Kumar, I., Reed, M. W. R., & Brown, N. J. (2007). Neuropilins in physiological and pathological angiogenesis. *Journal of Pathology*, *212*, 237–248. https://doi.org/10.1002/path.2182

Stephenson, J. M., Banerjee, S., Saxena, N. K., Cherian, R., & Banerjee, S. K. (2002). Neuropilin-1 is differentially expressed in myoepithelial cells and vascular smooth muscle cells in preneoplastic and neoplastic human breast: A possible marker for the progression of breast cancer. *International Journal of Cancer*, *101*(5), 409–414. https://doi.org/10.1002/ijc.10611

Stevenson, J. P., Rosen, M., Sun, W., Gallagher, M., Haller, D. G., Vaughn, D., Giantonio, B., Zimmer, R., Petros, W. P., Stratford, M., Chaplin, D., Young, S. L., Schnall, M., & O'Dwyer, P. J. (2003). Phase I trial of the antivascular agent combretastatin A4 phosphate on a 5-day schedule to patients with cancer: Magnetic resonance imaging evidence for altered tumor blood flow. *Journal of Clinical Oncology: Official Journal of the American Society of Clinical Oncology*, *21*(23), 4428–4438. https://doi.org/10.1200/JCO.2003.12.986

Straume, O., & Akslen, L. A. (2003). Increased expression of VEGF-receptors (FLT-1, KDR, NRP-1) and thrombospondin-1 is associated with glomeruloid microvascular proliferation, an aggressive angiogenic phenotype, in malignant melanoma. *Angiogenesis*, *6*(4), 295–301. https://doi.org/10.1023/B:AGEN.0000029408.08638.aa

Sugahara, K. N., Scodeller, P., Braun, G. B., de Mendoza, T. H., Tatiana Hurtado de Mendoza, Yamazaki, C. M., Kluger, M. D., Kitayama, J., Alvarez, E. A., Howell, S. B., Teesalu, T., Ruoslahti, E., & Lowy, A. M. (2015). A Tumor-Penetrating Peptide Enhances Circulation-Independent Targeting of Peritoneal Carcinomatosis. *Journal of Controlled Release*, *212*, 59–69. https://doi.org/10.1016/j.jconrel.2015.06.009

Sugahara, K. N., Teesalu, T., Karmali, P. P., Kotamraju, V. R., Agemy, L., Girard, O. M., Hanahan, D., Mattrey, R. F., & Ruoslahti, E. (2009). Tissue-Penetrating Delivery of Compounds and Nanoparticles into Tumors. *Cancer Cell*, *8*(16), 510–520. https://doi.org/10.1016/j.ccr.2009.10.013

Sugahara, K. N., Teesalu, T., Karmali, P. P., Kotamraju, V. R., Agemy, L., Greenwald, D. R., & Ruoslahti, E. (2010). Coadministration of a Tumor-Penetrating Peptide Enhances the Efficacy of Cancer Drugs. *Science*, *328*(5981), 1031–1035. https://doi.org/10.1126/science.1183057

Sun, L., Liu, H., Ye, Y., Lei, Y., Islam, R., Tan, S., Tong, R., Miao, Y.-B., & Cai, L. (2023). Smart nanoparticles for cancer therapy. *Signal Transduction and Targeted Therapy*, *8*(1), Article 1. https://doi.org/10.1038/s41392-023-01642-x

Sun, X., Li, Y., Liu, T., Li, Z., Zhang, X., & Chen, X. (2017). Peptide-based imaging agents for cancer detection. *Advanced Drug Delivery Reviews*, *110–111*, 38–51. https://doi.org/10.1016/j.addr.2016.06.007

Suzuki, T., Minamide, S., Iwasaki, T., Yamamoto, H., & Kanda, H. (1997). Cardiotoxicity of a new anthracycline derivative (SM-5887) following intravenous administration to rabbits: Comparative study with doxorubicin. *Investigational New Drugs*, *15*(3), 219–225. https://doi.org/10.1023/A:1005862730941

Swenson, C. E., Perkins, W. R., Roberts, P., & Janoff, A. S. (2001). Liposome technology and the development of Myocet™ (liposomal doxorubicin citrate). *The Breast*, *2*, 1–7. https://doi.org/10.1054/brst.2000.0201

Tacar, O., Sriamornsak, P., & Dass, C. R. (2012). Doxorubicin: An update on anticancer molecular action, toxicity and novel drug delivery systems. *Journal of Pharmacy and Pharmacology*, *65*(2), 157–170. https://doi.org/10.1111/j.2042-7158.2012.01567.x

Tavano, L., Vivacqua, M., Carito, V., Muzzalupo, R., Caroleo, M. C., & Nicoletta, F. (2013). Doxorubicin loaded magneto-niosomes for targeted drug delivery. *Colloids and Surfaces. B, Biointerfaces*, *102*, 803–807. https://doi.org/10.1016/j.colsurfb.2012.09.019

Teesalu, T., Sugahara, K. N., Kotamraju, V. R., & Ruoslahti, E. (2009). C-end rule peptides mediate neuropilin-1-dependent cell, vascular, and tissue penetration. *Proceedings of the National Academy of Sciences*, *106*(38), 16157–16162. https://doi.org/10.1073/pnas.0908201106

Teesalu, T., Sugahara, K. N., & Ruoslahti, E. (2012). Mapping of vascular ZIP codes by phage display. *Methods in Enzymology*, *503*, 35–56. https://doi.org/10.1016/B978-0-12-396962-0.00002-1

Teesalu, T., Sugahara, K. N., & Ruoslahti, E. (2013). Tumor-penetrating peptides. *Frontiers in Oncology*, *3*, 216. https://doi.org/10.1016/B978-0-08-100736-5.00014-4

Tewey, K. M., Rowe, T. C., Yang, L., Halligan, B. D., & Liu, L. F. (1984). Adriamycin-induced DNA damage mediated by mammalian DNA topoisomerase II. *Science (New York, N.Y.)*, *226*(4673), 466–468. https://doi.org/10.1126/science.6093249

Thevenot, J., Oliveira, H., & Lecommandoux, S. (2013). Polymersomes for theranostics. *Journal of Drug Delivery Science and Technology*, *23*(1), 38–46. https://doi.org/10.1016/S1773-2247(13)50005-0

Thurber, G. M., Schmidt, M. M., & Wittrup, K. D. (2008). Antibody tumor penetration. *Advanced Drug Delivery Reviews*, *60*(12), 1421. https://doi.org/10.1016/j.addr.2008.04.012

Tian, X., Nyberg, S., Sharp, P. S., Madsen, J., Daneshpour, N., Armes, S. P., Berwick, J., Azzouz, M., Shaw, P., Abbott, N. J., & Battaglia, G. (2015). LRP-1-mediated intracellular antibody delivery to the Central Nervous System. *Scientific Reports*, *5*(1), 11990. https://doi.org/10.1038/srep11990

Tobi, A., Willmore, A. A., Kilk, K., Sidorenko, V., Braun, G. B., Soomets, U., Sugahara, K. N., Ruoslahti, E., & Teesalu, T. (2021). Silver Nanocarriers Targeted with a CendR Peptide Potentiate the Cytotoxic Activity of an Anticancer Drug. *Advanced Therapeutics*, *4*, 2000097. https://doi.org/10.1002/adtp.202000097

Tozer, G. M., Kanthou, C., & Baguley, B. C. (2005). Disrupting tumour blood vessels. *Nature Reviews Cancer*, *5*(6). https://doi.org/10.1038/nrc1628

Tsuchikama, K., Anami, Y., Ha, S. Y. Y., & Yamazaki, C. M. (2024). Exploring the next generation of antibody–drug conjugates. *Nature Reviews Clinical Oncology*, 1–21. https://doi.org/10.1038/s41571-023-00850-2

Ucaryilmaz Metin, C., & Ozcan, G. (2022). The HIF-1α as a Potent Inducer of the Hallmarks in Gastric Cancer. *Cancers*, *14*(11), 2711. https://doi.org/10.3390/cancers14112711

Uchegbu, I. F., & Vyas, S. P. (1998). Non-ionic surfactant based vesicles (niosomes) in drug delivery. *International Journal of Pharmaceutics*, *172*(1), 33–70. https://doi.org/10.1016/S0378-5173(98)00169-0

Uhlen, M., Zhang, C., Lee, S., Sjöstedt, E., Fagerberg, L., Bidkhori, G., Benfeitas, R., Arif, M., Liu, Z., Edfors, F., Sanli, K., Von Feilitzen, K., Oksvold, P., Lundberg, E., Hober, S., Nilsson, P., Mattsson, J., Schwenk, J. M., Brunnström, H., … Ponten, F. (2017). A pathology atlas of the human cancer transcriptome. *Science*, *357*(660), 1–11. https://doi.org/10.1126/science.aan2507

Vadevoo, S. M. P., Gurung, S., Lee, H.-S., Gunassekaran, G. R., Lee, S.-M., Yoon, J.-W., Lee, Y.-K., & Lee, B. (2023). Peptides as multifunctional players in cancer therapy.

Experimental & Molecular Medicine, *55*(6), Article 6. https://doi.org/10.1038/s12276-023-01016-x

Van Vlerken, L. E., Vyas, T. K., & Amiji, M. M. (2007). Poly(ethylene glycol)-modified nanocarriers for tumor-targeted and intracellular delivery. *Pharmaceutical Research*, *24*(8), 1405–1414. https://doi.org/10.1007/s11095-007-9284-6

Varshavsky-Yanovsky, A. N., & Goldstein, L. J. (2020). Role of Capecitabine in Early Breast Cancer. *Journal of Clinical Oncology*, *38*(3), 179–182. https://doi.org/10.1200/JCO.19.02946

Venkatesh, P., & Kasi, A. (2023). Anthracyclines. In *StatPearls*. StatPearls Publishing. http://www.ncbi.nlm.nih.gov/books/NBK538187/

Verma, N., & Vinayak, M. (2012). A low dose of doxorubicin improves antioxidant defence system and modulates anaerobic metabolism during the development of lymphoma. *Indian Journal of Pharmacology*, *44*(3), 308–313. https://doi.org/10.4103/0253-7613.96299

Vhora, I., Patil, S., Bhatt, P., & Misra, A. (2015). Chapter One - Protein– and Peptide–Drug Conjugates: An Emerging Drug Delivery Technology. In R. Donev (Ed.), *Advances in Protein Chemistry and Structural Biology* (Vol. 98, pp. 1–55). Academic Press. https://doi.org/10.1016/bs.apcsb.2014.11.001

Vincent, L., Kermani, P., Young, L. M., Cheng, J., Zhang, F., Shido, K., Lam, G., Bompais-Vincent, H., Zhu, Z., Hicklin, D. J., Bohlen, P., Chaplin, D. J., May, C., & Rafii, S. (2005). Combretastatin A4 phosphate induces rapid regression of tumor neovessels and growth through interference with vascular endothelial-cadherin signaling. *The Journal of Clinical Investigation*, *115*(11), 2992–3006. https://doi.org/10.1172/JCI24586

Wang, D., Zou, L., Jin, Q., Hou, J., Ge, G., & Yang, L. (2018). Human carboxylesterases: A comprehensive review. *Acta Pharmaceutica Sinica B*, *8*(5), 699–712. https://doi.org/10.1016/j.apsb.2018.05.005

Wang, L., Chierico, L., Little, D., Patikarnmonthon, N., Yang, Z., Azzouz, M., Madsen, J., Armes, S. P., & Battaglia, G. (2012). Encapsulation of Biomacromolecules within Polymersomes by Electroporation. *Angewandte Chemie International Edition*, *51*(44), 11122–11125. https://doi.org/10.1002/anie.201204169

Wayakanon, K., Thornhill, M. H., Douglas, C. W. I., Lewis, A. L., Warren, N. J., Pinnock, A., Armes, S. P., Battaglia, G., & Murdoch, C. (2013). Polymersome-mediated intracellular delivery of antibiotics to treat Porphyromonas gingivalis-infected oral epithelial cells. *FASEB Journal: Official Publication of the Federation of American Societies for Experimental Biology*, *27*(11), 4455–4465. https://doi.org/10.1096/fj.12-225219

Weiss, R. B. (1992). The anthracyclines: Will we ever find a better doxorubicin? *Seminars in Oncology*, *19*(6), 670–686.

Weiss, R. B., Donehower, R. C., Wiernik, P. H., Ohnuma, T., Gralla, R. J., Trump, D. L., Baker, J. R., Van Echo, D. A., Von Hoff, D. D., & Leyland-Jones, B. (1990). Hypersensitivity reactions from taxol. *Journal of Clinical Oncology*, *8*(7), 1263–1268. https://doi.org/10.1200/JCO.1990.8.7.1263

Wicki, A., Witzigmann, D., Balasubramanian, V., & Huwyler, J. (2015). Nanomedicine in cancer therapy: Challenges, opportunities, and clinical applications. *Journal of Controlled Release*, *200*, 138–157. https://doi.org/10.1016/j.jconrel.2014.12.030

Wilhelm, S., Tavares, A. J., Dai, Q., Ohta, S., Audet, J., Dvorak, H. F., & Chan, W. C. W. (2016). Analysis of nanoparticle delivery to tumours. *Nature Reviews Materials*, *1*(5), 1–12. https://doi.org/10.1038/natrevmats.2016.14

Williams, H. D., Trevaskis, N. L., Charman, S. A., Shanker, R. M., Charman, W. N., Pouton, C. W., & Porter, C. J. H. (2013). Strategies to Address Low Drug Solubility in Discovery and Development. *Pharmacological Reviews*, *65*(1), 315–499. https://doi.org/10.1124/pr.112.005660

Willmore, A.-M. A., Simón-Gracia, L., Toome, K., Paiste, P., Kotamraju, V. R., Mölder, T., Sugahara, K. N., Ruoslahti, E., Braun, G. B., & Teesalu, T. (2016). Targeted silver nanoparticles for ratiometric cell phenotyping. *Nanoscale*, *8*, 9096–9101. https://doi.org/10.1039/c5nr07928d

Witika, B. A., Bassey, K. E., Demana, P. H., Siwe-Noundou, X., & Poka, M. S. (2022). Current Advances in Specialised Niosomal Drug Delivery: Manufacture, Characterization and Drug Delivery Applications. *International Journal of Molecular Sciences*, *23*(17), Article 17. https://doi.org/10.3390/ijms23179668

Witkamp, A. J., de Bree, E., Van Goethem, R., & Zoetmulder, F. A. N. (2001). Rationale and techniques of intra-operative hyperthermic intraperitoneal chemotherapy. *Cancer Treatment Reviews*, *27*(6), 365–374. https://doi.org/10.1053/ctrv.2001.0232

World Health Organization. (2023). *Web Annex A. World Health Organization Model List of Essential Medicines – 23rd List, 2023 3. In: The selection and use of essential medicines 2023: Executive summary of the report of the 24th WHO Expert Committee on the Selection and Use of Essential Medicines, 24 – 28 April 2023.* https://www.who.int/publications-detail-redirect/WHO-MHP-HPS-EML-2023.02

Xu, G., Zhang, W., Ma, M. K., & McLeod, H. L. (2002). Human carboxylesterase 2 is commonly expressed in tumor tissue and is correlated with activation of irinotecan. *Clinical Cancer Research*, *8*, 2605–2611.

Xu, H., Meng, F., & Zhong, Z. (2009). Reversibly crosslinked temperature-responsive nano-sized polymersomes: Synthesis and triggered drug release. *Journal of Materials Chemistry*, *19*(24), 4183–4190. https://doi.org/10.1039/b901141b

Yamaoka, T., Hanada, M., Ichii, S., Morisada, S., Noguchi, T., & Yanagi, Y. (1998). Cytotoxicity of amrubicin, a novel 9-aminoanthracycline, and its active metabolite amrubicinol on human tumor cells. *Japanese Journal of Cancer Research*, *89*(10), 1067–1073. https://doi.org/10.1111/j.1349-7006.1998.tb00498.x

Yamaoka, T., Hanada, M., Ichii, S., Morisada, S., Noguchi, T., & Yanagi, Y. (1999). Uptake and Intracellular Distribution of Amrubicin, a Novel 9-Amino-anthracycline, and Its Active Metabolite Amrubicinol in P388 Murine Leukemia Cells. *Japanese Journal of Cancer Research : Gann*, *90*(6), 685–690. https://doi.org/10.1111/j.1349-7006.1999.tb00801.x

Yan, F., Wang, S., Yang, W., Goldberg, S. N., Wu, H., Duan, W.-L., Deng, Z.-T., Han, H.-B., & Zheng, H.-R. (2017). Tumor-penetrating Peptide-integrated Thermally Sensitive Liposomal Doxorubicin Enhances Efficacy of Radiofrequency Ablation in Liver Tumors. *Radiology*, *285*(2), 462–471. https://doi.org/10.1148/radiol.2017162405

Yaqoob, U., Cao, S., Shergill, U., Jagavelu, K., Geng, Z., Yin, M., De Assuncao, T. M., Cao, Y., Szabolcs, A., Thorgeirsson, S., Schwartz, M., Yang, J. D., Ehman, R., Roberts, L., Mukhopadhyay, D., & Shah, V. H. (2012). Neuropilin-1 stimulates tumor growth by increasing fibronectin fibril assembly in the tumor microenvironment. *Cancer Research*, *72*(16), 4047–4059. https://doi.org/10.1158/0008-5472.CAN-11-3907

Yenugonda, V., Nomura, N., Kouznetsova, V., Tsigelny, I., Fogal, V., Nurmemmedov, E., Kesari, S., & Babic, I. (2017). A novel small molecule inhibitor of p32 mitochondrial protein overexpressed in glioma. *Journal of Translational Medicine*, *15*(1), 210. https://doi.org/10.1186/s12967-017-1312-7

Yeo, P. L., Lim, C. L., Chye, S. M., Ling, A. P. K., & Koh, R. Y. (2017). Niosomes: A review of their structure, properties, methods of preparation, and medical applications. *Asian Biomedicine*, *11*(4), 301–314.

Yoo, J., Park, C., Yi, G., Lee, D., & Koo, H. (2019). Active Targeting Strategies Using Biological Ligands for Nanoparticle Drug Delivery Systems. *Cancers*, *11*(5), Article 5. https://doi.org/10.3390/cancers11050640

Young, S., Ostowari, A., Yu, J., Eng, O. S., Dayyani, F., & Senthil, M. (2022). The role of cytoreductive surgery and intraperitoneal chemotherapy in gastric cancer. *Clinical Advances in Hematology & Oncology: H&O*, *20*(11), 673–682.

Yu, M. K., Park, J., & Jon, S. (2012). Targeting strategies for multifunctional nanoparticles in cancer imaging and therapy. *Theranostics*, *2*(1), 3–44. https://doi.org/10.7150/thno.3463

Zahreddine, H., & Borden, K. L. B. (2013). Mechanisms and insights into drug resistance in cancer. *Frontiers in Pharmacology*, *28*. https://doi.org/10.3389/fphar.2013.00028

Zavaleta, C., Ho, D., & Chung, E. J. (2018). Theranostic Nanoparticles for Tracking and Monitoring Disease State. *SLAS Technology*, *23*(3), 281–293. https://doi.org/10.1177/2472630317738699

Zhang, J., Pan, L., Xu, Y., Wu, C., Wang, C., Cheng, Z., & Zhao, R. (2011). Total cholesterol content of erythrocyte membranes in acute coronary syndrome: Correlation with apolipoprotein a-i and lipoprotein (a). *Coronary Artery Disease*, *22*(3), 145–152. https://doi.org/10.1097/MCA.0b013e328343fbbb

Zhang, Y., Wang, D., Shen, D., Luo, Y., & Che, Y.-Q. (2020). Identification of exosomal miRNAs associated with the anthracycline-induced liver injury in postoperative breast cancer patients by small RNA sequencing. *PeerJ*, *8*, e9021. https://doi.org/10.7717/peerj.9021

Zinger, A., Koren, L., Adir, O., Poley, M., Alyan, M., Yaari, Z., Noor, N., Krinsky, N., Simon, A., Gibori, H., Krayem, M., Mumblat, Y., Kasten, S., Ofir, S., Fridman, E., Milman, N., Lübtow, M. M., Liba, L., Shklover, J., … Schroeder, A. (2019). Collagenase Nanoparticles Enhance the Penetration of Drugs into Pancreatic Tumors. *ACS Nano*, *13*(10), 11008–11021. https://doi.org/10.1021/acsnano.9b02395

Zunino, F., & Capranico, G. (1990). DNA topoisomerase II as the primary target of anti-tumor anthracyclines. *Anti-Cancer Drug Design*, *5*(4), 307–317.

Zuo, H., Houdong Zuo, & Zuo, H. (2019). iRGD: A Promising Peptide for Cancer Imaging and a Potential Therapeutic Agent for Various Cancers. *Journal of Oncology*, *2019*, 9367845–9367845. https://doi.org/10.1155/2019/9367845

ACKNOWLEDGEMENTS

I want to express my deepest and sincerest gratitude to my supervisors, Dr. Lorena Simón Gracia and Prof. Tambet Teesalu. Being accepted into this remarkable lab has been an incredible opportunity. 7 years ago, when I first knocked on Tambets' door, I couldn't have imagined the extraordinary journey that awaited me. The person I have become, the knowledge I have gained, the fantastic people I have met, and the unforgettable memories we've created have far exceeded my expectations. I am also very thankful to my reviewers, Prof. Jyrki Tapio Heinämäki and Dr. Piret Arukuusk, for their time and valuable feedback, which greatly helped refine my work.

Throughout this journey, I have experienced significant personal and professional growth. Each day in the lab has been filled with joy, wisdom, and great ideas. Being part of such important and groundbreaking work in the field of targeted drug delivery has been mind-blowing. I am incredibly lucky to have mentors who have opened up this fascinating nanoworld to me, and I owe a great deal to both of you for shaping me in countless ways.

This journey would not have been possible without the incredible group of people in our lab. To all past and present members, thank you all for making the lab feel like a second home. The time we've shared has flown by, filled with joy and purpose, perfectly echoing Kaarel's wise words that time passes quickly when we're having fun. I am also very grateful to Toomas for his great support with immunostainings and our stimulating coffee-time conversations! Our gatherings, discussions, and chats before work created a wonderful atmosphere that made the lab truly feel like home. Your wisdom, patience, and willingness to listen to my challenges and joys have been invaluable in keeping me going.

Lastly, my heartfelt gratitude goes to my family. To my dear parents, who supported me unconditionally and refrained from asking too often, "So, when will you defend?"— thank you for cheering me on in every situation and for accepting my decision to go abroad without hesitation. To my dearest husband, Max, you have been my biggest fan, my greatest support, and my constant source of inspiration. Thank you for agreeing to take this journey with me. And, of course, a special mention to my mom's cats, Cosmos and Sever, whose presence in my thoughts provided comfort during tough times like failed experiments.

PUBLICATIONS

CURRICULUM VITAE

Name: Valeria Sidorenko
Date of birth: December 19, 1994
E-mail: valeria.sidorenko7@gmail.com

Education:

2019–2024	University of Tartu, Doctor of Philosophy (PhD), medicine
2017–2019	University of Tartu, Master of Science (MSc), biomedicine
2014–2017	University of Tartu, Bachelor of Science (BSc), gene technology
2012–2014	Tallinn Mustamäe College, silver medal
2010–2012	Audentes Sport Gymnasium
2006–2010	Tallinn Õismäe Humanities Gymnasium
2002–2006	Narva Estonian Gymnasium

Institutions and positions:

02.2023–09.2024	Junior Research Fellow in Cancer Biology (1,00)
06.2018–09.2018	Laboratory assistant at a pathology center, The North Estonia Medical Centre (1,00)
06.2017–09.2017	Laboratory assistant at a pathology center, The North Estonia Medical Centre (1,00)

Qualifications:

2020	2 weeks stay at the University College London in the Lab of Molecular Bionics
2019	Laboratory Animal Science course, Estonian University of Life Sciences
2019	EV Winter School ‘’Basics to work with Extracellular Vesicles’’

Honors and awards:

2021	Scholarship from Valda and Bernard Õun Memorial Foundation, 5000 eur
2020	Financial assistance for study-related errands by the Doctoral School of Clinical Medicine – 2 weeks stay at the University College London (10.03–21.03.2020)
2020	Scholarship from Liisa Kolumbus Memorial Foundation, 3000 eur
2019	First prize for the MSc thesis entitled “Peptide-targeted polymersomes for cancer therapy and detection” in the Estonian National Contest for University Students in Health Research. Thesis supervisors: Dr. Lorena Simon Gracia, Prof. Tambet Teesalu

Additional information:
Teaching Assistant in course Practical Courses in Genetics (LOMR.03.023) (1.00)

Publications

1. **Sidorenko, V**., Scodeller, P., Uustare, A., Ogibalov, I., Tasa, A., Tshubrik, O., Salumäe, L., Sugahara, K.N., Simón-Gracia, L., & Teesalu, T. (2024). Targeting Vascular Disrupting Agent-Treated Tumor Microenvironment with Tissue-Penetrating Nanotherapy. Sci Rep 14, 17513. https://doi.org/10.1038/s41598-024-64610-7
2. d'Avanzo, N.*, **Sidorenko, V.***, Simón-Gracia, L., Rocchi, A., Ottonelli, I., Ruozi, B., Longo, F., Celia, C., & Teesalu, T. (2024). C-end rule peptide-guided niosomes for prostate cancer cell targeting. Journal of Drug Delivery Science and Technology, 91, 105162. https://doi.org/10.1016/j.jddst.2023.105162 **Equal contribution*
3. Simón-Gracia, L., Scodeller, P., Fisher, W. S., **Sidorenko, V**., Steffes, V. M., Ewert, K. K., Safinya, C. R., & Teesalu, T. (2022). Paclitaxel-Loaded Cationic Fluid Lipid Nanodiscs and Liposomes with Brush-Conformation PEG Chains Penetrate Breast Tumors and Trigger Caspase-3 Activation. ACS applied materials & interfaces, 14(51), 56613–56622. https://doi.org/10.1021/acsami.2c17961
4. Simón-Gracia, L., Loisel, S., **Sidorenko, V**., Scodeller, P., Parizot, C., Savier, E., Haute, T., Teesalu, T., & Rebollo, A. (2022). Preclinical Validation of Tumor-Penetrating and Interfering Peptides against Chronic Lymphocytic Leukemia. Molecular pharmaceutics, 19(3), 895–903. https://doi.org/10.1021/acs.molpharmaceut.1c00837
5. Simón-Gracia, L.*, **Sidorenko, V**.*, Uustare, A., Ogibalov, I., Tasa, A., Tshubrik, O., & Teesalu, T. (2021). Novel Anthracycline Utorubicin for Cancer Therapy. Angewandte Chemie (International ed. in English), 60(31), 17018–17027. https://doi.org/10.1002/anie.202016421 **Equal contribution*
6. Tobi, A., Willmore, A.-M.A., Kilk, K., **Sidorenko, V**., Braun, G.B., Soomets, U., Sugahara, K.N., Ruoslahti, E. and Teesalu, T. (2021), Silver Nanocarriers Targeted with a CendR Peptide Potentiate the Cytotoxic Activity of an Anticancer Drug. Adv. Therap., 4: 2000097. https://doi.org/10.1002/adtp.202000097
7. Lepland, A., Asciutto, E. K., Malfanti, A., Simón-Gracia, L., **Sidorenko, V.**, Vicent, M. J., Teesalu, T., & Scodeller, P. (2020). Targeting Pro-Tumoral Macrophages in Early Primary and Metastatic Breast Tumors with the CD206-Binding mUNO Peptide. Molecular pharmaceutics, 17(7), 2518–2531. https://doi.org/10.1021/acs.molpharmaceut.0c00226
8. Simón-Gracia, L., Scodeller, P., Fuentes, S. S., Vallejo, V. G., Ríos, X., San Sebastián, E., **Sidorenko, V**., Di Silvio, D., Suck, M., De Lorenzi, F., Rizzo, L. Y., von Stillfried, S., Kilk, K., Lammers, T., Moya, S. E., & Teesalu, T. (2018). Application of polymersomes engineered to target p32 protein for detection of small breast tumors in mice. Oncotarget, 9(27), 18682–18697. https://doi.org/10.18632/oncotarget.24588

ELULOOKIRJELDUS

Nimi: Valeria Sidorenko
Sünniaeg: 19. detsember 1994
E-mail: valeria.sidorenko7@gmail.com

Hariduskäik:

2019–2024	Tartu ülikool, filosoofiadoktor (PhD), arstiteadus
2017–2019	Tartu Ülikool, loodusteaduste magister (MSc), biomeditsiin
2014–2017	Tartu Ülikool, loodusteaduse bakalaureus (BSc), geenitehnoloogia
2012–2014	Tallinna Mustamäe Gümnaasium, hõbemedal
2010–2012	Audentese Spordigümnaasium
2006–2010	Tallinna Õismäe Humanitaargümnaasium
2002–2006	Narva Eesti Gümnaasium

Teenistuskäik:

02.2023–09.2024	Vähibioloogia nooremteadur (1,00)
06.2018–09.2018	Laboriassistent patoloogiakeskuses (1,00)
06.2017–09.2017	Laboriassistent patoloogiakeskuses (1,00)

Kvalifikatsioonid:

2020	kahe nädalane õppereis (Lab of Molecular Bionics, University College London)
2019	Laboratory Animal Science course, Eesti Maaülikool
2019	EV Winter School "Basics to work with Extracellular Vesicles''

Teaduspreemiad ja tunnustused:

2021	Valda ja Bernard Õuna mälestusfondi stipendium, 5000 eurot
2020	Tartu Ülikooli Kliinilise meditsiini doktorikooli poolne toetus õppetööga seotud välislähetuseks (ASTRA projekti PER ASPERA raames, mida finantseerib Euroopa Liidu Regionaalarengu Fond) – 2 nädalane õppevisiit koostööpartnerite laboris (UCL, London)
2020	Liisa Kolumbuse mälestusfondi stipendium, 3000 eurot
2019	Üliõpilaste teadustööde riikliku konkursil 1. preemia magistriõppe üliõpilaste astmes konkursitöö „Kullerpeptiididega suunatud polümersoomid vähi raviks ja detekteerimiseks" eest; juhendajad: PhD Lorena Simón Gracia ja Prof. Tambet Teesalu

Lisainfo:

Õppeassistent aines LOMR.03.023 Geneetika praktikum (1,00)

Publikatsioonid

1. **Sidorenko, V.**, Scodeller, P., Uustare, A., Ogibalov, I., Tasa, A., Tshubrik, O., Salumäe, L., Sugahara, K.N., Simón-Gracia, L., & Teesalu, T. (2024). Targeting Vascular Disrupting Agent-Treated Tumor Microenvironment with Tissue-Penetrating Nanotherapy. Sci Rep 14, 17513. https://doi.org/10.1038/s41598-024-64610-7
2. d'Avanzo, N.*, **Sidorenko, V.***, Simón-Gracia, L., Rocchi, A., Ottonelli, I., Ruozi, B., Longo, F., Celia, C., & Teesalu, T. (2024). C-end rule peptide-guided niosomes for prostate cancer cell targeting. Journal of Drug Delivery Science and Technology, 91, 105162. https://doi.org/10.1016/j.jddst.2023.105162 **Equal contribution*
3. Simón-Gracia, L., Scodeller, P., Fisher, W. S., **Sidorenko, V.**, Steffes, V. M., Ewert, K. K., Safinya, C. R., & Teesalu, T. (2022). Paclitaxel-Loaded Cationic Fluid Lipid Nanodiscs and Liposomes with Brush-Conformation PEG Chains Penetrate Breast Tumors and Trigger Caspase-3 Activation. ACS applied materials & interfaces, 14(51), 56613–56622. https://doi.org/10.1021/acsami.2c17961
4. Simón-Gracia, L., Loisel, S., **Sidorenko, V.**, Scodeller, P., Parizot, C., Savier, E., Haute, T., Teesalu, T., & Rebollo, A. (2022). Preclinical Validation of Tumor-Penetrating and Interfering Peptides against Chronic Lymphocytic Leukemia. Molecular pharmaceutics, 19(3), 895–903. https://doi.org/10.1021/acs.molpharmaceut.1c00837
5. Simón-Gracia, L.*, **Sidorenko, V.***, Uustare, A., Ogibalov, I., Tasa, A., Tshubrik, O., & Teesalu, T. (2021). Novel Anthracycline Utorubicin for Cancer Therapy. Angewandte Chemie (International ed. in English), 60(31), 17018–17027. https://doi.org/10.1002/anie.202016421 **Equal contribution*
6. Tobi, A., Willmore, A.-M.A., Kilk, K., **Sidorenko, V**., Braun, G.B., Soomets, U., Sugahara, K.N., Ruoslahti, E. and Teesalu, T. (2021), Silver Nanocarriers Targeted with a CendR Peptide Potentiate the Cytotoxic Activity of an Anticancer Drug. Adv. Therap., 4: 2000097. https://doi.org/10.1002/adtp.202000097
7. Lepland, A., Asciutto, E. K., Malfanti, A., Simón-Gracia, L., **Sidorenko, V.**, Vicent, M. J., Teesalu, T., & Scodeller, P. (2020). Targeting Pro-Tumoral Macrophages in Early Primary and Metastatic Breast Tumors with the CD206-Binding mUNO Peptide. Molecular pharmaceutics, 17(7), 2518–2531. https://doi.org/10.1021/acs.molpharmaceut.0c00226
8. Simón-Gracia, L., Scodeller, P., Fuentes, S. S., Vallejo, V. G., Ríos, X., San Sebastián, E., **Sidorenko, V**., Di Silvio, D., Suck, M., De Lorenzi, F., Rizzo, L. Y., von Stillfried, S., Kilk, K., Lammers, T., Moya, S. E., & Teesalu, T. (2018). Application of polymersomes engineered to target p32 protein for detection of small breast tumors in mice. Oncotarget, 9(27), 18682–18697. https://doi.org/10.18632/oncotarget.24588

DISSERTATIONES MEDICINAE UNIVERSITATIS TARTUENSIS

1. **Heidi-Ingrid Maaroos**. The natural course of gastric ulcer in connection with chronic gastritis and *Helicobacter pylori*. Tartu, 1991.
2. **Mihkel Zilmer**. Na-pump in normal and tumorous brain tissues: Structural, functional and tumorigenesis aspects. Tartu, 1991.
3. **Eero Vasar**. Role of cholecystokinin receptors in the regulation of behaviour and in the action of haloperidol and diazepam. Tartu, 1992.
4. **Tiina Talvik**. Hypoxic-ischaemic brain damage in neonates (clinical, biochemical and brain computed tomographical investigation). Tartu, 1992.
5. **Ants Peetsalu**. Vagotomy in duodenal ulcer disease: A study of gastric acidity, serum pepsinogen I, gastric mucosal histology and *Helicobacter pylori*. Tartu, 1992.
6. **Marika Mikelsaar**. Evaluation of the gastrointestinal microbial ecosystem in health and disease. Tartu, 1992.
7. **Hele Everaus**. Immuno-hormonal interactions in chronic lymphocytic leukaemia and multiple myeloma. Tartu, 1993.
8. **Ruth Mikelsaar**. Etiological factors of diseases in genetically consulted children and newborn screening: dissertation for the commencement of the degree of doctor of medical sciences. Tartu, 1993.
9. **Agu Tamm**. On metabolic action of intestinal microflora: clinical aspects. Tartu, 1993.
10. **Katrin Gross**. Multiple sclerosis in South-Estonia (epidemiological and computed tomographical investigations). Tartu, 1993.
11. **Oivi Uibo**. Childhood coeliac disease in Estonia: occurrence, screening, diagnosis and clinical characterization. Tartu, 1994.
12. **Viiu Tuulik**. The functional disorders of central nervous system of chemistry workers. Tartu, 1994.
13. **Margus Viigimaa**. Primary haemostasis, antiaggregative and anticoagulant treatment of acute myocardial infarction. Tartu, 1994.
14. **Rein Kolk**. Atrial versus ventricular pacing in patients with sick sinus syndrome. Tartu, 1994.
15. **Toomas Podar**. Incidence of childhood onset type 1 diabetes mellitus in Estonia. Tartu, 1994.
16. **Kiira Subi**. The laboratory surveillance of the acute respiratory viral infections in Estonia. Tartu, 1995.
17. **Irja Lutsar**. Infections of the central nervous system in children (epidemiologic, diagnostic and therapeutic aspects, long term outcome). Tartu, 1995.
18. **Aavo Lang**. The role of dopamine, 5-hydroxytryptamine, sigma and NMDA receptors in the action of antipsychotic drugs. Tartu, 1995.
19. **Andrus Arak**. Factors influencing the survival of patients after radical surgery for gastric cancer. Tartu, 1996.

20. **Tõnis Karki**. Quantitative composition of the human lactoflora and method for its examination. Tartu, 1996.
21. **Reet Mändar**. Vaginal microflora during pregnancy and its transmission to newborn. Tartu, 1996.
22. **Triin Remmel**. Primary biliary cirrhosis in Estonia: epidemiology, clinical characterization and prognostication of the course of the disease. Tartu, 1996.
23. **Toomas Kivastik**. Mechanisms of drug addiction: focus on positive reinforcing properties of morphine. Tartu, 1996.
24. **Paavo Pokk**. Stress due to sleep deprivation: focus on $GABA_A$ receptor-chloride ionophore complex. Tartu, 1996.
25. **Kristina Allikmets**. Renin system activity in essential hypertension. Associations with atherothrombogenic cardiovascular risk factors and with the efficacy of calcium antagonist treatment. Tartu, 1996.
26. **Triin Parik**. Oxidative stress in essential hypertension: Associations with metabolic disturbances and the effects of calcium antagonist treatment. Tartu, 1996.
27. **Svetlana Päi**. Factors promoting heterogeneity of the course of rheumatoid arthritis. Tartu, 1997.
28. **Maarike Sallo**. Studies on habitual physical activity and aerobic fitness in 4 to 10 years old children. Tartu, 1997.
29. **Paul Naaber**. *Clostridium difficile* infection and intestinal microbial ecology. Tartu, 1997.
30. **Rein Pähkla**. Studies in pinoline pharmacology. Tartu, 1997.
31. **Andrus Juhan Voitk**. Outpatient laparoscopic cholecystectomy. Tartu, 1997.
32. **Joel Starkopf**. Oxidative stress and ischaemia-reperfusion of the heart. Tartu, 1997.
33. **Janika Kõrv**. Incidence, case-fatality and outcome of stroke. Tartu, 1998.
34. **Ülla Linnamägi**. Changes in local cerebral blood flow and lipid peroxidation following lead exposure in experiment. Tartu, 1998.
35. **Ave Minajeva**. Sarcoplasmic reticulum function: comparison of atrial and ventricular myocardium. Tartu, 1998.
36. **Oleg Milenin**. Reconstruction of cervical part of esophagus by revascularised ileal autografts in dogs. A new complex multistage method. Tartu, 1998.
37. **Sergei Pakriev**. Prevalence of depression, harmful use of alcohol and alcohol dependence among rural population in Udmurtia. Tartu, 1998.
38. **Allen Kaasik**. Thyroid hormone control over β-adrenergic signalling system in rat atria. Tartu, 1998.
39. **Vallo Matto**. Pharmacological studies on anxiogenic and antiaggressive properties of antidepressants. Tartu, 1998.
40. **Maire Vasar**. Allergic diseases and bronchial hyperreactivity in Estonian children in relation to environmental influences. Tartu, 1998.
41. **Kaja Julge**. Humoral immune responses to allergens in early childhood. Tartu, 1998.

42. **Heli Grünberg**. The cardiovascular risk of Estonian schoolchildren. A cross-sectional study of 9-, 12- and 15-year-old children. Tartu, 1998.
43. **Epp Sepp**. Formation of intestinal microbial ecosystem in children. Tartu, 1998.
44. **Mai Ots**. Characteristics of the progression of human and experimental glomerulopathies. Tartu, 1998.
45. **Tiina Ristimäe**. Heart rate variability in patients with coronary artery disease. Tartu, 1998.
46. **Leho Kõiv**. Reaction of the sympatho-adrenal and hypothalamo-pituitary-adrenocortical system in the acute stage of head injury. Tartu, 1998.
47. **Bela Adojaan**. Immune and genetic factors of childhood onset IDDM in Estonia. An epidemiological study. Tartu, 1999.
48. **Jakov Shlik**. Psychophysiological effects of cholecystokinin in humans. Tartu, 1999.
49. **Kai Kisand**. Autoantibodies against dehydrogenases of α-ketoacids. Tartu, 1999.
50. **Toomas Marandi**. Drug treatment of depression in Estonia. Tartu, 1999.
51. **Ants Kask**. Behavioural studies on neuropeptide Y. Tartu, 1999.
52. **Ello-Rahel Karelson**. Modulation of adenylate cyclase activity in the rat hippocampus by neuropeptide galanin and its chimeric analogs. Tartu, 1999.
53. **Tanel Laisaar**. Treatment of pleural empyema — special reference to intrapleural therapy with streptokinase and surgical treatment modalities. Tartu, 1999.
54. **Eve Pihl**. Cardiovascular risk factors in middle-aged former athletes. Tartu, 1999.
55. **Katrin Õunap**. Phenylketonuria in Estonia: incidence, newborn screening, diagnosis, clinical characterization and genotype/phenotype correlation. Tartu, 1999.
56. **Siiri Kõljalg**. *Acinetobacter* – an important nosocomial pathogen. Tartu, 1999.
57. **Helle Karro**. Reproductive health and pregnancy outcome in Estonia: association with different factors. Tartu, 1999.
58. **Heili Varendi**. Behavioral effects observed in human newborns during exposure to naturally occurring odors. Tartu, 1999.
59. **Anneli Beilmann**. Epidemiology of epilepsy in children and adolescents in Estonia. Prevalence, incidence, and clinical characteristics. Tartu, 1999.
60. **Vallo Volke**. Pharmacological and biochemical studies on nitric oxide in the regulation of behaviour. Tartu, 1999.
61. **Pilvi Ilves**. Hypoxic-ischaemic encephalopathy in asphyxiated term infants. A prospective clinical, biochemical, ultrasonographical study. Tartu, 1999.
62. **Anti Kalda**. Oxygen-glucose deprivation-induced neuronal death and its pharmacological prevention in cerebellar granule cells. Tartu, 1999.
63. **Eve-Irene Lepist**. Oral peptide prodrugs – studies on stability and absorption. Tartu, 2000.

64. **Jana Kivastik**. Lung function in Estonian schoolchildren: relationship with anthropometric indices and respiratory symptomas, reference values for dynamic spirometry. Tartu, 2000.
65. **Karin Kull**. Inflammatory bowel disease: an immunogenetic study. Tartu, 2000.
66. **Kaire Innos**. Epidemiological resources in Estonia: data sources, their quality and feasibility of cohort studies. Tartu, 2000.
67. **Tamara Vorobjova**. Immune response to *Helicobacter pylori* and its association with dynamics of chronic gastritis and epithelial cell turnover in antrum and corpus. Tartu, 2001.
68. **Ruth Kalda**. Structure and outcome of family practice quality in the changing health care system of Estonia. Tartu, 2001.
69. **Annika Krüüner**. *Mycobacterium tuberculosis* – spread and drug resistance in Estonia. Tartu, 2001.
70. **Marlit Veldi**. Obstructive Sleep Apnoea: Computerized Endopharyngeal Myotonometry of the Soft Palate and Lingual Musculature. Tartu, 2001.
71. **Anneli Uusküla**. Epidemiology of sexually transmitted diseases in Estonia in 1990–2000. Tartu, 2001.
72. **Ade Kallas**. Characterization of antibodies to coagulation factor VIII. Tartu, 2002.
73. **Heidi Annuk**. Selection of medicinal plants and intestinal lactobacilli as antimicrobil components for functional foods. Tartu, 2002.
74. **Aet Lukmann**. Early rehabilitation of patients with ischaemic heart disease after surgical revascularization of the myocardium: assessment of health-related quality of life, cardiopulmonary reserve and oxidative stress. A clinical study. Tartu, 2002.
75. **Maigi Eisen**. Pathogenesis of Contact Dermatitis: participation of Oxidative Stress. A clinical – biochemical study. Tartu, 2002.
76. **Piret Hussar**. Histology of the post-traumatic bone repair in rats. Elaboration and use of a new standardized experimental model – bicortical perforation of tibia compared to internal fracture and resection osteotomy. Tartu, 2002.
77. **Tõnu Rätsep**. Aneurysmal subarachnoid haemorrhage: Noninvasive monitoring of cerebral haemodynamics. Tartu, 2002.
78. **Marju Herodes**. Quality of life of people with epilepsy in Estonia. Tartu, 2003.
79. **Katre Maasalu**. Changes in bone quality due to age and genetic disorders and their clinical expressions in Estonia. Tartu, 2003.
80. **Toomas Sillakivi**. Perforated peptic ulcer in Estonia: epidemiology, risk factors and relations with *Helicobacter pylori*. Tartu, 2003.
81. **Leena Puksa**. Late responses in motor nerve conduction studies. F and A waves in normal subjects and patients with neuropathies. Tartu, 2003.
82. **Krista Lõivukene**. *Helicobacter pylori* in gastric microbial ecology and its antimicrobial susceptibility pattern. Tartu, 2003.

83. **Helgi Kolk**. Dyspepsia and *Helicobacter pylori* infection: the diagnostic value of symptoms, treatment and follow-up of patients referred for upper gastrointestinal endoscopy by family physicians. Tartu, 2003.
84. **Helena Soomer**. Validation of identification and age estimation methods in forensic odontology. Tartu, 2003.
85. **Kersti Oselin**. Studies on the human MDR1, MRP1, and MRP2 ABC transporters: functional relevance of the genetic polymorphisms in the *MDR1* and *MRP1* gene. Tartu, 2003.
86. **Jaan Soplepmann**. Peptic ulcer haemorrhage in Estonia: epidemiology, prognostic factors, treatment and outcome. Tartu, 2003.
87. **Margot Peetsalu**. Long-term follow-up after vagotomy in duodenal ulcer disease: recurrent ulcer, changes in the function, morphology and *Helicobacter pylori* colonisation of the gastric mucosa. Tartu, 2003.
88. **Kersti Klaamas**. Humoral immune response to *Helicobacter pylori* a study of host-dependent and microbial factors. Tartu, 2003.
89. **Pille Taba**. Epidemiology of Parkinson's disease in Tartu, Estonia. Prevalence, incidence, clinical characteristics, and pharmacoepidemiology. Tartu, 2003.
90. **Alar Veraksitš**. Characterization of behavioural and biochemical phenotype of cholecystokinin-2 receptor deficient mice: changes in the function of the dopamine and endopioidergic system. Tartu, 2003.
91. **Ingrid Kalev**. CC-chemokine receptor 5 (CCR5) gene polymorphism in Estonians and in patients with Type I and Type II diabetes mellitus. Tartu, 2003.
92. **Lumme Kadaja**. Molecular approach to the regulation of mitochondrial function in oxidative muscle cells. Tartu, 2003.
93. **Aive Liigant**. Epidemiology of primary central nervous system tumours in Estonia from 1986 to 1996. Clinical characteristics, incidence, survival and prognostic factors. Tartu, 2004.
94. **Andres, Kulla**. Molecular characteristics of mesenchymal stroma in human astrocytic gliomas. Tartu, 2004.
95. **Mari Järvelaid**. Health damaging risk behaviours in adolescence. Tartu, 2004.
96. **Ülle Pechter**. Progression prevention strategies in chronic renal failure and hypertension. An experimental and clinical study. Tartu, 2004.
97. **Gunnar Tasa**. Polymorphic glutathione S-transferases – biology and role in modifying genetic susceptibility to senile cataract and primary open angle glaucoma. Tartu, 2004.
98. **Tuuli Käämbre**. Intracellular energetic unit: structural and functional aspects. Tartu, 2004.
99. **Vitali Vassiljev**. Influence of nitric oxide syntase inhibitors on the effects of ethanol after acute and chronic ethanol administration and withdrawal. Tartu, 2004.

100. **Aune Rehema**. Assessment of nonhaem ferrous iron and glutathione redox ratio as markers of pathogeneticity of oxidative stress in different clinical groups. Tartu, 2004.
101. **Evelin Seppet**. Interaction of mitochondria and ATPases in oxidative muscle cells in normal and pathological conditions. Tartu, 2004.
102. **Eduard Maron**. Serotonin function in panic disorder: from clinical experiments to brain imaging and genetics. Tartu, 2004.
103. **Marje Oona**. *Helicobacter pylori* infection in children: epidemiological and therapeutic aspects. Tartu, 2004.
104. **Kersti Kokk**. Regulation of active and passive molecular transport in the testis. Tartu, 2005.
105. **Vladimir Järv**. Cross-sectional imaging for pretreatment evaluation and follow-up of pelvic malignant tumours. Tartu, 2005.
106. **Andre Õun**. Epidemiology of adult epilepsy in Tartu, Estonia. Incidence, prevalence and medical treatment. Tartu, 2005.
107. **Piibe Muda**. Homocysteine and hypertension: associations between homocysteine and essential hypertension in treated and untreated hypertensive patients with and without coronary artery disease. Tartu, 2005.
108. **Külli Kingo**. The interleukin-10 family cytokines gene polymorphisms in plaque psoriasis. Tartu, 2005.
109. **Mati Merila**. Anatomy and clinical relevance of the glenohumeral joint capsule and ligaments. Tartu, 2005.
110. **Epp Songisepp**. Evaluation of technological and functional properties of the new probiotic *Lactobacillus fermentum* ME-3. Tartu, 2005.
111. **Tiia Ainla**. Acute myocardial infarction in Estonia: clinical characteristics, management and outcome. Tartu, 2005.
112. **Andres Sell**. Determining the minimum local anaesthetic requirements for hip replacement surgery under spinal anaesthesia – a study employing a spinal catheter. Tartu, 2005.
113. **Tiia Tamme**. Epidemiology of odontogenic tumours in Estonia. Pathogenesis and clinical behaviour of ameloblastoma. Tartu, 2005.
114. **Triine Annus**. Allergy in Estonian schoolchildren: time trends and characteristics. Tartu, 2005.
115. **Tiia Voor**. Microorganisms in infancy and development of allergy: comparison of Estonian and Swedish children. Tartu, 2005.
116. **Priit Kasenõmm**. Indicators for tonsillectomy in adults with recurrent tonsillitis – clinical, microbiological and pathomorphological investigations. Tartu, 2005.
117. **Eva Zusinaite**. Hepatitis C virus: genotype identification and interactions between viral proteases. Tartu, 2005.
118. **Piret Kõll**. Oral lactoflora in chronic periodontitis and periodontal health. Tartu, 2006.
119. **Tiina Stelmach**. Epidemiology of cerebral palsy and unfavourable neurodevelopmental outcome in child population of Tartu city and county, Estonia Prevalence, clinical features and risk factors. Tartu, 2006.

120. **Katrin Pudersell**. Tropane alkaloid production and riboflavine excretion in the field and tissue cultures of henbane (*Hyoscyamus niger* L.). Tartu, 2006.
121. **Külli Jaako**. Studies on the role of neurogenesis in brain plasticity. Tartu, 2006.
122. **Aare Märtson**. Lower limb lengthening: experimental studies of bone regeneration and long-term clinical results. Tartu, 2006.
123. **Heli Tähepõld**. Patient consultation in family medicine. Tartu, 2006.
124. **Stanislav Liskmann**. Peri-implant disease: pathogenesis, diagnosis and treatment in view of both inflammation and oxidative stress profiling. Tartu, 2006.
125. **Ruth Rudissaar**. Neuropharmacology of atypical antipsychotics and an animal model of psychosis. Tartu, 2006.
126. **Helena Andreson**. Diversity of *Helicobacter pylori* genotypes in Estonian patients with chronic inflammatory gastric diseases. Tartu, 2006.
127. **Katrin Pruus**. Mechanism of action of antidepressants: aspects of serotoninergic system and its interaction with glutamate. Tartu, 2006.
128. **Priit Põder**. Clinical and experimental investigation: relationship of ischaemia/reperfusion injury with oxidative stress in abdominal aortic aneurysm repair and in extracranial brain artery endarterectomy and possibilities of protection against ischaemia using a glutathione analogue in a rat model of global brain ischaemia. Tartu, 2006.
129. **Marika Tammaru**. Patient-reported outcome measurement in rheumatoid arthritis. Tartu, 2006.
130. **Tiia Reimand**. Down syndrome in Estonia. Tartu, 2006.
131. **Diva Eensoo**. Risk-taking in traffic and Markers of Risk-Taking Behaviour in Schoolchildren and Car Drivers. Tartu, 2007.
132. **Riina Vibo**. The third stroke registry in Tartu, Estonia from 2001 to 2003: incidence, case-fatality, risk factors and long-term outcome. Tartu, 2007.
133. **Chris Pruunsild**. Juvenile idiopathic arthritis in children in Estonia. Tartu, 2007.
134. **Eve Õiglane-Šlik**. Angelman and Prader-Willi syndromes in Estonia. Tartu, 2007.
135. **Kadri Haller**. Antibodies to follicle stimulating hormone. Significance in female infertility. Tartu, 2007.
136. **Pille Ööpik**. Management of depression in family medicine. Tartu, 2007.
137. **Jaak Kals**. Endothelial function and arterial stiffness in patients with atherosclerosis and in healthy subjects. Tartu, 2007.
138. **Priit Kampus**. Impact of inflammation, oxidative stress and age on arterial stiffness and carotid artery intima-media thickness. Tartu, 2007.
139. **Margus Punab**. Male fertility and its risk factors in Estonia. Tartu, 2007.
140. **Alar Toom**. Heterotopic ossification after total hip arthroplasty: clinical and pathogenetic investigation. Tartu, 2007.

141. **Lea Pehme**. Epidemiology of tuberculosis in Estonia 1991–2003 with special regard to extrapulmonary tuberculosis and delay in diagnosis of pulmonary tuberculosis. Tartu, 2007.
142. **Juri Karjagin**. The pharmacokinetics of metronidazole and meropenem in septic shock. Tartu, 2007.
143. **Inga Talvik**. Inflicted traumatic brain injury shaken baby syndrome in Estonia – epidemiology and outcome. Tartu, 2007.
144. **Tarvo Rajasalu**. Autoimmune diabetes: an immunological study of type 1 diabetes in humans and in a model of experimental diabetes (in RIP-B7.1 mice). Tartu, 2007.
145. **Inga Karu**. Ischaemia-reperfusion injury of the heart during coronary surgery: a clinical study investigating the effect of hyperoxia. Tartu, 2007.
146. **Peeter Padrik**. Renal cell carcinoma: Changes in natural history and treatment of metastatic disease. Tartu, 2007.
147. **Neve Vendt**. Iron deficiency and iron deficiency anaemia in infants aged 9 to 12 months in Estonia. Tartu, 2008.
148. **Lenne-Triin Heidmets**. The effects of neurotoxins on brain plasticity: focus on neural Cell Adhesion Molecule. Tartu, 2008.
149. **Paul Korrovits**. Asymptomatic inflammatory prostatitis: prevalence, etiological factors, diagnostic tools. Tartu, 2008.
150. **Annika Reintam**. Gastrointestinal failure in intensive care patients. Tartu, 2008.
151. **Kristiina Roots**. Cationic regulation of Na-pump in the normal, Alzheimer's and CCK_2 receptor-deficient brain. Tartu, 2008.
152. **Helen Puusepp**. The genetic causes of mental retardation in Estonia: fragile X syndrome and creatine transporter defect. Tartu, 2009.
153. **Kristiina Rull**. Human chorionic gonadotropin beta genes and recurrent miscarriage: expression and variation study. Tartu, 2009.
154. **Margus Eimre**. Organization of energy transfer and feedback regulation in oxidative muscle cells. Tartu, 2009.
155. **Maire Link**. Transcription factors FoxP3 and AIRE: autoantibody associations. Tartu, 2009.
156. **Kai Haldre**. Sexual health and behaviour of young women in Estonia. Tartu, 2009.
157. **Kaur Liivak**. Classical form of congenital adrenal hyperplasia due to 21-hydroxylase deficiency in Estonia: incidence, genotype and phenotype with special attention to short-term growth and 24-hour blood pressure. Tartu, 2009.
158. **Kersti Ehrlich**. Antioxidative glutathione analogues (UPF peptides) – molecular design, structure-activity relationships and testing the protective properties. Tartu, 2009.
159. **Anneli Rätsep**. Type 2 diabetes care in family medicine. Tartu, 2009.
160. **Silver Türk**. Etiopathogenetic aspects of chronic prostatitis: role of mycoplasmas, coryneform bacteria and oxidative stress. Tartu, 2009.

161. **Kaire Heilman**. Risk markers for cardiovascular disease and low bone mineral density in children with type 1 diabetes. Tartu, 2009.
162. **Kristi Rüütel**. HIV-epidemic in Estonia: injecting drug use and quality of life of people living with HIV. Tartu, 2009.
163. **Triin Eller**. Immune markers in major depression and in antidepressive treatment. Tartu, 2009.
164. **Siim Suutre**. The role of TGF-β isoforms and osteoprogenitor cells in the pathogenesis of heterotopic ossification. An experimental and clinical study of hip arthroplasty. Tartu, 2010.
165. **Kai Kliiman**. Highly drug-resistant tuberculosis in Estonia: Risk factors and predictors of poor treatment outcome. Tartu, 2010.
166. **Inga Villa**. Cardiovascular health-related nutrition, physical activity and fitness in Estonia. Tartu, 2010.
167. **Tõnis Org**. Molecular function of the first PHD finger domain of Autoimmune Regulator protein. Tartu, 2010.
168. **Tuuli Metsvaht**. Optimal antibacterial therapy of neonates at risk of early onset sepsis. Tartu, 2010.
169. **Jaanus Kahu**. Kidney transplantation: Studies on donor risk factors and mycophenolate mofetil. Tartu, 2010.
170. **Koit Reimand**. Autoimmunity in reproductive failure: A study on associated autoantibodies and autoantigens. Tartu, 2010.
171. **Mart Kull**. Impact of vitamin D and hypolactasia on bone mineral density: a population based study in Estonia. Tartu, 2010.
172. **Rael Laugesaar**. Stroke in children – epidemiology and risk factors. Tartu, 2010.
173. **Mark Braschinsky**. Epidemiology and quality of life issues of hereditary spastic paraplegia in Estonia and implemention of genetic analysis in everyday neurologic practice. Tartu, 2010.
174. **Kadri Suija**. Major depression in family medicine: associated factors, recurrence and possible intervention. Tartu, 2010.
175. **Jarno Habicht**. Health care utilisation in Estonia: socioeconomic determinants and financial burden of out-of-pocket payments. Tartu, 2010.
176. **Kristi Abram**. The prevalence and risk factors of rosacea. Subjective disease perception of rosacea patients. Tartu, 2010.
177. **Malle Kuum**. Mitochondrial and endoplasmic reticulum cation fluxes: Novel roles in cellular physiology. Tartu, 2010.
178. **Rita Teek**. The genetic causes of early onset hearing loss in Estonian children. Tartu, 2010.
179. **Daisy Volmer**. The development of community pharmacy services in Estonia – public and professional perceptions 1993–2006. Tartu, 2010.
180. **Jelena Lissitsina**. Cytogenetic causes in male infertility. Tartu, 2011.
181. **Delia Lepik**. Comparison of gunshot injuries caused from Tokarev, Makarov and Glock 19 pistols at different firing distances. Tartu, 2011.
182. **Ene-Renate Pähkla**. Factors related to the efficiency of treatment of advanced periodontitis. Tartu, 2011.

183. **Maarja Krass**. L-Arginine pathways and antidepressant action. Tartu, 2011.
184. **Taavi Lai**. Population health measures to support evidence-based health policy in Estonia. Tartu, 2011.
185. **Tiit Salum**. Similarity and difference of temperature-dependence of the brain sodium pump in normal, different neuropathological, and aberrant conditions and its possible reasons. Tartu, 2011.
186. **Tõnu Vooder**. Molecular differences and similarities between histological subtypes of non-small cell lung cancer. Tartu, 2011.
187. **Jelena Štšepetova**. The characterisation of intestinal lactic acid bacteria using bacteriological, biochemical and molecular approaches. Tartu, 2011.
188. **Radko Avi**. Natural polymorphisms and transmitted drug resistance in Estonian HIV-1 CRF06_cpx and its recombinant viruses. Tartu, 2011, 116 p.
189. **Edward Laane**. Multiparameter flow cytometry in haematological malignancies. Tartu, 2011, 152 p.
190. **Triin Jagomägi**. A study of the genetic etiology of nonsyndromic cleft lip and palate. Tartu, 2011, 158 p.
191. **Ivo Laidmäe**. Fibrin glue of fish (*Salmo salar*) origin: immunological study and development of new pharmaceutical preparation. Tartu, 2012, 150 p.
192. **Ülle Parm**. Early mucosal colonisation and its role in prediction of invasive infection in neonates at risk of early onset sepsis. Tartu, 2012, 168 p.
193. **Kaupo Teesalu**. Autoantibodies against desmin and transglutaminase 2 in celiac disease: diagnostic and functional significance. Tartu, 2012, 142 p.
194. **Maksim Zagura**. Biochemical, functional and structural profiling of arterial damage in atherosclerosis. Tartu, 2012, 162 p.
195. **Vivian Kont**. Autoimmune regulator: characterization of thymic gene regulation and promoter methylation. Tartu, 2012, 134 p.
196. **Pirje Hütt**. Functional properties, persistence, safety and efficacy of potential probiotic lactobacilli. Tartu, 2012, 246 p.
197. **Innar Tõru**. Serotonergic modulation of CCK-4- induced panic. Tartu, 2012, 132 p.
198. **Sigrid Vorobjov**. Drug use, related risk behaviour and harm reduction interventions utilization among injecting drug users in Estonia: implications for drug policy. Tartu, 2012, 120 p.
199. **Martin Serg**. Therapeutic aspects of central haemodynamics, arterial stiffness and oxidative stress in hypertension. Tartu, 2012, 156 p.
200. **Jaanika Kumm**. Molecular markers of articular tissues in early knee osteoarthritis: a population-based longitudinal study in middle-aged subjects. Tartu, 2012, 159 p.
201. **Kertu Rünkorg**. Functional changes of dopamine, endopioid and endocannabinoid systems in CCK2 receptor deficient mice. Tartu, 2012, 125 p.
202. **Mai Blöndal**. Changes in the baseline characteristics, management and outcomes of acute myocardial infarction in Estonia. Tartu, 2012, 127 p.

203. **Jana Lass**. Epidemiological and clinical aspects of medicines use in children in Estonia. Tartu, 2012, 170 p.
204. **Kai Truusalu**. Probiotic lactobacilli in experimental persistent *Salmonella* infection. Tartu, 2013, 139 p.
205. **Oksana Jagur**. Temporomandibular joint diagnostic imaging in relation to pain and bone characteristics. Long-term results of arthroscopic treatment. Tartu, 2013, 126 p.
206. **Katrin Sikk**. Manganese-ephedrone intoxication – pathogenesis of neurological damage and clinical symptomatology. Tartu, 2013, 125 p.
207. **Kai Blöndal**. Tuberculosis in Estonia with special emphasis on drug-resistant tuberculosis: Notification rate, disease recurrence and mortality. Tartu, 2013, 151 p.
208. **Marju Puurand**. Oxidative phosphorylation in different diseases of gastric mucosa. Tartu, 2013, 123 p.
209. **Aili Tagoma**. Immune activation in female infertility: Significance of autoantibodies and inflammatory mediators. Tartu, 2013, 135 p.
210. **Liis Sabre**. Epidemiology of traumatic spinal cord injury in Estonia. Brain activation in the acute phase of traumatic spinal cord injury. Tartu, 2013, 135 p.
211. **Merit Lamp**. Genetic susceptibility factors in endometriosis. Tartu, 2013, 125 p.
212. **Erik Salum**. Beneficial effects of vitamin D and angiotensin II receptor blocker on arterial damage. Tartu, 2013, 167 p.
213. **Maire Karelson**. Vitiligo: clinical aspects, quality of life and the role of melanocortin system in pathogenesis. Tartu, 2013, 153 p.
214. **Kuldar Kaljurand**. Prevalence of exfoliation syndrome in Estonia and its clinical significance. Tartu, 2013, 113 p.
215. **Raido Paasma**. Clinical study of methanol poisoning: handling large outbreaks, treatment with antidotes, and long-term outcomes. Tartu, 2013, 96 p.
216. **Anne Kleinberg**. Major depression in Estonia: prevalence, associated factors, and use of health services. Tartu, 2013, 129 p.
217. **Triin Eglit**. Obesity, impaired glucose regulation, metabolic syndrome and their associations with high-molecular-weight adiponectin levels. Tartu, 2014, 115 p.
218. **Kristo Ausmees**. Reproductive function in middle-aged males: Associations with prostate, lifestyle and couple infertility status. Tartu, 2014, 125 p.
219. **Kristi Huik**. The influence of host genetic factors on the susceptibility to HIV and HCV infections among intravenous drug users. Tartu, 2014, 144 p.
220. **Liina Tserel**. Epigenetic profiles of monocytes, monocyte-derived macrophages and dendritic cells. Tartu, 2014, 143 p.
221. **Irina Kerna**. The contribution of *ADAM12* and *CILP* genes to the development of knee osteoarthritis. Tartu, 2014, 152 p.

222. **Ingrid Liiv**. Autoimmune regulator protein interaction with DNA-dependent protein kinase and its role in apoptosis. Tartu, 2014, 143 p.
223. **Liivi Maddison**. Tissue perfusion and metabolism during intra-abdominal hypertension. Tartu, 2014, 103 p.
224. **Krista Ress**. Childhood coeliac disease in Estonia, prevalence in atopic dermatitis and immunological characterisation of coexistence. Tartu, 2014, 124 p.
225. **Kai Muru**. Prenatal screening strategies, long-term outcome of children with marked changes in maternal screening tests and the most common syndromic heart anomalies in Estonia. Tartu, 2014, 189 p.
226. **Kaja Rahu**. Morbidity and mortality among Baltic Chernobyl cleanup workers: a register-based cohort study. Tartu, 2014, 155 p.
227. **Klari Noormets**. The development of diabetes mellitus, fertility and energy metabolism disturbances in a Wfs1-deficient mouse model of Wolfram syndrome. Tartu, 2014, 132 p.
228. **Liis Toome**. Very low gestational age infants in Estonia. Tartu, 2014, 183 p.
229. **Ceith Nikkolo**. Impact of different mesh parameters on chronic pain and foreign body feeling after open inguinal hernia repair. Tartu, 2014, 132 p.
230. **Vadim Brjalin**. Chronic hepatitis C: predictors of treatment response in Estonian patients. Tartu, 2014, 122 p.
231. **Vahur Metsna**. Anterior knee pain in patients following total knee arthroplasty: the prevalence, correlation with patellar cartilage impairment and aspects of patellofemoral congruence. Tartu, 2014, 130 p.
232. **Marju Kase**. Glioblastoma multiforme: possibilities to improve treatment efficacy. Tartu, 2015, 137 p.
233. **Riina Runnel**. Oral health among elementary school children and the effects of polyol candies on the prevention of dental caries. Tartu, 2015, 112 p.
234. **Made Laanpere**. Factors influencing women's sexual health and reproductive choices in Estonia. Tartu, 2015, 176 p.
235. **Andres Lust**. Water mediated solid state transformations of a polymorphic drug – effect on pharmaceutical product performance. Tartu, 2015, 134 p.
236. **Anna Klugman**. Functionality related characterization of pretreated wood lignin, cellulose and polyvinylpyrrolidone for pharmaceutical applications. Tartu, 2015, 156 p.
237. **Triin Laisk-Podar**. Genetic variation as a modulator of susceptibility to female infertility and a source for potential biomarkers. Tartu, 2015, 155 p.
238. **Mailis Tõnisson**. Clinical picture and biochemical changes in blood in children with acute alcohol intoxication. Tartu, 2015, 100 p.
239. **Kadri Tamme**. High volume haemodiafiltration in treatment of severe sepsis – impact on pharmacokinetics of antibiotics and inflammatory response. Tartu, 2015, 133 p.

240. **Kai Part**. Sexual health of young people in Estonia in a social context: the role of school-based sexuality education and youth-friendly counseling services. Tartu, 2015, 203 p.
241. **Urve Paaver**. New perspectives for the amorphization and physical stabilization of poorly water-soluble drugs and understanding their dissolution behavior. Tartu, 2015, 139 p.
242. **Aleksandr Peet**. Intrauterine and postnatal growth in children with HLA-conferred susceptibility to type 1 diabetes. Tartu. 2015, 146 p.
243. **Piret Mitt**. Healthcare-associated infections in Estonia – epidemiology and surveillance of bloodstream and surgical site infections. Tartu, 2015, 145 p.
244. **Merli Saare**. Molecular Profiling of Endometriotic Lesions and Endometria of Endometriosis Patients. Tartu, 2016, 129 p.
245. **Kaja-Triin Laisaar**. People living with HIV in Estonia: Engagement in medical care and methods of increasing adherence to antiretroviral therapy and safe sexual behavior. Tartu, 2016, 132 p.
246. **Eero Merilind**. Primary health care performance: impact of payment and practice-based characteristics. Tartu, 2016, 120 p.
247. **Jaanika Kärner**. Cytokine-specific autoantibodies in AIRE deficiency. Tartu, 2016, 182 p.
248. **Kaido Paapstel**. Metabolomic profile of arterial stiffness and early biomarkers of renal damage in atherosclerosis. Tartu, 2016, 173 p.
249. **Liidia Kiisk**. Long-term nutritional study: anthropometrical and clinico-laboratory assessments in renal replacement therapy patients after intensive nutritional counselling. Tartu, 2016, 207 p.
250. **Georgi Nellis**. The use of excipients in medicines administered to neonates in Europe. Tartu, 2017, 159 p.
251. **Aleksei Rakitin**. Metabolic effects of acute and chronic treatment with valproic acid in people with epilepsy. Tartu, 2017, 125 p.
252. **Eveli Kallas**. The influence of immunological markers to susceptibility to HIV, HBV, and HCV infections among persons who inject drugs. Tartu, 2017, 138 p.
253. **Tiina Freimann**. Musculoskeletal pain among nurses: prevalence, risk factors, and intervention. Tartu, 2017, 125 p.
254. **Evelyn Aaviksoo**. Sickness absence in Estonia: determinants and influence of the sick-pay cut reform. Tartu, 2017, 121 p.
255. **Kalev Nõupuu**. Autosomal-recessive Stargardt disease: phenotypic heterogeneity and genotype-phenotype associations. Tartu, 2017, 131 p.
256. **Ho Duy Binh**. Osteogenesis imperfecta in Vietnam. Tartu, 2017, 125 p.
257. **Uku Haljasorg**. Transcriptional mechanisms in thymic central tolerance. Tartu, 2017, 147 p.
258. **Živile Riispere**. IgA Nephropathy study according to the Oxford Classification: IgA Nephropathy clinical-morphological correlations, disease progression and the effect of renoprotective therapy. Tartu, 2017, 129 p.

259. **Hiie Soeorg**. Coagulase-negative staphylococci in gut of preterm neonates and in breast milk of their mothers. Tartu, 2017, 216 p.
260. **Anne-Mari Anton Willmore**. Silver nanoparticles for cancer research. Tartu, 2017, 132 p.
261. **Ott Laius**. Utilization of osteoporosis medicines, medication adherence and the trend in osteoporosis related hip fractures in Estonia. Tartu, 2017, 134 p.
262. **Alar Aab**. Insights into molecular mechanisms of asthma and atopic dermatitis. Tartu, 2017, 164 p.
263. **Sander Pajusalu**. Genome-wide diagnostics of Mendelian disorders: from chromosomal microarrays to next-generation sequencing. Tartu, 2017, 146 p.
264. **Mikk Jürisson**. Health and economic impact of hip fracture in Estonia. Tartu, 2017, 164 p.
265. **Kaspar Tootsi**. Cardiovascular and metabolomic profiling of osteoarthritis. Tartu, 2017, 150 p.
266. **Mario Saare**. The influence of AIRE on gene expression – studies of transcriptional regulatory mechanisms in cell culture systems. Tartu, 2017, 172 p.
267. **Piia Jõgi**. Epidemiological and clinical characteristics of pertussis in Estonia. Tartu, 2018, 168 p.
268. **Elle Põldoja**. Structure and blood supply of the superior part of the shoulder joint capsule. Tartu, 2018, 116 p.
269. **Minh Son Nguyen**. Oral health status and prevalence of temporomandibular disorders in 65–74-year-olds in Vietnam. Tartu, 2018, 182 p.
270. **Kristian Semjonov**. Development of pharmaceutical quench-cooled molten and melt-electrospun solid dispersions for poorly water-soluble indomethacin. Tartu, 2018, 125 p.
271. **Janne Tiigimäe-Saar**. Botulinum neurotoxin type A treatment for sialorrhea in central nervous system diseases. Tartu, 2018, 109 p.
272. **Veiko Vengerfeldt**. Apical periodontitis: prevalence and etiopathogenetic aspects. Tartu, 2018, 150 p.
273. **Rudolf Bichele**. TNF superfamily and AIRE at the crossroads of thymic differentiation and host protection against *Candida albicans* infection. Tartu, 2018, 153 p.
274. **Olga Tšuiko**. Unravelling Chromosomal Instability in Mammalian Preimplantation Embryos Using Single-Cell Genomics. Tartu, 2018, 169 p.
275. **Kärt Kriisa**. Profile of acylcarnitines, inflammation and oxidative stress in first-episode psychosis before and after antipsychotic treatment. Tartu, 2018, 145 p.
276. **Xuan Dung Ho**. Characterization of the genomic profile of osteosarcoma. Tartu, 2018, 144 p.
277. **Karit Reinson**. New Diagnostic Methods for Early Detection of Inborn Errors of Metabolism in Estonia. Tartu, 2018, 201 p.

278. **Mari-Anne Vals**. Congenital N-glycosylation Disorders in Estonia. Tartu, 2019, 148 p.
279. **Liis Kadastik-Eerme**. Parkinson's disease in Estonia: epidemiology, quality of life, clinical characteristics and pharmacotherapy. Tartu, 2019, 202 p.
280. **Hedi Hunt**. Precision targeting of intraperitoneal tumors with peptide-guided nanocarriers. Tartu, 2019, 179 p.
281. **Rando Porosk**. The role of oxidative stress in Wolfram syndrome 1 and hypothermia. Tartu, 2019, 123 p.
282. **Ene-Ly Jõgeda**. The influence of coinfections and host genetic factor on the susceptibility to HIV infection among people who inject drugs. Tartu, 2019, 126 p.
283. **Kristel Ehala-Aleksejev**. The associations between body composition, obesity and obesity-related health and lifestyle conditions with male reproductive function. Tartu, 2019, 138 p.
284. **Aigar Ottas**. The metabolomic profiling of psoriasis, atopic dermatitis and atherosclerosis. Tartu, 2019, 136 p.
285. **Elmira Gurbanova**. Specific characteristics of tuberculosis in low default, but high multidrug–resistance prison setting. Tartu, 2019, 129 p.
286. **Van Thai Nguyeni**. The first study of the treatment outcomes of patients with cleft lip and palate in Central Vietnam. Tartu, 2019, 144 p.
287. **Maria Yakoreva**. Imprinting Disorders in Estonia. Tartu, 2019, 187 p.
288. **Kadri Rekker**. The putative role of microRNAs in endometriosis pathogenesis and potential in diagnostics. Tartu, 2019, 140 p.
289. **Ülle Võhma**. Association between personality traits, clinical characteristics and pharmacological treatment response in panic disorder. Tartu, 2019, 121 p.
290. **Aet Saar**. Acute myocardial infarction in Estonia 2001–2014: towards risk-based prevention and management. Tartu, 2019, 124 p.
291. **Toomas Toomsoo**. Transcranial brain sonography in the Estonian cohort of Parkinson's disease. Tartu, 2019, 114 p.
292. **Lidiia Zhytnik**. Inter- and intrafamilial diversity based on genotype and phenotype correlations of Osteogenesis Imperfecta. Tartu, 2019, 224 p.
293. **Pilleriin Soodla**. Newly HIV-infected people in Estonia: estimation of incidence and transmitted drug resistance. Tartu, 2019, 194 p.
294. **Kristiina Ojamaa**. Epidemiology of gynecological cancer in Estonia. Tartu, 2020, 133 p.
295. **Marianne Saard**. Modern Cognitive and Social Intervention Techniques in Paediatric Neurorehabilitation for Children with Acquired Brain Injury. Tartu, 2020, 168 p.
296. **Julia Maslovskaja**. The importance of DNA binding and DNA breaks for AIRE-mediated transcriptional activation. Tartu, 2020, 162 p.
297. **Natalia Lobanovskaya**. The role of PSA-NCAM in the survival of retinal ganglion cells. Tartu, 2020, 105 p.

298. **Madis Rahu**. Structure and blood supply of the postero-superior part of the shoulder joint capsule with implementation of surgical treatment after anterior traumatic dislocation. Tartu, 2020, 104 p.
299. **Helen Zirnask**. Luteinizing hormone (LH) receptor expression in the penis and its possible role in pathogenesis of erectile disturbances. Tartu, 2020, 87 p.
300. **Kadri Toome**. Homing peptides for targeting of brain diseases. Tartu, 2020, 152 p.
301. **Maarja Hallik**. Pharmacokinetics and pharmacodynamics of inotropic drugs in neonates. Tartu, 2020, 172 p.
302. **Raili Müller**. Cardiometabolic risk profile and body composition in early rheumatoid arthritis. Tartu, 2020, 133 p.
303. **Sergo Kasvandik**. The role of proteomic changes in endometrial cells – from the perspective of fertility and endometriosis. Tartu, 2020, 191 p.
304. **Epp Kaleviste**. Genetic variants revealing the role of STAT1/STAT3 signaling cytokines in immune protection and pathology. Tartu, 2020, 189 p.
305. **Sten Saar**. Epidemiology of severe injuries in Estonia. Tartu, 2020, 104 p.
306. **Kati Braschinsky**. Epidemiology of primary headaches in Estonia and applicability of web-based solutions in headache epidemiology research. Tartu, 2020, 129 p.
307. **Helen Vaher**. MicroRNAs in the regulation of keratinocyte responses in *psoriasis vulgaris* and atopic dermatitis. Tartu, 2020, 242 p.
308. **Liisi Raam**. Molecular Alterations in the Pathogenesis of Two Chronic Dermatoses – Vitiligo and Psoriasis. Tartu, 2020, 164 p.
309. **Artur Vetkas**. Long-term quality of life, emotional health, and associated factors in patients after aneurysmal subarachnoid haemorrhage. Tartu, 2020, 127 p.
310. **Teele Kasepalu**. Effects of remote ischaemic preconditioning on organ damage and acylcarnitines' metabolism in vascular surgery. Tartu, 2020, 130 p.
311. **Prakash Lingasamy**. Development of multitargeted tumor penetrating peptides. Tartu, 2020, 246 p.
312. **Lille Kurvits.** Parkinson's disease as a multisystem disorder: whole transcriptome study in Parkinson's disease patients' skin and blood. Tartu, 2021, 142 p.
313. **Mariliis Põld.** Smoking, attitudes towards smoking behaviour, and nicotine dependence among physicians in Estonia: cross-sectional surveys 1982–2014. Tartu, 2021, 172 p.
314. **Triin Kikas**. Single nucleotide variants affecting placental gene expression and pregnancy outcome. Tartu, 2021, 160 p.
315. **Hedda Lippus-Metsaots**. Interpersonal violence in Estonia: prevalence, impact on health and health behaviour. Tartu, 2021, 172 p.

316. **Georgi Dzaparidze.** Quantification and evaluation of the diagnostic significance of adenocarcinoma-associated microenvironmental changes in the prostate using modern digital pathology solutions. Tartu, 2021, 132 p.
317. **Tuuli Sedman.** New avenues for GLP1 receptor agonists in the treatment of diabetes. Tartu, 2021, 118 p.
318. **Martin Padar.** Enteral nutrition, gastrointestinal dysfunction and intestinal biomarkers in critically ill patients. Tartu, 2021, 189 p.
319. **Siim Schneider.** Risk factors, etiology and long-term outcome in young ischemic stroke patients in Estonia. Tartu, 2021, 131 p.
320. **Konstantin Ridnõi.** Implementation and effectiveness of new prenatal diagnostic strategies in Estonia. Tartu, 2021, 191 p.
321. **Risto Vaikjärv.** Etiopathogenetic and clinical aspects of peritonsillar abscess. Tartu, 2021, 115 p.
322. **Liis Preem.** Design and characterization of antibacterial electrospun drug delivery systems for wound infections. Tartu, 2022, 220 p.
323. **Keerthie Dissanayake.** Preimplantation embryo-derived extracellular vesicles: potential as an embryo quality marker and their role during the embryo-maternal communication. Tartu, 2022, 203 p.
324. **Laura Viidik.** 3D printing in pharmaceutics: a new avenue for fabricating therapeutic drug delivery systems. Tartu, 2022, 139 p.
325. **Kasun Godakumara.** Extracellular vesicle mediated embryo-maternal communication – A tool for evaluating functional competency of preimplantation embryos. Tartu, 2022, 176 p.
326. **Hindrek Teder.** Developing computational methods and workflows for targeted and whole-genome sequencing based non-invasive prenatal testing. Tartu, 2022, 138 p.
327. **Jana Tuusov.** Deaths caused by alcohol, psychotropic and other substances in Estonia: evidence based on forensic autopsies. Tartu, 2022, 157 p.
328. **Heigo Reima.** Colorectal cancer care and outcomes – evaluation and possibilities for improvement in Estonia. Tartu, 2022, 146 p.
329. **Liisa Kuhi.** A contribution of biomarker collagen type II neoepitope C2C in urine to the diagnosis and prognosis of knee osteoarthritis. Tartu, 2022, 157 p.
330. **Reeli Tamme.** Associations between pubertal hormones and physical activity levels, and subsequent bone mineral characteristics: a longitudinal study of boys aged 12–18. Tartu, 2022, 118 p.
331. **Deniss Sõritsa.** The impact of endometriosis and physical activity on female reproduction. Tartu, 2022, 152 p.
332. **Mohammad Mehedi Hasan.** Characterization of follicular fluid-derived extracellular vesicles and their contribution to periconception environment. Tartu, 2022, 194 p.
333. **Priya Kulkarni.** Osteoarthritis pathogenesis: an immunological passage through synovium-synovial fluid axis. Tartu, 2022, 268 p.

334. **Nigul Ilves.** Brain plasticity and network reorganization in children with perinatal stroke: a functional magnetic resonance imaging study. Tartu, 2022, 169 p.
335. **Marko Murruste.** Short- and long-term outcomes of surgical management of chronic pancreatitis. Tartu, 2022, 180 p.
336. **Marilin Ivask.** Transcriptomic and metabolic changes in the WFS1-deficient mouse model. Tartu, 2022, 158 p.
337. **Jüri Lieberg.** Results of surgical treatment and role of biomarkers in pathogenesis and risk prediction in patients with abdominal aortic aneurysm and peripheral artery disease. Tartu, 2022, 160 p.
338. **Sanna Puusepp.** Comparison of molecular genetics and morphological findings of childhood-onset neuromuscular disorders. Tartu, 2022, 216 p.
339. **Khan Nguyen Viet.** Chemical composition and bioactivity of extracts and constituents isolated from the medicinal plants in Vietnam and their nanotechnology-based delivery systems. Tartu, 2023, 172 p.
340. **Getnet Balcha Midekessa.** Towards understanding the colloidal stability and detection of Extracellular Vesicles. Tartu, 2023, 172 p.
341. **Kristiina Sepp.** Competency-based and person-centred community pharmacy practice – development and implementation in Estonia. Tartu, 2023, 242 p.
342. **Linda Sõber.** Impact of thyroid disease and surgery on patient's quality of voice and swallowing. Tartu, 2023, 114 p.
343. **Anni Lepland.** Precision targeting of tumour-associated macrophages in triple negative breast cancer. Tartu, 2023, 160 p.
344. **Sirje Sammul.** Prevalence and risk factors of arterial hypertension and cardiovascular mortality: 13-year longitudinal study among 35- and 55-year-old adults in Estonia and Sweden. Tartu, 2023, 158 p.
345. **Maarjaliis Paavo**. Short-Wavelength and Near-Infrared Autofluorescence Imaging in Recessive Stargardt Disease, Choroideremia, *PROM1*-Macular Dystrophy and Ocular Albinism. Tartu, 2023, 202 p.
346. **Kaspar Ratnik.** development of predictive multimarker test for preeclampsia in early and late pregnancy. Tartu, 2023, 134 p.
347. **Kärt Simre.** Development of coeliac disease in two populations with different environmental backgrounds. Tartu, 2023, 161 p.
348. **Qurat Ul Ain Reshi.** Characterization of the maternal reproductive tract and spermatozoa communication during periconception period via extracellular vesicles. Tartu, 2023, 182 p.
349. **Stanislav Tjagur.** *Mycoplasma genitalium* and other sexually transmitted infections causing urethritis – their prevalence, impact on male fertility parameters and prostate health. Tartu, 2023, 225 p.
350. **Lagle Lehes.** The first study of voice and resonance related treatment outcomes of Estonian cleft palate children. Tartu, 2023, 126 p.
351. **Liis Ilves.** Metabolomic profiling of chronic inflammatory skin diseases. Tartu, 2023, 146 p.

352. **Marina Šunina**. Flow cytometric analysis of T and B cell properties in healthy donors and subjects with vitiligo. Tartu, 2023, 164 p.
353. **Jaanus Suumann.** Gastric biomarkers and their dynamics as a less invasive method to evaluate stomach health in bariatric surgery patients. Tartu, 2023, 122 p.
354. **Ele Hanson.** Clinical and biochemical markers for the prediction and early diagnosis of pregnancy related complications. Tartu, 2023, 145 p.
355. **Priit Pauklin.** Hemodynamic and biochemical characteristics of patients with atrial fibrillation and anticoagulation of ≥65-year-old patients with atrial fibrillation in Estonia. Tartu, 2023, 144 p.
356. **Triinu Keskpaik.** Quality Indicators and Non-Ischemic Myocardial Injury in Emergency Medicine. Tartu, 2023, 121 p.
357. **Laura Roht.** Hereditary colorectal cancer syndromes in Estonia. Tartu, 2023, 178 p.
358. **Norman Ilves.** Risk factors and onset time of periventricular hemorrhagic infarction in preterm born children and periventricular venous infarction in term born children. Tartu, 2024, 177 p.
359. **Edgar Lipping.** Postoperative antibacterial therapy in complicated appendicitis and appendectomy in pregnancy. Tartu, 2024, 121 p.
360. **Celia Teresa Pozo Ramos.** Preparation and assessment of antimicrobial electrospun matrices for prospective applications in wound healing. Tartu, 2024, 203 p.
361. **Karl Kuusik.** Effects of remote ischaemic preconditioning on arterial stiffness, organ damage and metabolomic profile in patients with lower extremity artery disease. Tartu, 2024, 173 p.
362. **Kelli Somelar-Duracz.** The molecular and cellular mechanisms of brain plasticity impairing factors. Tartu, 2024, 245 p.
363. **Aleksei Baburin.** Breast cancer incidence, mortality and survival in Estonia in the context of health care system changes and screening. Tartu, 2024, 130 p.
364. **Marina Loid.** Molecular and cellular determinants of healthy receptive and aged endometrium. Tartu, 2024, 159 p.
365. **Ulvi Vaher.** Epilepsy after ischemic perinatal stroke in term born children: neuroimaging predictors, clinical course and cognitive outcome. Tartu, 2024, 160 p.
366. **Allan Tobi.** Development of Smart Nanoparticles for Experimental Treatment of Cancer. Tartu, 2024, 160 p.
367. **Leho Rips.** The influence of vitamin D on the physical performance of conscripts in the Estonian Defence Forces. Tartu, 2024, 147 p.
368. **Kati Kärberg.** Factors and markers predicting subclinical atherosclerosis in type 2 diabetes. Tartu, 2024, 161 p.